Charles University in Prague
Faculty of Science
Department of Cell Biology

Study programme: Biology
Branch of study: Cellular and Developmental Biology

Bc. Katarína Vaškovičová

The determination of the role of protein kinase C α in amoeboid invasion of cancer cells

Určení úlohy protein kinázy C α v améboidní invazivitě nádorových buněk

Master's thesis

Supervisor: doc. RNDr. Jan Brábek, PhD.

Prague, 2012

Declaration

I declare that I elaborated the master's thesis „The determination of the role of protein kinase C α in amoeboid invasion of cancer cells“ independently, guided by my supervisor. I also declare that I have mentioned all the used literature and other sources. Neither this thesis, nor the part of it, was used to gain another or the same academic degree.

Prague, August 2012

Katarína Vaškovičová

Acknowledgements

I would like to thank to my supervisor, RNDr. Jan Brábek, PhD., for his professional advice and guidance during my work in his laboratory. Thanks also for his useful suggestions and support while writing this master's thesis.
Thanks also to Mgr. Radoslav Janoštiak for his help with confocal microscope.
I would also like to thank to my family and friends for always being very caring and supportive of me. Special thanks belong to my sister who is always here for me.

Contents

1. Abstract

Protein kinase C α (PKCα) is a serine/threonine protein kinase regulating many different signaling pathways. The aim of this study was to investigate the potential role of PKCα in amoeboid morphology and invasion of cancer cells.

It was observed, that expression of PKCα as well as its phosphorylation on Thr497 remained unchanged upon amoeboid-mesenchymal transition of A375m2 cells (induced by inhibition of ROCK kinase) both in 3D and in 2D environment.

However, activation of PKCα by PKC activator treatment resulted in mesenchymal-amoeboid transition of K2 and MDA-MB-231 mesenchymal cell lines, although it did not change overall invasivity ability of cells to invade 3D collagen. Notably, PKCα activation significantly reduced matrix degrading abilities of A375m2 cells. Conversely, inhibition of PKCα by PKCα inhibitor treatment caused amoeboid-mesenchymal transition of amoeboid A375m2 cells and it was associated with decreased invasiveness of all three cell lines used. PKCα inhibitor did not have any effect on gelatin degradation area of A375m2 cells. Consistently, specific siRNA mediated downregulation of PKCα lead to transition from amoeboid to mesenchymal morphology of A375m2 cells and reduced invasiveness of cells into 3D collagen. Moreover, gelatin degrading abilities of A375m2 cells were greatly increased upon siRNA treatment.

Taken together, our results suggest that PKCα is protein important for amoeboid morphology and invasiveness and could be involved in regulation of transitions between amoeboid and mesenchymal modes of cancer cell invasion.

Key words: protein kinase C α (PKCα), cell invasiveness, amoeboid invasion, mesenchymal invasion, invadopodia, extracellular matrix degradation

2. Abstrakt

Proteín kináza C α (PKCα) je serín/threonínová kináza regulujúca veľa rôznych signálnych kaskád v bunke. Cieľom tejto práce bolo preskúmať potenciálnu úlohu PKCα v améboidnej morfológii a invazivite nádorových buniek.

Bolo pozorované, že hladina expresie PKCα a takisto hladina jej fosforylácie na Thr497 zostala nezmenená po améboidne-mezenchymálnom prechode A375m2 buniek (indukovanom inhibítorom kinázy ROCK) ako v 3D, tak aj v 2D prostredí. Ukázalo sa však, že aktivácia PKCα jej aktivátorom viedla k mezenchymálne-améboidnému prechodu K2 a MDA-MB-231 mezenchymálnych bunkových línií, hoci celková schopnosť buniek invadovať do 3D kolagénu zostala nezmenená. Treba však poznamenať, že aktivácia PKCα významne znížila schopnosť A375m2 buniek degradovať extracelulárnu matrix. Naopak, inhibícia PKCα jej inhibítorom zapríčinila améboidne-mezenchymálny prechod améboidných buniek A375m2 a tento prechod bol spojený so zníženou invazivitou všetkých použitých bunkových línií. PKCα inhibítor nemal žiadny vplyv na degradovanú plochu A375m2 buniek. V súlade s týmito pozorovaniami, špecifické umlčanie PKCα pomocou siRNA viedlo k zmene morfológie A375m2 buniek z améboidnej na mezenchymálnu a tiež k zníženej schopnosti buniek invadovať do 3D kolagénu. Navyše, schopnosti A375m2 buniek degradovať želatín boli význačne zvýšené po siRNA transfekcií.

Tieto výsledky spoločne naznačujú, že PKCα je proteín dôležitý pre améboidnú morfológiu a invazivitu a môže byť zahrnutý do regulácie prechodov medzi améboidným a mezenchymálnym spôsobom invazivity.

Kľúčové slová: proteín kináza C α (PKCα), invazivita buniek, améboidná invazivita, mezenchymálna invazivita, invadopódiá, degradácia extracelulárnej matrix

3. List of abbreviations

A375m2 – human melanoma cell line

A-loop – activation loop

AMT – amoeboid – mesenchymal transition

AP1 – activator protein 1

aPKCs – atypical protein kinases C

ARHGAP22 – Rho GTPase activating protein 22

Arp2/3 complex – actin-related proteins 2/3 complex

ATPase – adenosine triphosphatase

C1, C2, C3, C4 – conserved regions of PKCα

Cdc42 – small GTPase of Rho family

cPKCs – conventional (classical) protein kinases C

CT – carboxy-terminal tail

DAG – diacylglycerol

DOCK3 – dedicator of cytokinesis 3

DOCK10 – dedicator of cytokinesis 10

ECM – extracellular matrix

EMT – epithelial-mesenchymal transition

EphA2 - ephrin type-A receptor 2

ERK1/2 – extracellular signal – regualted protein kinase 1/2

ERM – ezrin, radixin and moesin proteins

FAK – focal adhesion kinase

F-actin – filamentous actin

GAP – guanine nucleotide triphosphatase - activating protein

GEF – guanine nucleotide exchange factor

Gö6976 – PKCα and PKCβI inhibitor

GTPase – guanine nucleotide triphosphatase

HM – hydrophobic motif

HSP70 – heat shock protein 70

HSP90 – heat shock protein 90

JNK – c-Jun N-terminal kinase

K2 (LW13K2) – rat sarcoma cell line

LIMK1 – LIM kinase 1

LIMK2 – LIM kinase 2

MAPK – mitogen – activated protein kinase

MAT – mesenchymal – amoeboid transition

MDA-MB-231 – human breast cancer cell line

MEK – MAP kinase kinase (MAPKK)

MLC – myosin light chain

MLC2 – myosin light chain 2

MLCK – myosin light chain kinase

MLCP – myosin light chain phosphatase

MMP-2 – matrix metalloproteinase 2

MMP-9 – matrix metalloproteinase 9

MMPs – matrix metalloproteinases

MRCK - myotonic dystrophy kinase-related Cdc42-binding kinase

mTORC2 - mammalian target of rapamycin complex 2

MTs - microtubules

MT1-MMP – membrane – targeted matrix metalloproteinase 1, synonym MMP-14

Nck1 - non-catalytic region of tyrosine kinase adaptor protein 1

NEDD9 - neural precursor cell expressed, developmentally down-regulated 9

NFκB - nuclear factor kappa-light-chain-enhancer of activated B cells

NIK kinase - NFκB-inducing kinase

nPKCs – novel protein kinases C

NRP1 – neuropilin 1

N-WASP – neural-Wiskott-Aldrich syndrome protein

p115RhoGEF – Rho guanine nucleotide exchange factor

p130Cas – Crk-associated substrate

PAK1 – p21-activated kinase 1

PAK2 – p21-activated kinase 2

PDK1 – 3-phosphoinositide-dependent protein kinase 1

PHLPP - PH domain and Leucine rich repeat Protein Phosphatases

PIP_2 - phosphatidylinositol(4,5)bisphosphate

PKC – protein kinase C

PKCα – protein kinase C – α isoform

PKCβ – protein kinase C – β isoform

PKM – protein kinase M, cleavage fragment of PKCα

PLCγ – phospholipase C γ

PLD – phospholipase D

PP2a – protein phosphatase 2

PtdSer - phosphatidylserine

PMA – phorbol 12-myristate 13-acetate, synonym 12-O-tetradecanoylphorbol-13-acetate (TPA)

PS – pseudosubstrate sequence

Rac1 – small GTPase of Rho family

RACKs – receptor for activated protein kinase C

Raf - MAP kinase kinase kinase (MAPKKK)

Ras – monomeric GTPase of Ras superfamily

RhoA - small GTPase of Rho family

RhoC – small GTPase of Rho family

RhoE - small GTPase of Rho family, synonym Rnd3

RhoGDI – Rho GDP dissociation inhibitor

Rho GTPases – Rho family of small GTPases

RICKs – receptor for inactivated protein kinase C

Rnd3 - small GTPase of Rho family, synonym RhoE

ROCK – Rho-associated coiled-coil – containing protein kinase

siRNA – small interfering RNA

Src – non-receptor tyrosine – kinase

TM – turn motif

uPA – urokinase plasminogen-activator

uPAR – uPA receptor

V1, V2, V3, V4, V5 – variable regions of PKCα

VEGF – vascular endothelial growth factor

WASP – family of Wiskott-Aldrich syndrome protein

WAVE – Wiskott-Aldrich syndrome protein family Verprolin – homologous protein

WIP – WASP-interacting protein

Y27632 – ROCK kinase inhibitor

ZIPK – zipper-interacting protein kinase

4. Introduction

4.1 Metastatic cascade

The ability of forming metastases is the most dangerous feature that tumor cells can gain. It is very important, therefore, to study this process, so we could better understand its molecular mechanisms and possibly find new therapeutic targets for anti-metastatic therapy.

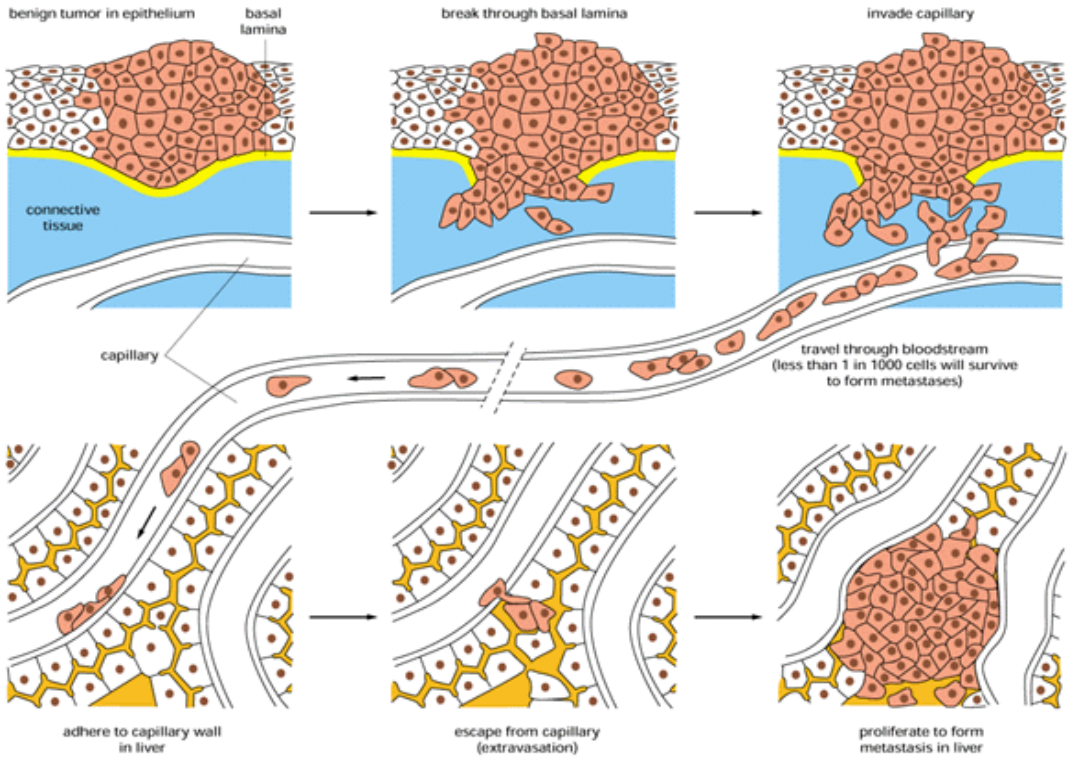

Figure 4.1. Metastatic cascade. Some cells of primary tumor are able to invade surrounding tissue, enter bloodstream or lymphatic vessel system and spread throughout the body for long distances. In the distant body part, cells that are able to leave vessel system can invade through surrounding tissue and establish new secondary tumor – metastase.
(Adapted from Alberts et al., Molecular biology of the cell, 4th ed.,, p. 1325)

Cells of primary tumor can disseminate throughout the body and potentially establish secondary tumors – metastases - in the process called metastatic cascade (reviewed in Kopfstein and Christofori, 2006) (Figure 4.1). First, primary tumor cells detach from primary tumor and invade the adjacent tissue and extracellular matrix (ECM). As this local invasion is generally too slow and undirected, tumor cells most likely soon after

the separation from primary tumor overcome endothelial barrier and basement membrane (in the process of intravasation) and enter the nearest blood or lymphatic vessel. Through the bloodstream or lymph vessel system, tumor cells can quickly and efficiently spread to distant body parts. Finally, at the distant location, tumor cells that are able to extravasate can leave blood or lymph vessel, once again invade the surrounding tissue and establish new secondary tumor there.

4.2 Modes of tumor cell invasion

Local invasion of tumor cells to surrounding tissue is the first and the most critical part of metastatic cascade and it also determines the metastatic potential of certain tumor cell types.

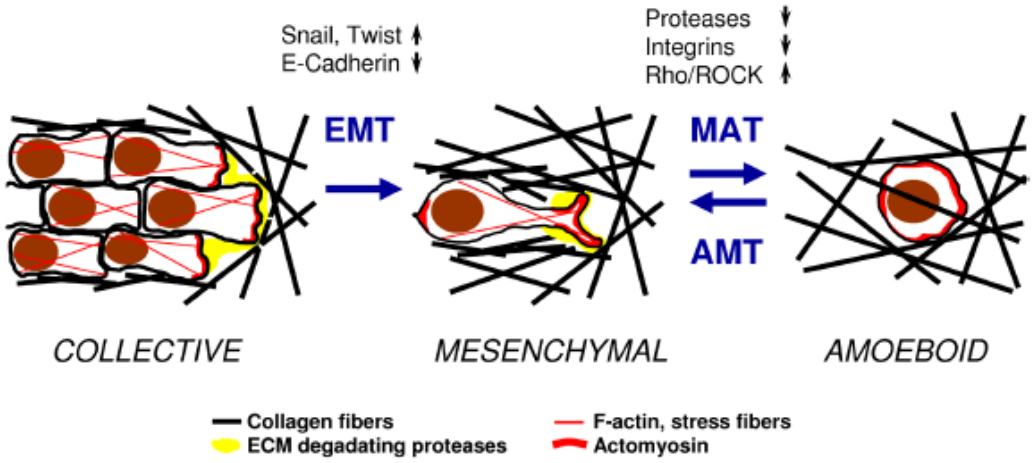

Figure 4.2. Collective, mesenchymal and amoeboid invasion and transitions between them. Cancer cells can invade either collectively or individually. In individual invasion, mesenchymal and amoeboid types of invasion can be further distinguished. Upon activation or inhibition of specific proteins important for specific type of invasion, transitions between invasion types can be observed.
(Adapted from Brábek J., Mierke C. T., Rösel D., Veselý P. and Fabry B. (2010). The role of the tissue microenvironment in the regulation of cancer cell motility and invasion. Cell Communication and Signaling 8:22).

Cells can invade through tissue and ECM either collectively, or individually. During collective invasion, the cell – cell adhesions between cells remain intact and cells migrate as a group of cells in the form of tubes, strands, sheets or irregular masses (Friedl and Gilmour, 2009; Farooqui and Fenteany, 2005; Friedl et al., 1995). Individual

invasion is the invasion of single cells and can occur in mesenchymal or amoeboid mode (reviewed in Paňková et al., 2010; Friedl, 2004) (Figure 4.2).

4.2.1 Mesenchymal invasion

Mesenchymal invasion reminds typical fibroblast-like migration (Lauffenburger and Horwitz, 1996). Also keratinocytes, endothelial cells, myoblasts, macrophages and some types of tumor cells (fibrosarcoma, glioblastoma) can migrate this way (Friedl, 2004; Sanz-Moreno and Marshall, 2010).

Mesenchymal cells have elongated, spindle-shaped morphology. In 3D matrices they are polarized - the leading and the trailing edge can be distinguished. On their leading edge, mesenchymal cells form actin-rich protrusions - filopodia or lamellipodia and formation of these migration structures is controlled by small GTPases of the Rho family, mostly by Rac and Cdc42 (Nobes and Hall, 1995; Ridley et al., 1992). The trailing edge contains nucleus, organelles and cytoplasm. Importantly, cells form contractile actin stress fibers that are anchored to integrin-based focal adhesions both at the front and the rear of the cell and are able to produce traction force that causes rear retraction and forward movement of the cell (Ballestrem et al., 2001; Sheetz et al., 1998). Moreover, into these sites of focal adhesions, also proteolytic enzymes are recruited to promote ECM degradation and remodeling (Wolf et al., 2003; Deryugina et al., 2001; Brooks et al., 1996; Wei et al, 1996). Therefore, mesenchymal cell is able to form a migration path for its own translocation in otherwise dense ECM. Because of the relative slow turnover of focal adhesions (Palecek et al., 1997), cell migration velocity in 3D matrices is relatively low as well – approximately 0,1 – 0,5 μm/min (Friedl et al., 1998).

Movement of mesenchymal cells can be divided into 5 steps that are continuously repeating (Friedl and Wolf, 2009) (Figure 4.3):

1. Cell polarization and formation of the leading protrusions (pseudopodia) by actin polymerization
2. Interaction between cell and ECM at the leading edge – formation of focal adhesions and downstream signaling

3. Local proteolysis of ECM

4. Contraction of actin stress fibers to promote traction force between leading and trailing edge of the cell

5. Displacement of the cell

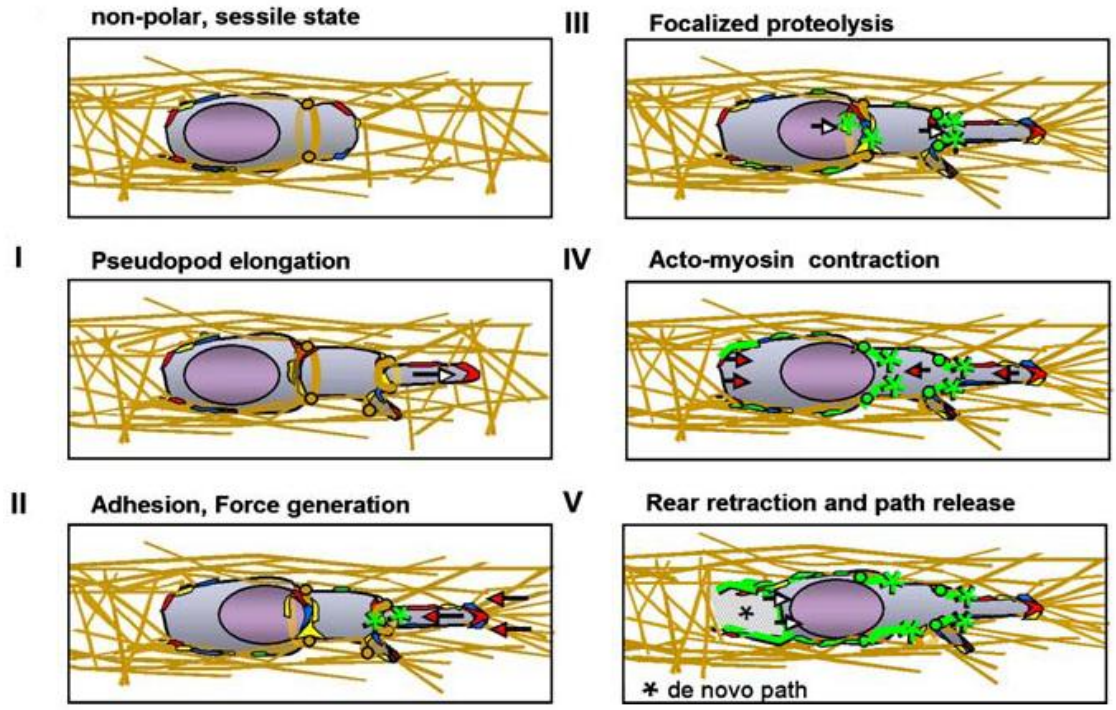

Figure 4.3. Five step process of cell invasion in 3D environment.
(Adapted from Friedl and Wolf (2009). Proteolytic intersticial cell migration: a five step process. Cancer Metastasis Rev 28(1-2):129-35).

For mesenchymal invasion, actin-based membrane protrusions at the leading edge are essential (Figure 4.4). In 2D environment, mesenchymal cells form lamellipodia – flat broad membrane protrusion composed of branched actin network, in 3D matrices cells form pseudopodia. Filopodia – thin rod-like protrusion consisting of parallel actin bundles - are formed both in 2D and 3D environment. Formation of these migration structures is based on actin polymerization and is regulated by small Rho GTPases Rac1 and Cdc42 (Figure 4.4). Rac1 and Cdc42 regulate WASP proteins family (Wiskott-Aldrich syndrome proteins) (Miki et al., 1998; Rohatgi et al., 1999), consisting of WASP, N-WASP and WAVE (Miki et al., 1998). These proteins subsequently activate Arp2/3 protein complex (actin-related protein) that promotes actin filament nucleation (Suetsugu et al., 2001). Formation of lamellipodia and filopodia is regulated by

Rac1/WAVE2/Arp2/3 signaling cascade (Yamazaki et al., 2003). Cdc42/N-WASP/Arp2/3 signaling cascade is important for filopodia formation (Carlier et al., 1999).

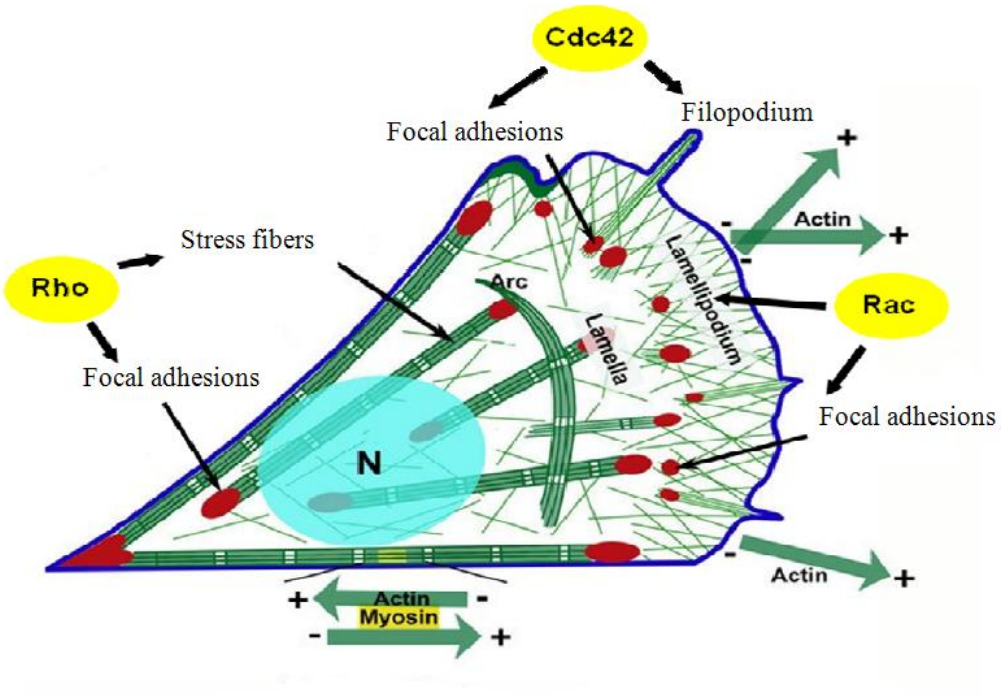

Figure 4.4. Membrane protrusions that mediate cell migration and their regulation by small Rho GTPases. To migrate, cells form actin-based membrane protrusions such as lamellipodia and filopodia. For cell contraction, stress fibers and focal adhesions are necessary. Formation of all of these structures is controlled by small Rho GTPases. Rac controls lamellipodia and focal adhesions formation. Cdc42 regulates filopodia and focal adhesions formation. Rho is important for stress fibers and focal adhesions formation.
(Adapted from web pages of Vic Small laboratory, Austrian Academy of Sciences in Salzburg and Vienna).

Besides actin polymerization, small Rho GTPases have also other functions necessary for mesenchymal invasion. Cdc42 regulates filopodia formation (Nobes and Hall, 1995; Yang et al., 2006), furthermore, it also influences initial cell polarity through organization of microtubules (Cau and Hall, 2005). Rac1 is important for lamellipodia (Ridley et al., 1992) and pseudopodia (Dharmawardhane et al., 1999) formation, but it regulates focal adhesions at the leading edge as well (Nobes and Hall, 1995). It affects stress fiber formation too (Guo et al., 2006). Stress fiber formation is also regulated by RhoA (Nobes and Hall, 1995) and in addition, RhoA controls focal adhesions formation (Amano et al., 1997; Totsukawa et al., 2004) (Figure 4.4).

The movement of mesenchymal cell and its body dislocation is based on traction force generated by actin stress fibers (Sheetz et al., 1998). This contraction is particularly regulated by Rho/ROCK signaling (as described below). For the record, Rho/ROCK signaling is dispensable for mesenchymal invasion of BE colon carcinoma and SW962 squamous cell carcinoma cells (Sahai and Marshall, 2003), because activated Cdc42/MRCK pathway can substitute it efficiently (Wilkinson et al., 2005). Only inactivation of both ROCK and MRCK leads to the decreased mesenchymal cell motility (Wilkinson et al., 2005).

Mesenchymal cells form many interactions with ECM – these are called focal adhesions. Focal adhesions also anchor stress fibers to the cell membrane and due to their contact with ECM they also stabilize lamellipodia, pseudopodia and filopodia. The basis of focal adhesions is formed by integrins – heterodimer transmembrane receptors that mechanically mediate interaction between actin cytoskeleton and ECM components (Tamariz and Grinnell, 2002). Integrins are organized into clusters by adaptor protein talin that mediates interaction between integrins and actin (Calderwood et al., 1999). Integrin clusters afterwards attract other adaptor proteins such as α-actinin, vinculin, paxillin, zyxin and signaling proteins – focal adhesion kinase (FAK) or Src, that further stabilize focal adhesions (Zaidel-Bar et al., 2004). Mesenchymal invasion is highly dependent on cell-ECM contacts, HT-1080 fibrosarcoma cells were after blocking of the β1 integrins immotile (Wolf et al., 2003).
As stated previously, focal adhesion contacts are regulated by small Rho GTPases. Interestingly, Rac and Cdc42 have somehow opposing effects to Rho in this regulation (Friedl, 2004). Whereas Rac and Cdc42 are important for elevated dynamics of focal adhesions (Keely et al., 1997), Rho activation leads to increased adhesiveness, stress fiber formation and lower migration speed (Clark et al., 1998; Nobes and Hall, 1999).

For mesenchymal invasion, also proteolytic degradation of ECM is essential (Birkedal-Hansen, 1995). At the sites of focal adhesions, clustered integrins recruit extracellular proteolytic enzymes such as matrix metalloproteinases (MMPs), cathepsins and serine proteases (Stetler-Stevenson et al., 1993; Brooks et al., 1996; Wei et al., 1996). These enzymes degrade ECM and form tube-like migratory pathways for migrating cells (Murphy and Gavrilovic, 1999; Friedl and Bröcker, 2000; Wolf and Friedl, 2005).

Proteolytic activity is localized a few micrometers behind actin polymerization of pseudopodia (Wolf et al., 2007; Tolde et al., 2010).

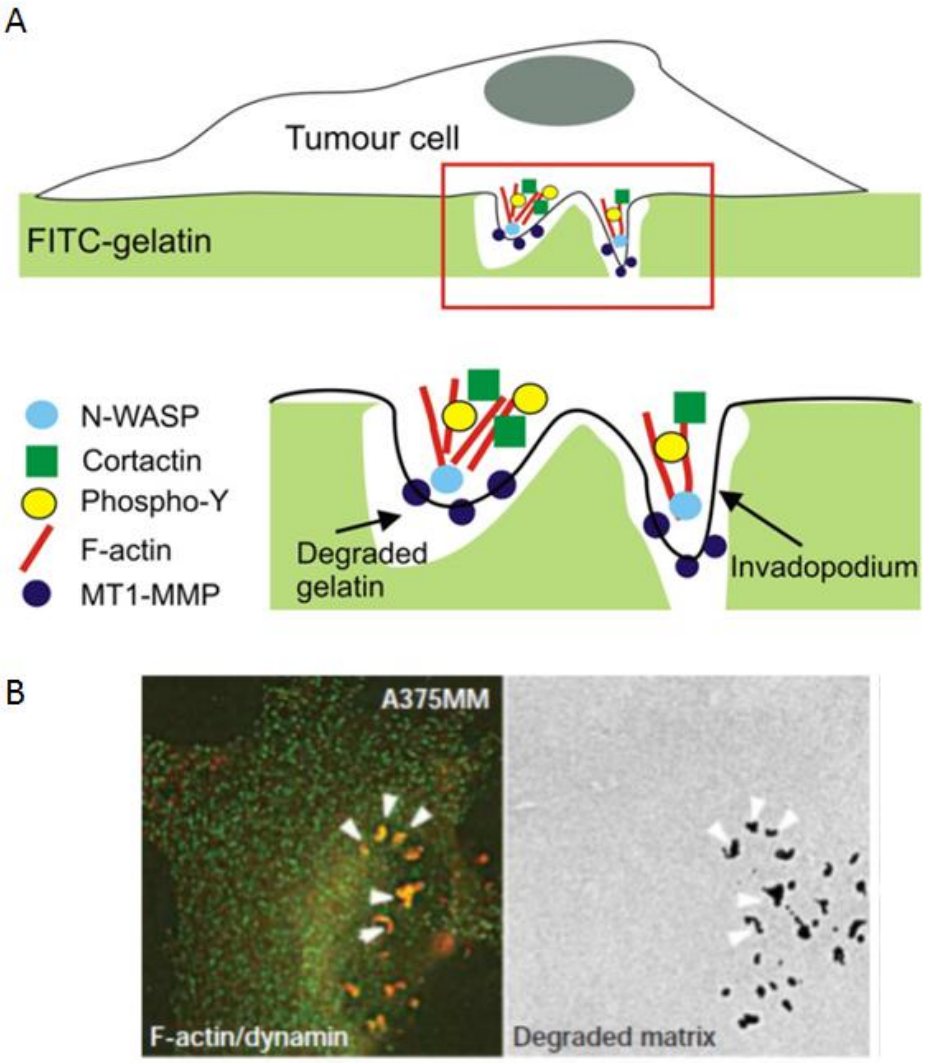

Figure 4.5. Invadopodia.

A) Invadopodia structure. Invadopodia are actin-based protrusions where also cortactin and MT1-MMP co-localize. (Adapted from Stylli, S. S., Kaye, A. H. and Lock, P. (2008). Invadopodia: At the cutting edge of tumor invasion. Journal of Clinical Neuroscience 15, 725-737).

B) Invadopodia function – ECM degradation. Invadopodia are sites, where F-actin and dynamin co-localize (left panel). These sites also co-localize with ECM degradation sites (right panel). (Adapted from Buccione, R., Orth, J. D. and McNiven, M. A. (2004). Foot and mouth: podosomes, invadopodia and circular dorsal ruffles Nature Reviews, Molecular Cell Biology 5, 647-657).

If cell is plated onto 3D matrix ECM-degrading pseudopodia are sometimes also called invadopodia (Figure 4.5). Invadopodia are dynamic membrane protrusions at the ventral surface of the cell that can be organized into clusters – where many smaller protrusions expand from one larger invagination (Buccione et al., 2004; Stylli et al., 2008; Tolde et

al., 2010). Invadopodia formation is induced by actin polymerization through N-WASP-Arp2/3-cortactin-dynamin signaling cascade (Buccione et al., 2004). N-WASP can be activated by Cdc42, Nck1 and WASP-interacting protein (WIP) in response to extracellular signals such as EGF (Yamaguchi et al., 2005). Besides F-actin, invadopodia also contains actin-regulatory proteins (Arp2/3, N-WASP, cortactin), adhesion molecules (integrins and focal adhesion molecules), signaling molecules (Src) and already mentioned MMPs (Weaver, 2006). Specifically, invadopodia contain membrane-associated collagenase MT1-MMP (also known as MMP-14) and soluble gelatinases MMP-2 and MMP-9 (Stylli et al., 2008). Interestingly, soluble MMPs are synthetized as inactive precursors and cleavage by MT1-MMP is essential for their activity (Kelly et al., 1998). Importantly, invadopodia were shown to be essential for cancer cell invasion as their formation is characteristic for highly invasive cancer cells and their markers are over-expressed in many human tumors (Weaver, 2006). Furthermore, the ability of cells to form invadopodia correlates with their invasive potential *in vitro* as well as *in vivo* (Stylli et al., 2008; Weaver, 2006). In addition, invasive potential of cancer cells is also dependent on MMPs levels and invadopodial ability to degrade ECM (Kelly et al., 1998; Stylli et al., 2008).

Regulation of MMPs expression is mediated (among others) also by Raf/MAPK signaling cascade. Upon extracellular signal, small monomeric GTPase Ras interact with Raf kinase and causes Raf translocation to the membrane and launching of MAPK cascade. Raf kinase phosphorylates MEK (mitogen-activated protein kinase kinase, also known as MAPKK) that phosphorylates MAPK (mitogen-activated protein kinase) (Hilger et al., 2002). This leads to activation of ERK (extracellular signal-regulated protein kinase), JNK (c-Jun N-terminal kinase) and p38 MAPK which activate AP1 and NF-κB transcription factors to switch on MMPs transcription (Kar et al., 2010; Liacini et al., 2003).

Actually, when cell is cultured in 3D environment, it is possible to distinguish few distinct ECM-degrading structures (Wolf and Friedl, 2009) (Figure 4.6). The cell movement begins with leading pseudopodia that attach to the ECM and generate traction force, but their tips are proteolysis-free. When ECM sterically obstructs cell movement, belt-like cell compressions are formed and belt-like cleavage of ECM is performed at these sites. Moreover, lateral spikes and other pseudopodia are formed that

do not contribute to pulling force of the cell movement, but focally degrade adjacent ECM fibers and rapidly retract. This could contribute to anchoring and stabilization of the cell and additional ECM degradation. The trailing edge contains a lot of protease activity and executes constitutive ECM remodeling and fragmentation. Partially cleaved fiber ends stay bound to the cell and as cell moves forward, they are re-aligned into parallel oriantation. This way cell generates its own tube-like track to move forward.

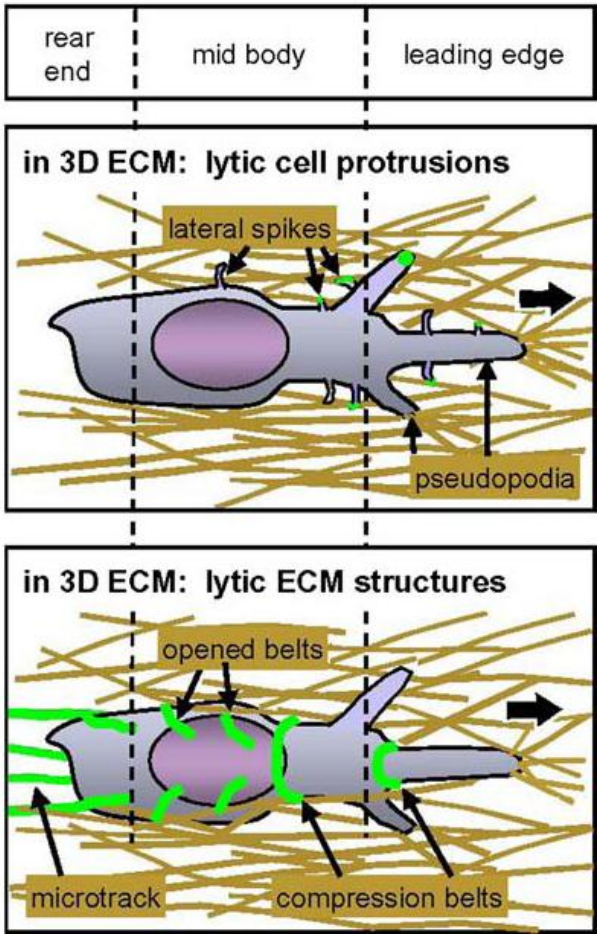

Figure 4.6. Distinct proteolytic structures of invading cell. At the leading edge, invading cells form leading pseudopodia, but these are mostly proteolysis-free. ECM cleavage is mainly mediated by compression belts. Additional ECM degradation is maintained by lateral spikes and other pseudopodia. (Adapted from Wolf and Friedl (2009). Mapping proteolytic cancer cell-extracellular matrix interface. Clin Exp Metastasis 26: 289-298).

Interestingly, ECM fragments from laminin, fibronectin and collagen can chemotactically attract nearby cells (Giannelli et al., 1997). Moreover, soluble protease can cleave and release ECM-bound growth factors and chemokines (Mueller et al., 2004; Egeblad et al., 2002). By this mechanism, also other tumor cells can be attracted

into this already pre-formed microtrack and can generate macrotrack through which they can migrate collectively (Friedl and Wolf, 2008).

4.2.2 Amoeboid invasion

Amoeboid invasion resembles the motility of amoeba *Dictyostelim discoideum* (Friedl et al., 2001; Devreotes and Zigmond, 1988). In higher eukaryotes, leukocytes (Mandeville et al., 1997; Friedl et al., 2001) and few types of cancer cells such as lymphoma, leukaemia, small cell lung and prostate carcinoma cells (Sahai and Marshall, 2003; Wolf et al., 2003; Friedl, 2004; Wyckoff et al., 2006; Rösel et al., 2008) use this type of migration.

Amoeboid cells show rounded or ellipsoid morphology in 3D substrates, they lack mature focal adhesion contacts and stress fibers (Friedl et al., 2001; Lämmermann and Sixt, 2009) and their migration is independent of proteolytic degradation of ECM (Wolf et al., 2003; Wyckoff et al., 2006). Amoeboid cells can move forward by utilizing cycles of cell body expansion and contraction, mediated by cortically localized acto-myosin (Yumura et al., 1984). The enhanced contractility of these cells is regulated by Rho/ROCK signaling pathway (Sahai and Marshall, 2003; Wyckoff et al., 2006). Thus, cells can adapt their shape to fit into the gaps in the ECM and are consequently able to squeeze through ECM fibers (Mandeville et al., 1997; Friedl et al., 2001; Wolf et al., 2003). The other option for amoeboid cells is generation of force sufficient to deform ECM fibers and make a path for migrating amoeboid cell (Wyckoff et al., 2006; Rösel et al., 2008; Provenzano et al., 2008). As a result of this acto-myosin contractility, bleb-like protrusions are observed at the membranes of amoeboid cell that also contribute to the migration by generating traction forces (Keller and Eggli, 1998; Charras et al., 2006). Amoeboid cells are relatively little adherent to the ECM, so the migration speed of cells is higher comparing to mesenchymal cells.

As noted previously, generation of contractile force is essential for amoeboid invasion (Mierke et al., 2008). Contractile force is in the cells produced by myosin II that is activated by its myosin light chain (MLC) phosphorylation. This phosphorylation allows myosin to interact with actin and stimulates myosin ATPase activity, therefore

promotes enhanced cell contractility. This process is regulated by small GTPases from Rho family – RhoA, RhoC, Rac1, Cdc42 and their effector kinases - MLC kinases and MLC phosphatases, that directly determine the MLC phosphorylation status (Zhao and Manser, 2005) (Figure 4.7).

Small GTPases RhoA and RhoC activate Rho-associated kinase (ROCK) (Ishizaki et al., 1996; Sahai and Marshall, 2002) that can either directly phosphorylate MLC (Amano et al., 1996; Totsukawa et al., 2000; Wyckoff et al., 2006), or can inhibit myosin light chain phosphatase (MLCP) by its phosphorylation at inhibitory sites (Tan et al., 2001; Velasco et al., 2002) and thus prevent MLC dephoshorylation (Kimura et al., 1996; Sward et al., 2000). ROCK also phosphorylates and activates zipper-interacting protein kinase (ZIPK) that directly phosphorylates MLC or inhibits MLCP by its phosphorylation (Hagerty et al., 2007).

Small GTPase Rac acts opposite to Rho. Rac effector p21-activated kinase 1 (PAK1) inhibits myosin light chain kinase (MLCK) (Sanders et al., 1999).

Small GTPase Cdc42 can activate myotonic dystrophy kinase-related Cdc42-binding kinase (MRCK) that activates MLC phosphorylation directly and also indirectly through MLCP inhibitory phosphorylation (Leung et al. 1998; Wilkinson et al., 2005). On the contrary, Cdc42 can also inhibit MLC phosphorylation by its interaction with PAK1 (Manser et al., 1995).

Obviously, regulation of MLC phosphorylation by small Rho GTPases is very complex and the result depends both on temporal and spatial coordination of Rho GTPases. For example, ROCK and MLCK were shown to regulate distinct subpopulations of MLC (Totsukawa et al., 2004) and have overall different roles in regulation of cell shape, adhesion and migration (Niggli et al., 2006). Inhibition of both ROCK and MLCK leads into complete abolition of MLC phosphorylation (Niggli et al., 2006), however, only ROCK is able to generate sufficient contractile force for migration (Wyckoff et al., 2006). Importantly, ROCK-mediated MLC phosphorylation is needed also for correct MLC localization and cortex assembly (Wyckoff et al., 2006).

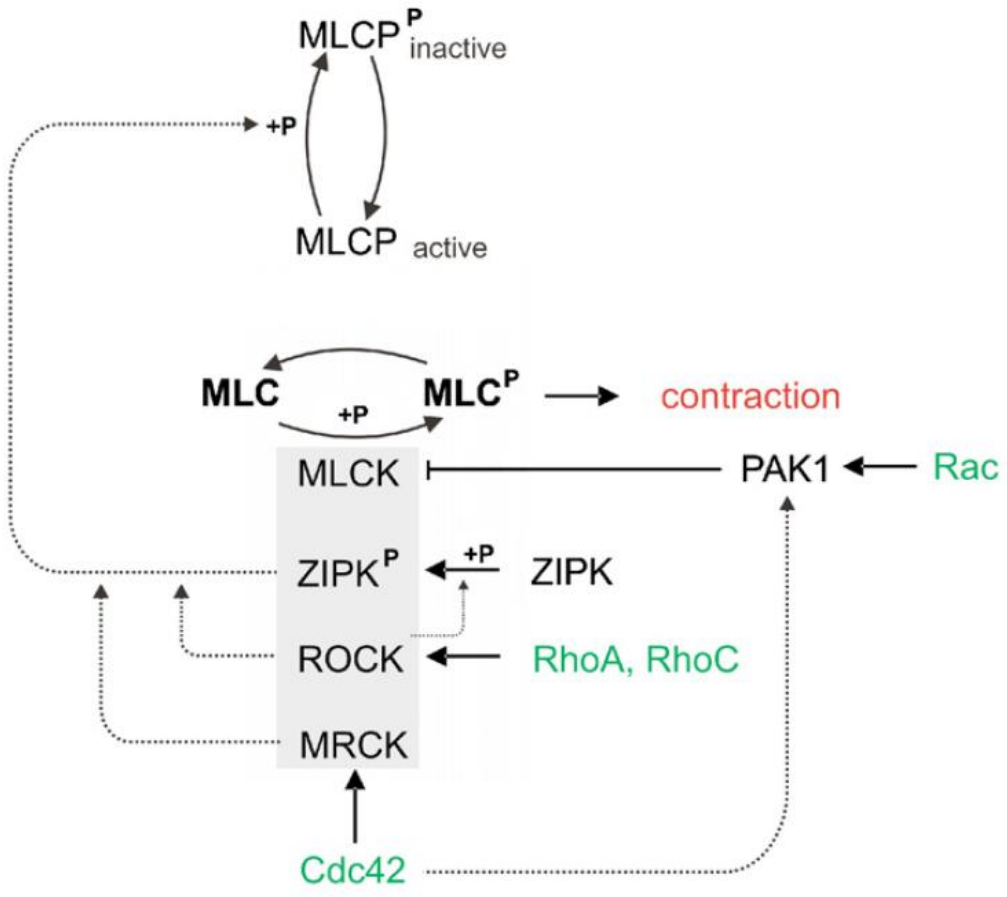

Figure 4.7. Regulation of myosin light chain phosphorylation (MLC) by small Rho GTPases. Phosphorylation of MLC results in increased contractility important for amoeboid invasion. Phosphorylation of MLC is mediated by MLCK, ROCK, MRCK, ZIPK that are regulated by small GTPases RhoA, RhoC, Cdc42 and Rac. Dephosphorylation is caused by MLCP activity.
(Adapted from Mierke C. T., Rösel D., Fabry B. and Brábek J. (2008). Contractile forces in tumor cell migration. Eur. J. Cell Biol. 87(8-9): 669-76).

The amoeboid movement of cells is partly dependent also on formation of spherical membrane protrusions called blebs, localized preferentially at the leading edge of the cell (Keller and Eggli, 1998). Blebbing of cells is regulated by ROCK kinase and myosin contractility (Coleman et al., 2001; Paluch et al., 2005), but it is not mediated by actin polymerization. Rather, blebs are formed by hydrostatic pressure-driven inflow of cytoplasm into sites under the membrane, where actomyosin cortex was either disrupted (Keller and Eggli, 1998) or detached from the membrane (Cunningham, 1995). Local differences in actomyosin contractility can lead to local differences in the pressure towards the membrane (Lecuit and Lenne, 2007) and so hydrostatic pressure pushes cytoplasm in the direction of cortex disruption (Yanai et al., 1996). In the formed bleb, actomyosin network is renewed (Cunningham, 1995; Charras et al., 2006) and by its contractility can lead to the bleb retraction. Bleb can be also stabilized by ERM proteins

(Sahai and Marshall, 2003), predominantly by ezrin (Charras et al., 2006). It is noteworthy, therefore, that also cortical actin is attached to the plasma membrane through ERM proteins (ezrin / radixin / moesin) (Bretscher et al., 2002; Niggli and Rossy, 2008). ERM proteins can be phosphorylated and subsequently activated by ROCK (Bretscher et al., 2002), PKCα and NIK kinase (Niggli and Rossy, 2008) and the localization of ezrin is regulated by RhoA (Yonemura et al., 2002).

Amoeboid cells do not form stable focal adhesions and their integrins are diffusely localized throughout the membrane. Amoeboid cells show reduced requirement for the cell – ECM contacts comparing to mesenchymal cells (Carragher et al., 2006; Wolf et al., 2003; Friedl et al., 1998). Primary amoeboid melanoma cells were shown to migrate independently of β1 integrins (Hegerfeldt et al., 2002). Consistently, HT-1080 cells after mesenchymal – amoeboid transition (MAT) lost their integrin clusters (Wolf et al., 2003). However, presumably, amoeboid cells utilize different types of ECM-contact molecules, maybe other types of glycoproteins (Schmidt and Friedl, 2010). Recently, NG2 chondroitin sulfate glycoprotein was identified as a possible non-integrin ECM receptor of amoeboid cells (Paňková et al., 2012).
Because of the short-lived and relatively weak interactions of cells with the ECM, amoeboid cells can migrate more quickly than mesenchymal cells. Migration velocity can vary from 2 μm/min (observed in A375m2 melanoma cells) (Sahai and Marshall, 2003) to 25 μm/min (lymphocyte migration) (Friedl et al., 1994).

Actually, two types of amoeboid invasion can be distinguished (Mierke et al., 2008) – first, the cells that squeeze through pre-existing gaps in ECM and show very high deformability (Friedl et al., 1998, 2001; Sahai and Marshall, 2003; Wolf et al., 2003) and second, the cells that are able to generate force to structurally remodel ECM fibers to make a path for their movement (Wyckoff et al., 2006; Rösel et al., 2008; Provenzano et al., 2006, 2008). First type was observed in HT-1080 fibrosarcoma cells upon protease inhibitor cocktail treatment that convert their invasion from mesenchymal to amoeboid (Wolf et al., 2003). These cells align their bodies according to collagen fibers, form pseudopodia to get into gaps between ECM fibers and then constrict their body to squeeze through (Wolf et al., 2003). Second type was observed in primarily amoeboid MTLn3E breast carcinoma cells (Wyckoff et al., 2006; Rösel et al., 2008). These amoeboid cells localize their ROCK-mediated contractile acto-myosin force together

with cell-matrix adhesions towards the leading edge of the cell and therefore are able to push away collagen fibers at the front of the cell to make space for cell translocation (Wyckoff et al., 2006). This invasion mechanism also leads to the re-organization of collagen fibers from parallel to perpendicular orientation and this can stimulate local invasion of also other cancer cells (Provenzano et al., 2006, 2008).

4.3 Mesenchymal vs. amoeboid invasion

Characteristic	Mesenchymal invasion	Amoeboid invasion
Shape	Elongated, polarized	Rounded
Membrane protrusions	Pseudopodia, lamellipodia, filopodia	Blebs
Adhesion	Strong, β integrin clusters	Weak, β integrins diffusely
Actin cytoskeleton	Stress fibers	Actomyosin cortex
Signalization	Rac	Rho/ROCK
Movement through	ECM degradation	Actomyosin contraction – morphological adaptation
Velocity	0.1 – 1 μm/min	2 – 25 μm/min

Figure 4.7. Comparison between key characteristics of mesenchymal and amoeboid modes of cancer cell invasion.
(Adapted from Kasalová (2010). In vitro analysis of amoeboid-mesenchymal transitionof A375m2 melanoma cells. Charles University in Prague, diploma thesis).

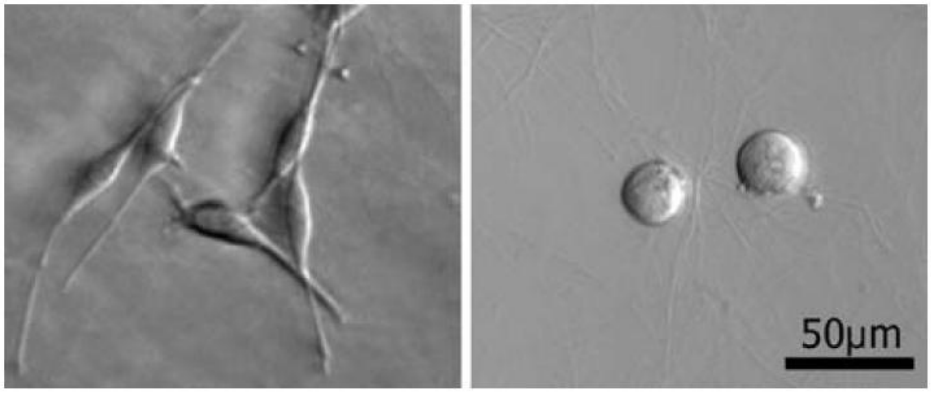

Figure 4.8. Microscopic pictures of typical mesenchymal (left panel) and amoeboid (right panel) morphology of cancer cells.
(Adapted from Paňková K., Rösel D., Novotný M. and Brábek J. (2010). The molecular mechanisms of transition between mesenchymal and amoeboid invasiveness in tumor cells. Cll Mol Life Sci 67:63-71).

4.4 Mesenchymal – amoeboid transition (MAT) and amoeboid – mesenchymal transition (AMT)

Cancer cell invasion is very complex and plastic process and mesenchymal and amoeboid modes of invasion are mutually interchangeable. Activation or inhibition of specific signaling cascades leading to specific mode of invasion can cause a switch from one invasion mode to another (reviewed in Paňková et al., 2010; Friedl, 2004; Sanz-Moreno and Marshall, 2010, Friedl and Wolf, 2009) (Figure 4.9).

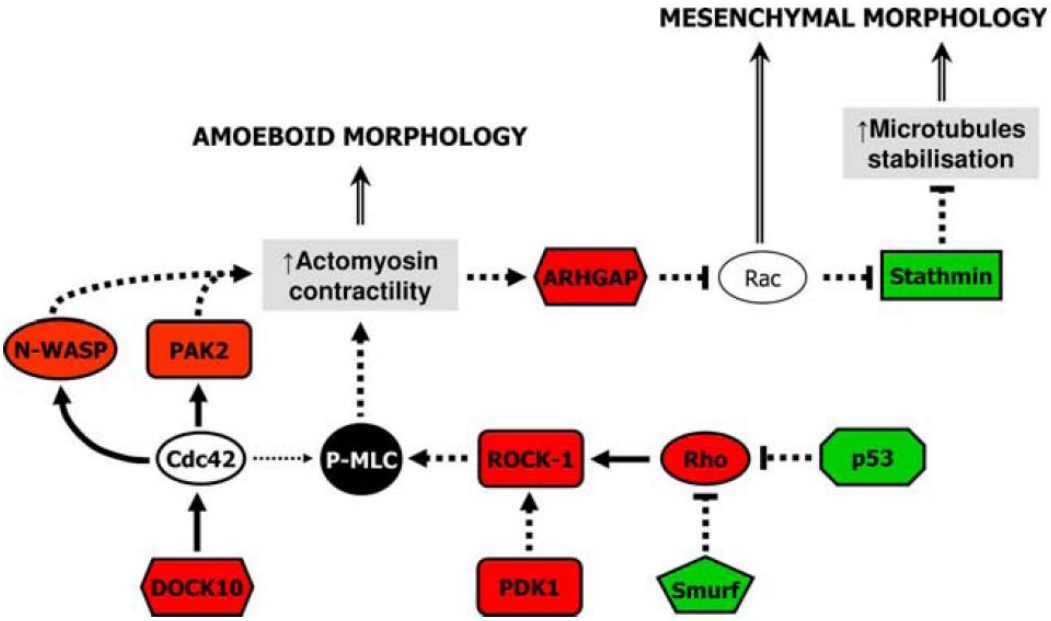

Figure 4.9. Important proteins regulating mesenchymal-amoeboid transition or amoeboid-mesenchymal transition. Inhibition of proteins marked red leads to amoeboid-mesenchymal transition. Inhibition of proteins marked green results in mesenchymal-amoeboid transition. For further explanation, see text.
(Adapted from Paňková K., Rösel D., Novotný M. and Brábek J. (2010). The molecular mechanisms of transition between mesenchymal and amoeboid invasiveness in tumor cells. Cell. Mol. Life Sci. 67:63-71).

Therefore, mechanisms as mesenchymal – amoeboid transition (MAT) or amoeboid – mesenchymal transition (AMT) were observed. Unlike epithelial – mesenchymal transition (EMT) (the process of changing invasion from collective mode to mesenchymal), that is accompanied by wide changes in gene transcription, MAT and AMT are very quick processes, sometimes lasting just a few minutes. It is remarkable, that cell invasion also depends on characteristics of surrounding tissue and ECM and

migrating cells can adjust themselves to specific conditions of environment. Therefore, MAT and AMT can be also seen as the escape mechanisms if one mode of invasion is blocked.

4.4.1 Acto-myosin contractility changes mediating MAT/AMT

As stated previously, Rho/ROCK signalization is critical for amoeboid invasion of cancer cells (Figure 4.10). Inhibiting of this signaling cascade in amoeboid cells that resulted in mesenchymal phenotype was the first identified mechanism of AMT (Sahai and Marshall, 2003). Rho inactivation, as well as ROCK inactivation, in A375m2 melanoma cells leads to transition to mesenchymal mode of invasion (Sahai and Marshall, 2003).

The other way around, activation of both RhoA and ROCK results in MAT (Sahai and Marshall, 2003). Constitutively active ROCK leads to cortical contraction, cell rounding, blebs formation in 3T3 fibroblasts and HT-1080 fibrosarcoma cells (Sahai and Marshall, 2003). Interestingly, in some other cell types, ROCK activation also stabilizes stress fibers and causes cell spreading, flattening and loss of motility (Nobes and Hall, 1999). Therefore, probably also additional factors are needed to cooperate with Rho/ROCK signaling pathway in amoeboid invasion (Friedl, 2004).

Obviously, activation or inhibition of important regulators of Rho/ROCK pathway also influences AMT/MAT (Figure 4.10).

3-phosphoinositide-dependent protein kinase 1 (PDK1) is one of these proteins. In amoeboid cells, PDK1 activates ROCK1-mediated acto-myosin contractility by correct ROCK1 localization to the plasma membrane (Pinner and Sahai, 2008). This function is independent of PDK1 kinase activity, rather, PDK1 competes with RhoE that prevents ROCK1 localization to the plasma membrane (Pinner and Sahai, 2008). Lowering of PKD1 expression in A375m2, MTLn3 and BE amoeboid cells leads to actin cortex disruption, mesenchymal morphology and decreased motility (Pinner and Sahai, 2008). ROCK1 localization to the membrane is also regulated by RhoA, however, RhoA is not sufficient for correct ROCK1 localization (Pinner and Sahai, 2008).

Rho/ROCK signalization has in amoeboid cells also negative effect on one of the mesenchymal features – Rac-mediated formation of lamellipodia. Rho/ROCK pathway leads to activation of ARHGAP22 that is Rac-specific GAP (guanine nucleotide

triphosphatase - activating protein). So, inhibition of ARHGAP22 leads to increased presence of elongated cells with MLC decreased levels (Sanz-Moreno et al., 2008).

Cdc42 is also partly important for amoeboid type of invasion of A375m2 cells (Gadea et al., 2008). Inhibition of Cdc42 upstream regulator DOCK10 leads to lower MLC phosphorylation, higher Rac1 activity and consequently, to AMT (Gadea et al., 2008). Inhibition of Cdc42 downstream effectors N-WASP and PAK2 results in mesenchymal shape of the cells, nonetheless, only inhibition of PAK2 leads to decreased MLC phosphorylation (Gadea et al., 2008). As Cdc42 is essential protein for cell migration, depletion of Cdc42 results in non-motile cells (Gadea et al., 2008).
Cdc42 also regulates MRCK that subsequently phosphorylates MLC. However, because MLC phosphorylation is mostly dependent on ROCK activation, inhibition of MRCK has only a mild effect on A375m2 cells (Wilkinson et al., 2005).

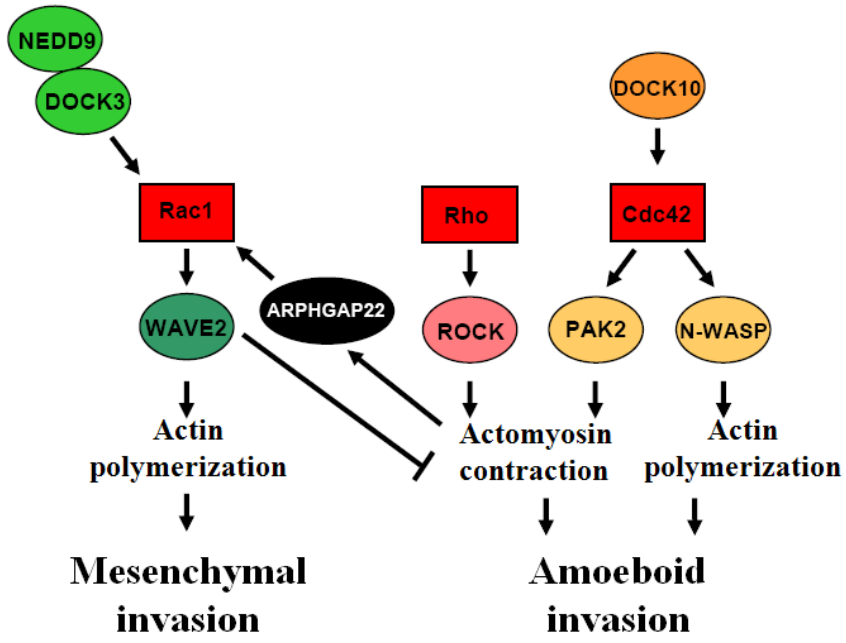

Figure 4.10. Small Rho GTPases regulating mesenchymal-amoeboid transition or amoeboid-mesenchymal transition. Small GTPases Rac1, Rho and Cdc42 control acto-myosin contraction and actin polymerization (resulting in membrane protrusions formation) that are essential for cell invasion. Their upstream regulators and downstream effectors are important signaling proteins through which mesenchymal and amoeboid modes of invasion can be controlled. For further information, see text.
(Adapted from Kasalová (2010). In vitro analysis of amoeboid-mesenchymal transition of A375m2 melanoma cells. Charles University in Prague, diploma thesis).

4.4.2 Role of cell polarization and formation of protrusions in MAT/AMT

Rac is very important GTPase for mesenchymal invasion, as it regulates lamellipodia and pseudopodia formation (Ridley et al., 1992; Miki et al., 1998; Bosco et al., 2009).
Rac inactivation therefore leads to MAT both in 2D and in 3D environment (Sanz-Moreno et al., 2008; Yamazaki et al., 2009). Nevertheless, the result of Rac inhibition depends on the cell type. In primarily mesenchymal MEF cells and U87M6 glioblastoma cells Rac1 inactivation results in loss of invasiveness (Guo et al., 2006; Yamazaki et al., 2009). In contrast, in HT-1080 fibrosarcoma cells and A375P, Rac inhibition causes MAT with rounded morphology and increased MLC phosphorylation levels (Sanz-Moreno et al., 2008; Yamazaki et al., 2009). Inactivation of Rac regulatory proteins - DOCK3 (Rac guanine nucleotide exchange factor (GEF)) or NEDD9 (adaptor protein interacting with DOCK3) leads to rounded morphology as well (Sanz-Moreno et al., 2008). The other way around, expression of constitutively active Rac GTPase (Rac1 Q61L) in A375m2 melanoma cells leads to elongated shape of the cells on top of the thick collagen (Sanz-Moreno et al., 2008). However, in 3D environment, this change was not observed yet.
Rac1 also regulates focal adhesions and stress fibers formation (Guo et al., 2006). Furthermore, WAVE2 is Rac effector that suppresses MLC2 phosphorylation and decreases cell contractility (Sanz-Moreno et al., 2008). Pseudopodia formation is also regulated by Rac through WAVE2/Arp2/3 complex. So, depletion of WAVE2 or Arp2/3 complex in HT-1080 fibrosarcoma cells results in MAT (Yamazaki et al., 2009).

In mesenchymal cells to form protrusions at the leading edge, local inhibition of cell contractility is needed. Decrease in RhoA level at these sites is kept by E3 ubiquitin ligase Smurf1 that mediates proteolytic degradation of RhoA (Wang et al., 2006). Accordingly, inactivation of Smurf1 leads to blebs formation and RhoA accumulation in these sites, as well as cortical localization of actin, peripheral localization of ROCK and increase in MLC phosphorylation. Inhibition of Smurf1 is enough to promote MAT of BE colon carcinoma cells (Sahai et al., 2007).

Cdc42 is another GTPase regulating mesenchymal invasion as it regulates filopodia formation. In mouse embryonic fibroblasts, this process can be inhibited by p53 (tumor suppressor transcription factor) that probably acts downstream of Cdc42 (Gadea et al., 2002). For that reason, depletion of p53 causes rounded morphology, increased RhoA activity and membrane blebbing (Gadea et al., 2007). p53 also regulates β1 integrin and ezrin distribution (Gadea et al., 2007), that are proteins participating in cell polarization (Sahai and Marshall, 2003). The effector of p53 could be RhoE as it is one of transcription targets of p53 during genotoxic stress (Gadea et al., 2007). RhoE binds to ROCK and blocks it kinase activity at the plasma membrane (Riento et al., 2003).

Cdc42 is also needed for cell polarity of fibroblasts that is determined by microtubules (MT) (Cau and Hall, 2005). MT dynamics is important for adhesion, migration and cell shape.

The MT-destabilizing factor stathmin 1 (Curmi et al., 1999) stimulates cell migration *in vitro* and increases metastatic potential (Belletti et al., 2008). Stathmin is negatively regulated by phosphorylation (Curmi et al., 1999). After interaction of cell with ECM, stathmin is phosphorylated (Belletti et al., 2008) and MTs are stabilized (Palazzo et al., 2004). Non-phosphorylable mutant of stathmin disrupts MT stability and enhances migration of mesenchymal HT-1080 fibrosarcoma cells which was associated with rounded morphology of cells, suggesting MAT (Belletti et al., 2008). However, MAT caused by activated stathmin was not confirmed by manifestation of any other amoeboid features in these cells (Belletti et al., 2008).

Also in amoeboid-like migration of neutrophils, MT destabilization causes enhanced motility connected with ROCK activation and increased MLC2 phosphorylation levels (Niggli et al., 2003).

MTs stability and cell-matrix adhesion can be also regulated by p27 protein. p27 is cyklin-dependent kinases (CDK) inhibitor, but also plays role in both modes of invasion. Deletion of p27 results in rounded morphology of Src-transformed fibroblasts that is accompanied by cortical actin formation, loss of β1 integrin clusters and translocation of MTs (Berton et al., 2009). In mesenchymal cells, p27 binds stathmin, causes its inhibition and therefore stabilizes MTs (Baldassarre et al., 2005). In amoeboid cells, p27 regulates Rho signalization, exact mechanism is not known (Berton et al., 2009; Besson et al., 2004).

LIM kinase 1 (LIMK1) is important regulator of actin cytoskeleton through regulation of cofilin. LIMK1 phosphorylates cofilin of Ser3 and prevents its actin-degradation function (Yang et al., 1998). In amoeboid cells, LIMK1 can therefore stabilize acto-myosin structure of blebs (Mishima et al., 2010). In mesenchymal cells, LIMK1 can regulate Rac-dependent lamellipodia formation (Nishita et al., 2005).

LIMK1 is activated upon protease inhibitors treatment or ROCK1 inhibitor in HT-1080 fibrosarcoma cells (Mishima et al., 2010). ROCK1 phosphorylates and activates LIMK1 (Maekawa et al., 1999). Moreover, decrease in cofilin levels in MTLn3 cells leads to mesenchymal morphology (Sidani et al., 2007) and correlates with decreased metastatic potential of cells (Mouneimne et al., 2006; Sidani et al., 2007).

Direct interaction of ROCK1 with LIMK2 was observed in MDA-MB-231 breast cancer cells (Shea et al., 2008). In this context, this complex regulate mesenchymal invasion by stabilizing acto-myosin fibers through cofilin inactivation (Shea et al., 2008).

4.4.3 Proteolytic remodeling of the ECM influencing MAT/AMT

Mesenchymal cells express and membrane-target or secrete proteolytic enzymes such as matrix metalloproteinases (MMPs), cathepsins and serine proteases to cleave ECM fibers and invade surrounding tissue. Matrix metalloproteinases (MMPs) and cathepsins degrade mostly collagen fibers, the main component of connective tissue (Montcourrier et al., 1990; Aimes and Quigley et al., 1995). Proteases are also able to cleave substrates used in *in vitro* experiments – matrigel, gelatin, fibronectin (Nakahara et al., 1997; d'Ortho et al., 1998).

However, upon treatment with protease inhibitor cocktail in mesenchymal cells, proteolysis-independent mechanism of invasion occurred (Wolf et al., 2003; Wyckoff et al., 2006; Carragher et al., 2006). This mode of invasion was associated with all the features of amoeboid invasion – rounded shape of cells, diffuse integrins in the plasma membrane, dependence on acto-myosin contractility (Wolf et al., 2003; Wyckoff et al., 2006; Carragher et al., 2006). Proteolysis inhibition of HT-1080 fibrosarcoma cells was also connected to decreased surface expression of α2β1 integrins and a lower lever of phosphorylated FAK, suggesting lower need for focal adhesion contacts (Carragher et al., 2006).

The failure of matrix metalloproteinase inhibitors in clinical trials suggests that mesenchymal-amoeboid transition could be possible escape mechanism of invading cancer cells (Ramnath and Creaven, 2004).

Nevertheless, Sabeh et al., (2009) argued that amoeboid invasion is not very efficient process *in vivo*, because it can occur only under specific conditions. They state that amoeboid invasion was studied mostly on artificial 3D ECM constructs that lack covalent cross-links typical for normal tissues. To prove their presumption, they studied invasion of HT-1080 fibrosarcoma and MDA-MB-231 breast cancer cells in matrices that either had or did not have these cross-links. They found out that cells invaded more efficiently in matrices without cross-links and therefore claimed that amoeboid invasion can be used only if structural pores in collagen are not stabilized by covalent cross-links (Sabeh et al., 2009). However, in their study, they did not use primarily amoeboid cells that can be fully adapted for amoeboid invasion and could overcome also this kind of barrier. So, it would be interesting to evaluate also invasiveness of primarily amoeboid cells (such as A311 sarcoma cells) in both types of matrices to prove or falsify this hypothesis (Paňková et al., 2010).

4.4.4 Cell-cell and cell-matrix adhesive interactions that mediate MAT/AMT

Signalization through β1 integrins is essential for mesenchymal invasion and inhibition of β1 integrins in mesenchymal cells leads to loss of adhesion and following MAT (Maaser et al., 1999; Friedl et al., 2004) as amoeboid invasion was thought to be β1 integrin-independent (Hegerfeldt et al., 2002).

However, this is not always the case, as depletion of β1 integrins in HT-1080 fibrosarcoma cells was not sufficient for MAT induction, rather it resulted in the loss of motility, not in MAT (Carragher et al., 2006).

Although intracellular pathways regulating invasion are being studied very extensively, very little is known about extra-cellular signals and their receptors.

Receptor tyrosine kinase signaling is mainly responsible for Rac-mediated mesenchymal signaling. Surprisingly, EphA2 receptor tyrosine kinase seems to be important for amoeboid movement. There was shown increased level of EphA2 in aggressive melanoma cells (Kinch and Carles-Kinch, 2003). EphA2 re-expression and

activation in little metastatic melanoma cells F10-M3 leads to increased invasivity and MAT (Parri et al., 2009). Activation of EphA2 results in Src-FAK activation that afterwards leads to RhoA-mediated acto-myosin contractility (Parri et al., 2007, 2009). Moreover, EphA2 activation mediates Rac1 inhibition (Parri et al., 2009) as well as to integrin signalization inactivation (Miao et al., 2000).

Another receptor involved in invasion is neuropilin 1 (NRP1). NRP1 is receptor for semaphorins (He et al., 1997) and vascular endothelial growth factor (VEGF) (Soker et al., 1998). Posttranslational modification by chondroitin sulphate on Ser612 of NRP1 determines invasive character of migrating cells (Frankel et al., 2008). Mutation in Ser612 results in increased invasivity of glioma cells and increased level of p130Cas phosphorylation (Frankel et al., 2008). Inhibition of p130Cas in these cells causes MAT (Frankel et al., 2008).

Also other adaptor proteins connected to tyrosine kinase signaling such as NEDD9, Crk and Crk-L are involved in regulation of mesenchymal invasion (Sanz-Moreno et al., 2008, Kiyokawa et al., 1998). These proteins are linked to Src signaling that is essential for mesenchymal invasion (Carragher et al., 2006).

4.4.5 Properties of the ECM influencing MAT/AMT

Cell invasion is dependent on fiber network morphology and other features of ECM (reviewed in Brábek et al., 2010). If the cross-section of the mesenchymal cell matches the mesh size, there is no steric hindrance and cell can efficiently migrate through. If the gaps are too big, cell looses cell-ECM attachments and cell velocity is lower (Harley et al., 2008). Interestingly, large mesh sizes enable cells to migrate using amoeboid mode (Brábek et al., 2010). However, if there is only small amount of fibers, cell must switch into "1D" mode of migration (Doyle et al., 2009). The other way around, if the mesh size is too small, migration velocity decreases and cell might get stuck inside (Harley et al., 2008). Cell deformability depends mostly on the rigidity of nucleus, regulated by nuclear lamins A/C (Pajerowski et al., 2007; Dahl et al., 2008). But cells can overcome this situation, either by pushing fibers apart or by proteolytic degradation of ECM (Friedl and Wolf, 2010).

It is very important that cells can sense ECM mechanical properties and can adapt themselves. This mechano-sensing is mediated by integrin-based adhesions and adaptor proteins such as vinculin, talin, FAK and p130Cas (Brábek et al., 2010).

In response to increased stiffness, cell can strengthen focal adhesions, form pseudopodia and increase its protrusive force that is connected to mesenchymal mode of invasion (Peyton et al., 2008). On the contrary, soft matrix supports cell rounding and amoeboid morphology (Ulrich et al, 2009). Consequently, tissue stiffness can direct cell movement towards sites with higher rigidity in a process called durotaxis (Lo et al., 2000).

Also spatial organization of ECM fibers can influence cell invasion mode (Provenzano et al., 2008). To mimic tissue invasion of MDA-MB-231 cells from primary tumor, cells were cultured in high density in 3D collagen and then piece of this gel was transferred in fresh, isotropic gel. In this case, cells migrated in amoeboid way (Provenzano et al., 2008). When the gel was inserted into anisotropic gel with aligned collagen fibers and stiffer gel, cells migrated mesenchymally (Provenzano et al., 2008).

Human macrophage mode of migration is also dependent on ECM architecture. Macrophages migrate amoeboidly in fibrillate collagen I, although in Matrigel and gelled collagen they used mesenchymal migration (Van Goethem et al., 2010). Macrophage migration depended on tissue stiffness too (Van Goethem et al., 2010).

4.5 Protein kinase C α (PKCα)

Protein kinase C α (PKCα) is a calcium and phospholipid dependent serine/threonine protein kinase belonging to the group of conventional (classical) protein kinases C (cPKCs). PKCα is widely expressed in all tissues and plays essential role in signal transduction. PKCα regulates cell proliferation, differentiation, apoptosis, secretion, polarity, adhesion, migration and cancer progression.

The role of PKCα in tumorigenesis is controversial, as the level of expression and its function depend on tumor cell type. Overexpression of PKCα was found in prostate cancer, endometrial cancer, urinary bladder cancer and hepatocellular carcinoma. However, in colon cancer, lower expression was detected. Inconclusive results were obtained in hematological malignancies and breast carcinoma, where both higher and lower expression of PKCα was observed (Martiny-Baron and Fabbro, 2007).

More importantly, PKCα also plays essential role in cell migration. The activation of PKCα is connected to increased migration and invasivity of cells in several *in vitro* and *in vivo* models. Inhibition of PKCα in these models resulted in decreased migration and invasivity. However, mechanisms of PKCα-mediated invasion remain unclear.

4.5.1 Family of protein kinases C (PKCs)

Protein kinases C (PKCs) are enzymes belonging to the AGC kinases that catalyze covalent transfer of phosphate from ATP to serine or threonine residues on proteins. Phosphorylation of target protein usually results in a conformational change of protein and subsequent alteration of its function.

Family of PKCs was discovered in 1977 by Inoue and coworkers (Inoue et al., 1977) and then identified by Takai and coworkers as an enzyme activated by Ca^{2+} and diacylglycerol (DAG) (Takai et al., 1979).

Family of PKCs evolved from one PKC in *Saccharomyces cerevisiae* (PKC1) (Watanabe et al., 1994). In mammals this family consists of at least ten members and is divided into 3 groups according to their structure from which arises their regulation by cofactors. There are classical (conventional) PKCs (cPKCs) (α, βI, βII, γ), novel PKCs (nPKCs) (δ, ε, η, θ) and atypical PKCs (aPKCs) (ζ, τ/λ).

Every isoform has different cofactor requirements, cell compartmentalization and tissue distribution. This suggests specific function and specific signaling cascades that it takes part in for every isoform. PKCs can be activated by range of different extracellular stimuli and in response, regulate activities of many cellular proteins such as receptors, enzymes, cytoskeletal proteins and transcription factors. On that account, PKCs are essential in cellular signal processing (Breitkreutz et al., 2007).

As cPKCs are activated by Ca^{2+} and DAG, PKCs act rapidly downstream of phospholipase C γ (PLCγ) or more slowly of phospholipase D (PLD) that are activated by G protein-coupled receptors, receptor tyrosine kinases and non-receptor tyrosine kinases (Newton, 1995; Martiny-Baron and Fabbro, 2007). Moreover, PKCs were identified as major intracellular receptors of tumor promoting phorbol esters, suggesting the role of PKCs in cell transformation and carcinogenesis (Castagna et al., 1982). As phorbol esters such as phorbol 12-myristate 13-acetate (PMA) are not readily metabolized, short term exposure to phorbol ester leads to prolonged PKC activation

(Newton, 1995). However, long term treatment results in enhanced PKC degradation and consequently to lowering of PKC activity (Martiny-Baron and Fabbro, 2007). All PKCs also require phosphatidylserine (PtdSer) for their activation (Newton, 1995).

4.5.2 Structure of PKCα

PKCα belongs to the group of conventional PKC (cPKC). It consists of N-terminal regulatory domain and C-terminal kinase domain that are connected through hinge region. It can be also divided into four conserved (C1 – C4) and five variable (V1 – V5) regions (reviewed in Freeley et al., 2010, Newton, 2010) (Figure 4.11).

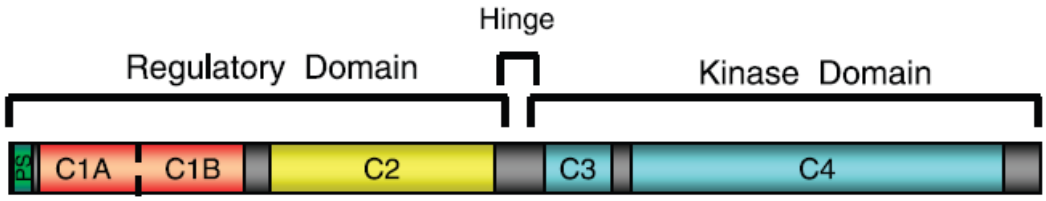

Figure 4.11. Domain structure of PKCα. N – terminal regulation domain contains pseudosubstrate sequence, C1A and C1B domains and C2 domain. C – terminal catalytic domain contains C3 and C4 conserved regions. These two domains are linked by hinge region. (Adapted from Steinberg (2008). Structural basis of Protein kinase C isoform function. Physiol Rev 88: 1341-1378).

4.5.2.1 Regulation domain of PKCα

N-terminal regulatory domain contains V1, C1, V2 and C2 regions.

In the most N-terminal region, there is an autoinhibitory pseudosubstrate sequence (PS). This sequence closely resembles substrate recognition motif except that serine/threonine residue is replaced by alanine (House and Kemp, 1987). In the absence of cofactors and activators, it occupies substrate-binding pocket and keeps enzyme in its inactive state (Orr et al., 1992; Orr and Newton, 1994).

PKCα contains tandem C1 domains (C1A and C1B) (Figure 4.12) that are able to bind DAG through its Cys-rich motif. This small globular domain is also binding site for phorbol esters (Hurley et al., 2006; Zhang et al., 1995), which bind competitively to DAG (Sharkey et al., 1984). C1 domain also stereospecifically binds to anionic lipid PtdSer (Johnson et al., 2000).

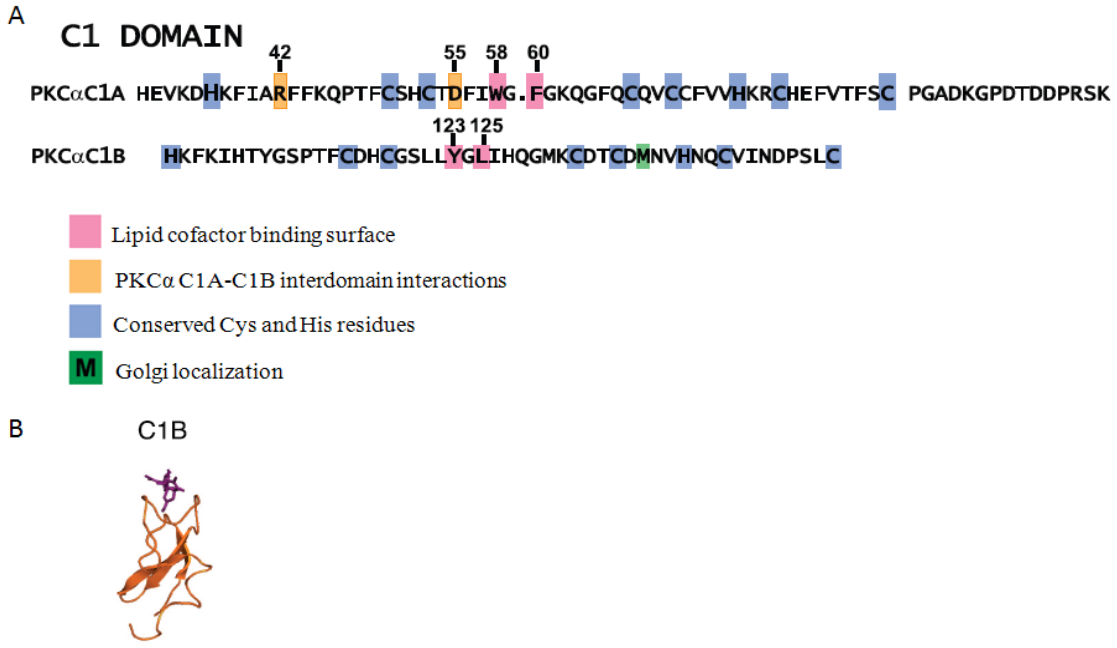

Figure 4.12. C1 region of PKCα.
A) Sequence of C1A and C1B domains of PKCα.
B) Ribbon structure of PKC C1B domain.
(Adapted from Steinberg (2008). Structural basis of Protein kinase C isoform function. Physiol Rev 88: 1341-1378).

C2 domain is responsible for Ca^{2+} dependent phospholipid binding (Figure 4.13). This domain forms four antiparallel β sheets and Ca^{2+} binding changes original negative charge in the site of membrane binding, so that the electrostatical interactions can be formed with phospholipids (Lemmon, 2008; Nalefski et al., 2001). It binds anionic phospholipids with little but not stereospecific preference for PtdSer (Cho and Stahelin, 2006; Conesa-Zamora et al., 2001). Importantly, it has bigger selectivity for phosphatidylinositol-4,5-bisphosphate (PIP_2) binding and this interaction targets PKCα to the plasma membrane (Corbalan-Garcia et al., 2007; Evans et al., 2006).

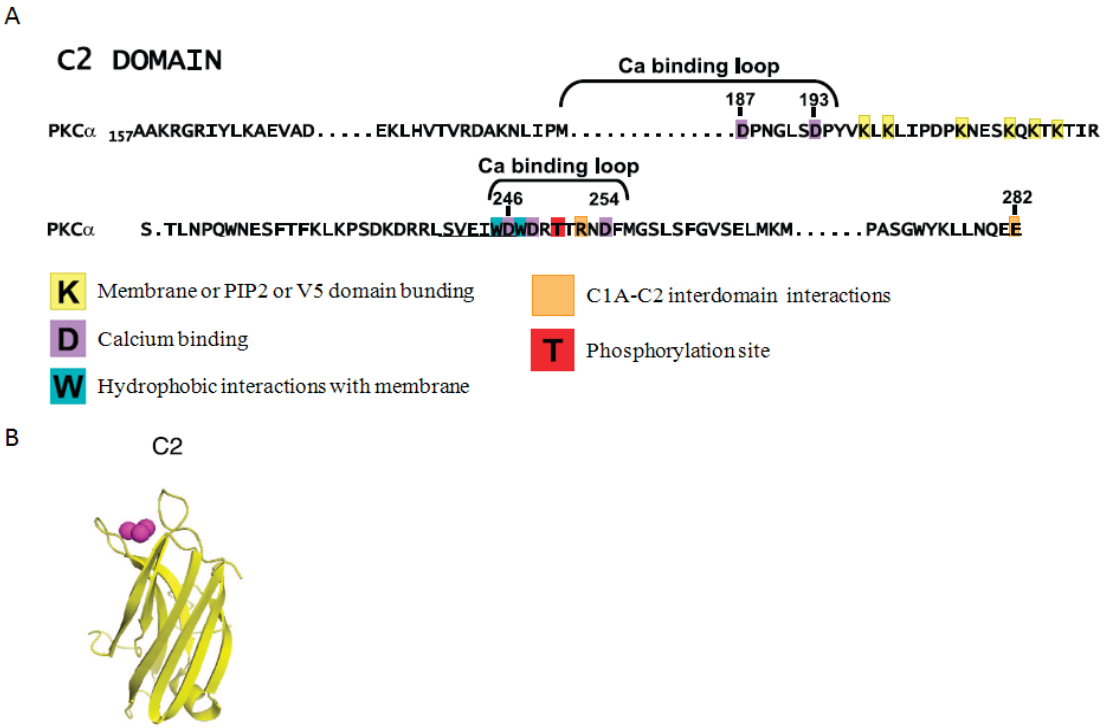

Figure 4.13. C2 region of PKCα.
A) Sequence of C2 domain of PKCα.
B) Ribbon structure of PKC C2 domain.
(Adapted from Steinberg (2008). Structural basis of Protein kinase C isoform function. Physiol Rev 88: 1341-1378).

4.5.2.2 Hinge region (V3 region) of PKCα

Hinge region (V3) connects regulation domain to the catalytic domain. When PKCα is bound to the membrane, hinge region can become proteolytically labile by Ca^{2+} dependent calpains (Kishimoto et al., 1989), caspases (Datta et al., 1997; Emoto et al., 1995) or trypsin (Orr and Newton, 1994). This cleavage produces kinase domain fragment also called protein kinase M (PKM) that is constitutively active also in absence of any lipid cofactors (Kishimoto et al., 1983).

4.5.2.3 Catalytic domain of PKCα

Catalytic kinase domain contains C3, C4, V4 and V5 regions (Figure 4.14).

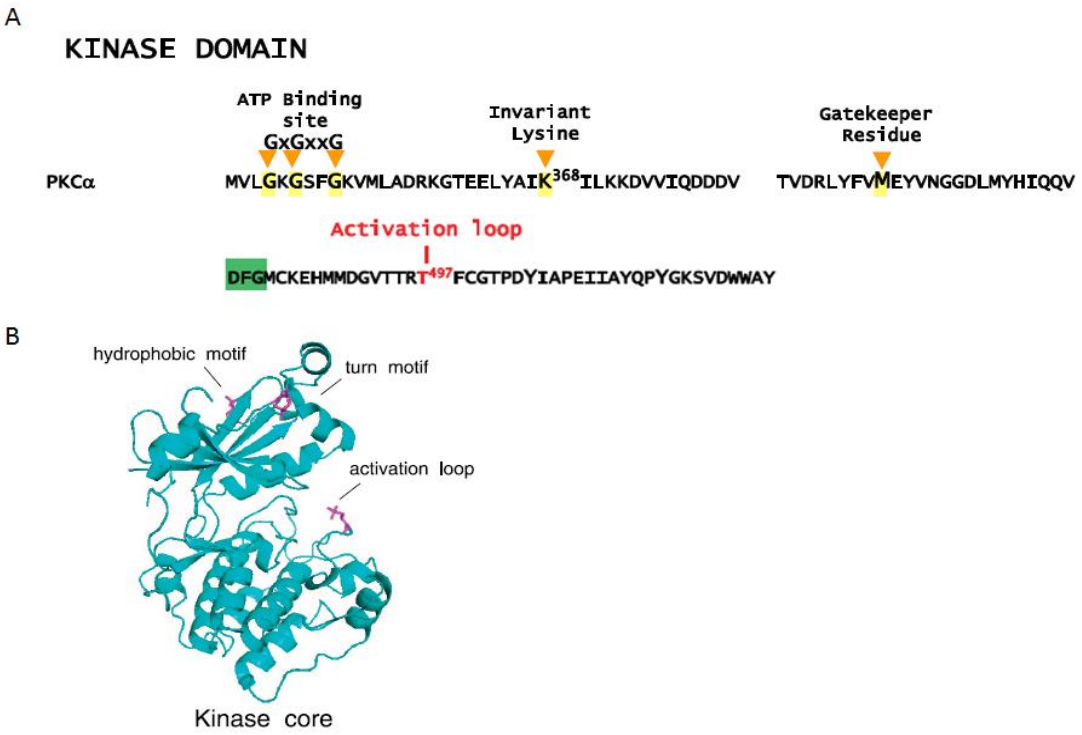

Figure 4.14. Kinase domain of PKCα.
A) Sequence of kinase domain of PKCα.
B) Ribbon structure of PKC kinase core.
(Adapted from Steinberg (2008). Structural basis of Protein kinase C isoform function. Physiol Rev 88: 1341-1378).

In C3 region, there is an essential ATP-binding site. It contains Gly-rich sequence that is characteristic ATP-binding motif (Coussens et al., 1986; Parker et al., 1986).

In C4 region, there is located substrate-binding cavity, but also very conserved structure, DFG motif that binds Mg^{2+}.

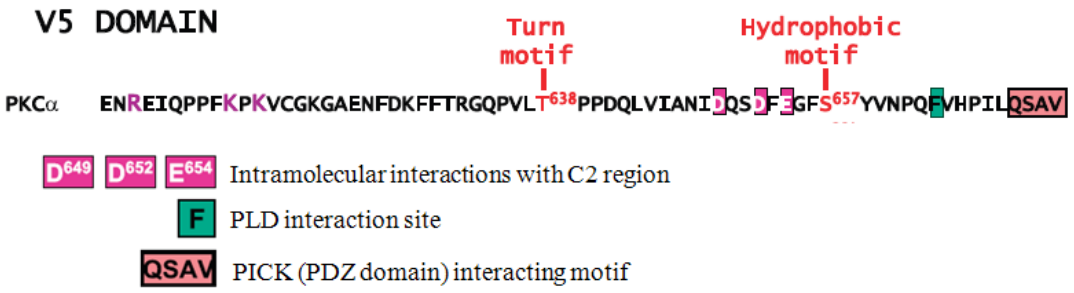

Figure 4.15. V5 region of PKCα. Sequence of V5 region of PKCα.
(Adapted from Steinberg (2008). Structural basis of Protein kinase C isoform function. Physiol Rev 88: 1341-1378).

On the most C-terminus, there is conserved carboxy-terminal tail (CT) (Figure 4.15). This site functions as phosphorylation dependent docking site for regulatory molecules and probably it is important for substrate specificity as well as for PKCα localization (Babwah et al., 2003; Newton, 2010).

4.5.3 Regulation of PKCα

PKCα is protein of 74 kDa in its inactive form and 80 kDa in its active form (Pears et al., 1992). PKCα is synthesized as an inactive precursor and after synthesis it has to be first maturated by three priming phosphorylations in kinase domain. These phosphorylations allow enzyme to adopt stable, closed conformation with pseudosubstrate occupying substrate-binding cavity. The enzyme is inactive, but signaling competent – it can be activated by lipid second messengers interaction and recruitment to the membrane. When PKCα is both phosphorylated and membrane-bound, it is fully activated and can finally phosphorylate its substrates (reviewed in Newton, 2010; Newton, 1995) (Figure 4.16).

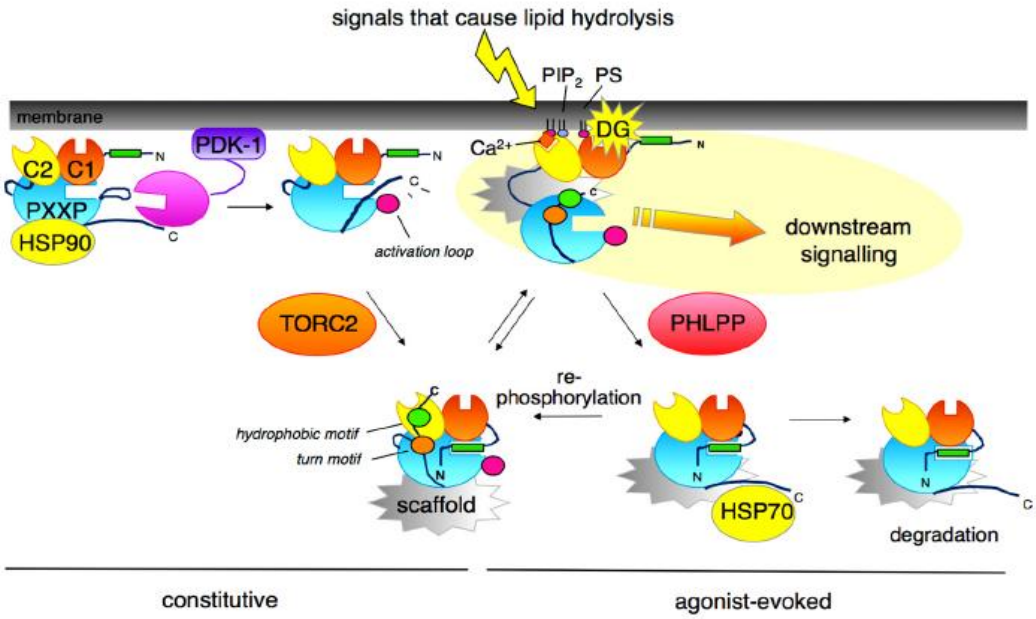

Figure 4.16. PKC regulation. After synthesis, PKCα is phosphorylated on three priming phosphorylation sites. In this state, enzyme localizes to the cytosol and is in its mature, but closed conformation with pseudosubstrate sequence bound to the substrate-binging cavity. Lipid hydrolysis upon specific signals recruits PKCα to the membrane. Membrane-bound conformation releases pseudosubstrate from substrate-binding site and in this open state, enzyme is catalytically active and can signal downstream. However, this open state can be easily dephosphorylated and subsequently degraded.
(Adapted from Newton (2010). Protein kinase C: poised to signal. Am J Physiol Endocrinol Metab 298: E395-E402).

4.5.3.1 Maturation of PKCα - regulation by priming phosphorylations

PKCα maturation is highly ordered process of serial tightly coupled phosphorylations leading to increased stability and catalytic competence of PKCα. There are three phosphorylation sites needed for PKCα maturation and all of them are located in the catalytic domain. These sites are known as the activation loop (A-loop) (Thr497), turn motif (TM) (Thr638) and hydrophobic motif (HM) (Ser657) (reviewed in Freeley et al., 2011; Newton, 2010).

However, first, chaperone HSP90 and co-chaperon Cdc37 have to bind to the PXXP clamp in CT region (Gould et al., 2008). The integrity of this motif and these interactions are necessary for the following phosphorylations events (Newton, 2010).

The first phosphorylation event is the phosphorylation of A-loop at Thr497 that is mediated by PDK1 (Chou et al., 1998; Dutil et al., 1998). Interestingly, it is independent of phosphoinositides. Rather, newly synthesized PKCα has open conformation where PS is relieved from substrate-binding site and therefore activation site is accessible for

phosphorylation (Dutil and Newton, 2000). This phosphorylation is necessary for correct alignment of active site, but also for other phosphorylations at CT (Cazaubon et al., 1994; Orr and Newton, 1994) and therefore for processing of enzyme into fully phosphorylated form (Newton, 2010). However, as soon as the other sites are phosphorylated, this phosphorylation becomes dispensable (Dutil and Newton, 2000) and only one half of the pool of PKC in cultured cells is phosphorylated at this site (Keranen et al., 1995). This phosphorylation is also important for enzyme stabilization by forming ionic interactions with positively-charged residues in the proximity of catalytic domain (Balendran et al., 2000).

Phosphorylation of turn motif (at Thr638) is dependent on mTORC2 complex (Facchinetti et al., 2008; Ikenoue et al., 2008). However, whether this is happening directly or indirectly is still not known. Notably, mTORC2 cannot phosphorylate this site *in vitro* (Ikenoue et al., 2008). This phosphorylation is important for stabilization of PKCα in its catalytically competent form by anchoring C-terminal tail on the upper lobe of the kinase (Hauge et al., 2007) rather than playing role in catalytic activity. Although mutation in this site has no effect on catalytic activity, it is more susceptible to proteolysis, dephosphorylation, oxidation or thermal instability (Bornancin and Parker, 1996).

PKCα can autophosphorylate itself on its HM *in vitro* (at Ser657) (Behn-Krappa and Newton, 1999). Whether this is also its *in vivo* regulation remains unclear as this motif can be phosphorylated also by other kinases *in vitro*, including mTORC2 complex (Ikenoue et al., 2008). For this site phosphorylation, also interaction of PXXP clamp with HSP90 is necessary – it both facilitates this phosphorylation event and helps to stabilize the enzyme (Gould et al., 2008). This phosphorylation is also important for protein stability because it closes its conformation and prevents the dephosphorylation by phosphatases (Gysin et al., 1996; Bornancin et al., 1997).

Phosphorylation on these sites does not actually correlate with catalytic activation of the kinase, rather, it correlates with closed enzyme conformation (Freeley et al., 2011).

Besides these three priming phosphorylations, there were identified also other non-conserved phosphorylation sites on PKCα.

Phosphorylation on Thr250 in the C2 domain was observed upon treatment with phorbol esters (Ng et al., 1999), but also as result of cells adhering to fibronectin (Anilkumar et al., 2003). PKCα autophosphorylates on Thr250 itself, so it can be used as marker of PKCα activity (Ng et al., 1999). Under specific conditions also phosphorylation on Thr209 (in the C2 domain), Ser319 (in the hinge domain) and Tyr658 (after HM site) occurred (Sharma et al., 2010; Daub et al., 2008; Kawakami et al., 2003).

4.5.3.2 Regulation by lipid second messengers

Priming phosphorylations occur immediately after synthesis and result in stable, closed conformation of the enzyme with pseudosubstrate bound to the substrate-binding site. Mature enzyme is localized to cytoplasm, but it is inactive, and can become activated by lipid second messengers interactions.

As a signal to PKCα activation, hydrolysis of PIP_2 occurs and produces Ca^{2+} and DAG both to activate enzyme (Newton, 2010).

Ca^{2+} binds to the C2 region and pre-targets enzyme to the membrane where it can interact with anionic phospholipids, preferentially PIP_2 (Bazzi and Nelsestuen, 1990; Newton and Keranen, 1994; Corbalan-Garcia et al., 2007). This binding is relatively weak. Although it is connected to conformational change with exposure of hinge region, it still does not release the pseudosubstrate (Orr et al., 1992; Newton and Keranen, 1994; Orr and Newton, 1992).

Then, PKCα can interact with DAG through C1 region and bind tightly to the membrane. DAG (as well as phorbol esters) serves as a hydrophobic anchor and increases enzyme membrane affinity. Alone, this interaction is reversible and can occur also in the absence of C2 domain interactions (Kazanietz et al., 1995; Mosior and Epand, 1993; Mosior and Newton, 1995; Newton and Keranen, 1994; Orr and Newton, 1992). DAG also decreases Ca2+ concentration that is needed for Ca^{2+} binding in a synergic manner (Nishizuka, 1984). Moreover, DAG binding to the enzyme is enhanced by stereospecific PtdSer binding.

All of these interactions lead to the pseudosubstrate release from substrate-binding site and enzyme is finally catalytically competent to promote its substrate phosphorylations (Newton, 1993; Newton and Keranen, 1994; Orr et al., 1992; Orr and Newton, 1992).

4.5.3.3 Spatial and temporal control of PKCα activity

As stated before, stimulation causes translocation of PKCα from cytosol to membranes. Upon phorbol ester treatment (non-specific activator), PKCα is redistributed to entire membrane, however, specific activator treatment results in redistribution to specific membrane compartments, such as plasma membrane, focal adhesion, cell-cell contacts, caveolae and nucleus (Nakashima, 2002).

This specific translocation is mediated by docking (anchoring) proteins. Without these proteins, translocation of PKCα is dependent on the content of DAG, PtdSer and PIP_2 in specific membranes and localized pool of Ca^{2+} (Nakashima, 2002).

Scaffold proteins for PKC are called RACKs (receptor for activated protein kinase C) (or, potentionally, RICKs - receptor for inactivated protein kinase C) (Ron et al., 1994; Ron and Mochly-Rosen, 1995; Mochly-Rosen and Gordon, 1998; Schechtman and Mochly-Rosen, 2001). These proteins bind PKCα specifically and release pseudosubstrate from substrate-binding cavity, therefore also have the ability to activate PKCα without second lipid messengers (Newton, 2010).

Other proteins that target PKCα to specific membrane sites were identified too. For example, vinculin, talin and β1 integrin target PKCα to focal contacts (Hyatt et al,, 1994; Ng et al., 2001) and caveolin to caveolae (Oka et al., 1997). Also other proteins as syndecans (Keum et al., 2004) were found to affect PKCα localization.

Together, these observations confirm that PKCα regulation is very complex. PKCα activity can depend on its phosphorylation status, presence of second lipid messengers (temporal regulation) and also its localization to specific membranes (spatial regulation) to promote selection of specific substrate under specific stimuli and context.

4.5.3.4 Termination of PKCα signaling

PKCα signaling is terminated by DAG metabolism that leads to the translocation of PKCα back into the cytoplasm. PKCα has relatively long half-life. However, upon prolonged activation (by phorbol esters) PKCα is rapidly degraded in proteasome.

During the process of downregulation, also dephosphorylation events at A-loop, TM and HM sites occur (Hansra, 1999). In its inactive conformation, PKCα is relatively resistant to dephosphorylation. However, open, membrane-bound conformation increases its sensitivity to dephosphorylation that favors protein instability (Dutil et al., 1994). These dephosphorylations are dependent on PP2a-like phosphatases (Lee et al., 2000; Hansra et al., 1996; Gatti and Robinson, 1997) or PHLPP phosphatases (Gao et al., 2008).

Although these dephosphorylations occur prior to PKCα degradation and act to decrease its activity, it is not always the case. Downregulation of PKCα does not have to involve enzyme dephosphorylation (Hansra et al., 1996; Leontieva and Black, 2004). The other way around, when the dephosphorylations occur, HSP70, keratins and Cdc37 can bind to PKCα, stabilizes it and assists its re-phosphorylation (Gao and Newton, 2002; Mashukova et al., 2009).

4.6 Role of PKCα in cancer cell invasion

As stated before, PKCα is very important for cell migration and invasion. PKCα is connected to invasivity in urinary bladder carcinoma (Koivunen et al., 2004), colon carcinoma (Masur et al., 2001), kidney cancer (Engers et al., 2000), breast cancer (Parsons et al., 2002) and myeloma (Podar et al., 2002). However, mechanisms by which PKCα regulates cell migration remain unclear.

PKCα could regulate migration through integrin signalization, adherens junctions, desmosomes and hemidesmosomes (Liu et al., 2010; Koivunen et al., 2004; Rabinovitz et al., 2004; Parsons et al., 2002; Masur et al., 2001; Ng et al., 1999; Rabinovitz et al., 1999), ezrin (Ng et al., 2010), Rac1 GTPase (Elfenbein et al., 2009; Sun and Rotenberg, 1999), NG2 proteoglycan (Makagensar et al., 2007) or matrix metalloproteinase 9 expression (Hwang and Jeong, 2010; Lin et al., 2010). This way, PKCα could regulate mesenchymal mode of invasion.

Role of PKCα in amoeboid migration was not described yet. However, PKCα could regulate signaling leading to RhoA activation (Holinstat et al., 2003; Dovas et al., 2010; Madigan et al., 2009) which is essential for amoeboid mode of invasion.

4.6.1 Potential role of PKCα in amoeboid invasion

As said previously, Rho/ROCK signaling cascade is essential for amoeboid invasion. This cascade has several levels of regulation that could be influenced by PKCα (Figure 4.17).

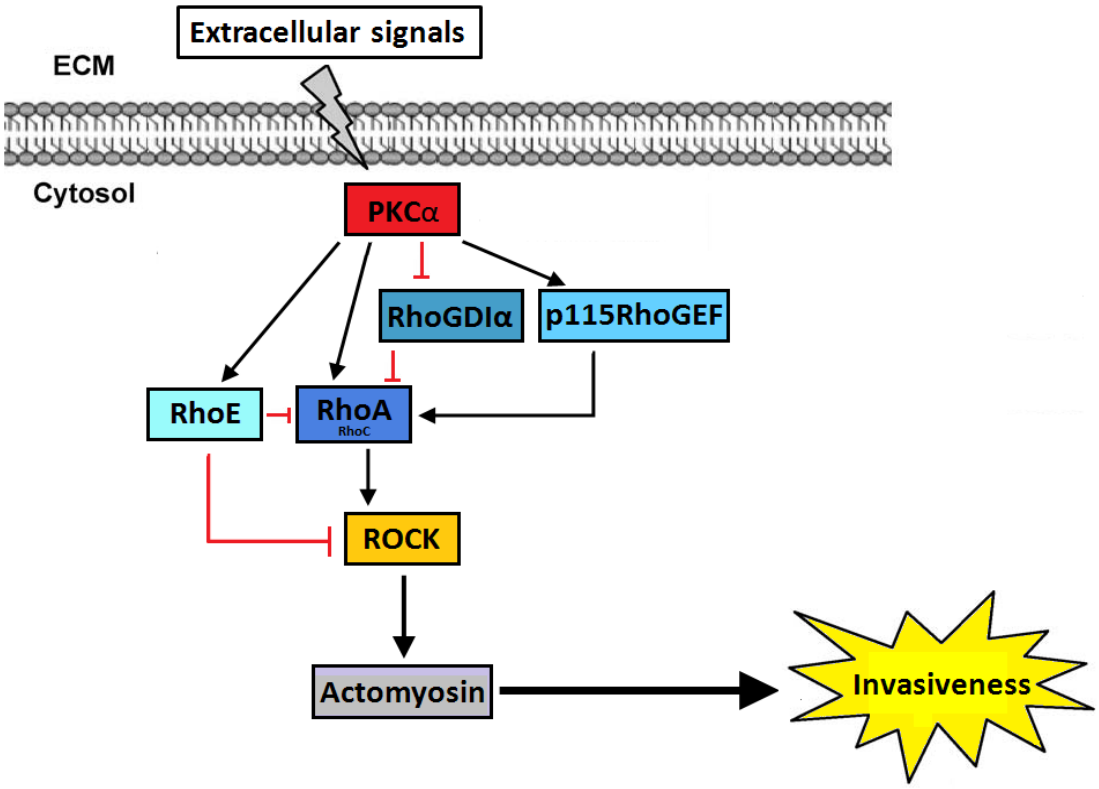

Figure 4.17. PKCα could regulate Rho/ROCK signaling cascade.
(Adapted from Szabadosová (2011). The role of protein kinase C α in individual cancer cell invasiveness)

4.6.1.1 Regulation of ROCK through RhoE

First of all, PKCα can influence Rnd3 protein (also known as RhoE) (Madigan et al., 2009).

Rnd proteins belong to the family of small Rho GTPases, however, they lack GTPase activity (Nobes et al., 1998) and therefore are in constitutively GTP-bound state (Foster et al., 1996). They are known to act to downregulate Rho signaling and decrease stress fiber formation and focal adhesion (Nobes et al., 1998; Guasch et al., 1998).

Rnd3 protein competes with PDK1 (3-phosphoinositide-dependent protein kinase 1) to binding to ROCK1 kinase. PDK1 recruits ROCK kinase to the plasma membrane (Pinner and Sahai, 2008). However, binding of Rnd3 to ROCK prevents this correct localization of ROCK and inhibits ROCK activity and downstream signaling (Pinner and Sahai, 2008; Riento et al., 2003).
Importantly, localization of Rnd3 is dependent on PKCα (Madigan et al., 2009). PKCα is able to phosphorylate Rnd3 and causes its translocation to intrinsic membranes. Subsequently, Rnd3 cannot inhibit ROCK activity and activity of Rho/ROCK pathway is increased (Madigan et al., 2009).
Interestingly, RhoE expression decreases RhoA levels in cells (Riento et al., 2003).

Another way of regulation is that RhoE expression can be induced by loss of cortical acto-myosin fibers in response to Raf activation (Hansen et al., 2000). Raf activation can be regulated by PKCα (Hwang et al., 2010; McGrew et al., 1992; Schonwasser et al., 1998).

4.6.1.2 Regulation of RhoA through RhoGDI

PKCα could also influence RhoA activity through RhoGDIα (Dovas et al., 2010).
RhoGDIs are cytosolic proteins that sequester small RhoGTPases in their inactive, GDP-bound state. This way, they block cycling of these proteins through GTPase-activating proteins (GAPs) and guanine nucleotide-exchange factors (GEFs) proteins (DerMardirossian and Bokoch, 2005; Dovas and Couchman, 2005). This leads to decreased pool of GTPases that can be used for another action.
RhoGDIα is the most expressed isoform and can bind RhoA, Rac1 and Cdc42 GTPases (DerMardirossian and Bokoch, 2005). It was shown that PKCα can phosphorylate RhoGDIα on Ser34 resulting in specific decrease in affinity for RhoA, but not for Rac1 or Cdc42 (Dovas et al., 2010). This leads to increase in RhoA activity (Dovas et al., 2010). For this phosphorylation, also PIP_2 is required, possibly for correct PKCα activation, localization and orientation in the membrane (Dovas et al., 2010). Moreover, higher levels of GTP-RhoA detected upon phorbol ester treatment were connected to loss of focal adhesions (Dovas et al., 2010).

Significantly, fibroblasts adhesion to fibronectin activates PKCα and this event leads to more active RhoA and associated cytoskeletal reorganizations (Dovas et al., 2006; Bass et al., 2008).

4.6.1.3 Regulation of RhoA through RhoGEF

Another way how PKCα could regulate RhoA activity is through its GEF p115RhoGEF (Holinstat et al., 2003). This group already previously showed that PKCα is able to activate RhoA in response to thrombin and consequently mediate actin cytoskeletal changes in endothelial cells (Mehta et al., 2001).
p115RhoGEF is Rho-specific GEF. Upon thrombin treatment, PKCα directly interacts with p115RhoGEF and phosphorylates it (Holinstat et al., 2003). This phosphorylation is associated with RhoA activation and regulation of actin stress fiber formation and cell contraction (Holinstat et al., 2003).

4.6.1.4 Regulation of ERM proteins

PKCα could regulate amoeboid invasion also by other mechanism – activation of ERM proteins (ezrin / radixin / moesin).
ERM proteins are important for cortical actin attachment to the membrane (Bretscher et al., 2002), but also for blebs stabilization (Sahai and Marshall, 2003) and so, they play significant role in amoeboid invasion. It was shown that PKCα can directly interact with ezrin and localize to plasma membrane protrusions (Ng et al., 2001). Furthermore, PKCα can phosphorylate ezrin on Thr567 in wound migratory response (Ng et al., 2001) and this can lead to its activation.
Activated ERM proteins can also regulate interaction of RhoGDIs with Rho GTPases (Ivetic and Ridley, 2004).

4.6.1.5 PKCα and MAT/AMT – preliminary results from our laboratory

Proteomic analysis (Kinexus) of A375m2 melanoma cells was done to identify proteins that are differentially expressed or phosphorylated in amoeboid comparing to mesenchymal cells. Among others, this analysis detected decreased level of PKCα

phosphorylation on Ser657 in cells after amoeboid-mesenchymal transition (induced by ROCK inhibition - inhibitor Y27632) both in 2D (culture dish) and in 3D (matrigel) environment (Figure 4.18) (Kasalová, 2010). Decreased level of PKCα phosphorylation on Ser657 after amoeboid-mesenchymal transition was confirmed by using phospho-specific antibody against PKCα Ser657 (Figure 4.19) (Kasalová, 2010). These results suggest that PKCα could possibly be involved in amoeboid invasion of melanoma A375m2 cells.

Target protein name	Phospho-site (Human)	Full target protein name	2DY/2D	3DY/3D
PKCa	Pan-specific	Protein-serine kinase C alpha	1,21	1,00
PKCa	S657	Protein-serine kinase C alpha	0,39	0,31

Figure 4.18. Results of proteomic analysis of A375m2 cell line (Kinexus) – results for total PKCα and PKCα phosphorylated on Ser657.
2DY/2D = expression of PKCα in cells treated with ROCK inhibitor Y27632 divided expression of PKCα in control cells for 2D environment
3DY/3D = expression of PKCα in cells treated with ROCK inhibitor Y27632 divided expression of PKCα in control cells for 3D environment
(Adapted from Kasalová (2010). In vitro analysis of amoeboid-mesenchymal transition of A375m2 melanoma cells. Charles University in Prague, diploma thesis).

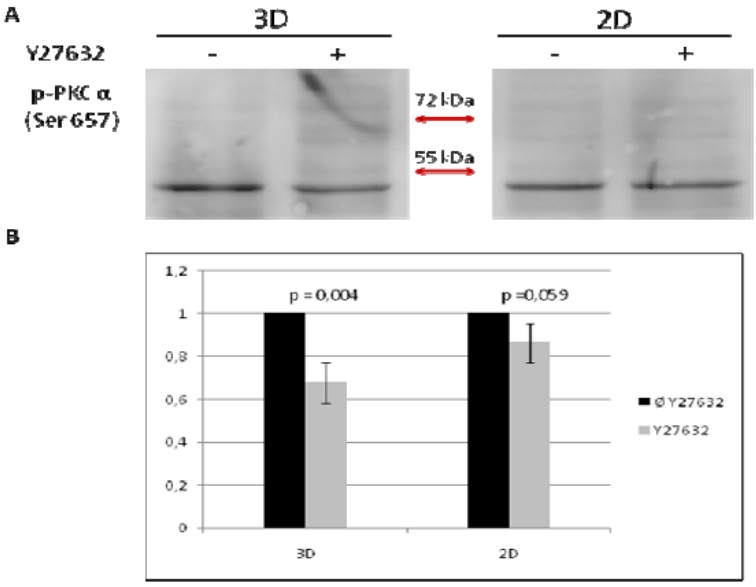

Figure 4.19. Immunoblots of phosphorylated PKCα on Ser657. Using specific antibody, native 80 kDa form of PKCα was not detected, only lower band of 50 kDa was detected. In 3D environment, decreased phosphorylation on Ser657 upon AMT (induced by ROCK inhibitor Y27632) was observed. This decrease was not seen in 2D environment.
A) Representative immunoblot of phosphorylated PKCα on Ser657 in A365m2 cells non-treated (-) and treated (+) with ROCK inhibitor Y27632 both in 2D and 3D environment.
B) Densitometric quantification of three independent experiments.
(Adapted from Kasalová (2010). In vitro analysis of amoeboid-mesenchymal transition of A375m2 melanoma cells. Charles University in Prague, diploma thesis).

5. Material

5.1 Model organisms

A375M2 - human melanoma cell line

K2 (LW13K2) – rat sarcoma cell line

MDA-MB231 – human breast cancer cell line

5.2 Solutions for cell cultivation

Complete growth medium M1H (500 ml, pH 7.4) (for K2 cell line culturing)

380 ml	millipore water, 2x steamed sterilized
50 ml	H-MEM 10x
50 ml	fetal bovine serum (FBS) (Hustopeče)
10 ml	antibiotic – antimycotic solution (ATB 100x) (GE Life Sciences / PAA Laboratories)
5 ml	L-glutamine (100x) (Sigma)
5 ml	$NaHCO_3$ 7.5% (sodium bicarbonate solution) (Sigma)

Complete growth medium DMEM (500 ml) (for A375m2 cell line culturing)

DMEM (Dulbecco's modified Eagle's minimal essential medium) (Gibco, Invitrogen)

10% fetal bovine serum (FBS) (Sigma)

1% non-essential amino acid solution (NEAA) (Sigma)

2% antibiotic – antimycotic solution (ATB 100x) (GE Life Sciences / PAA Laboratories)

Complete growth medium RPMI (500 ml) (for MDA-MB231 cell line culturing)

RPMI 1640 (Roswell Park Memorial Institute medium) (Gibco, Invitrogen)

10% fetal bovine serum (FBS) (Sigma)

1% non-essential amino acid solution (NEAA) (Sigma)

2% antibiotic – antimycotic solution (ATB 100x) (GE Life Sciences / PAA Laboratories)

Solution for cell splitting - 25% trypsin – EDTA (Gibco, Invitrogen)

2.5 g/l	trypsin
0.38 g/l	EDTA (ethylenediaminetetraacetic acid)

Freezing solution

10%	DMSO (dimethyl sulfoxide) (Sigma)
90%	FBS (fetal bovine serum)

10x PBS

137 mM	NaCl
2.7 mM	KCl
4.3 mM	Na_2HPO_4 . 12 H_2O
1.4 mM	KH_2PO_4

pH adjusted to 7,3

Inhibitors and activators

Y27632 – ROCK kinase inhibitor, 10μM (Sigma)

Gö6976 – PKCα and PKCβ inhibitor, 1μM (Sigma)

PMA (phorbol 12-myristate 13-acetate) – PKC activator, 162nM (100ng/ml)

Transfection solutions

jetPRIME™ in vitro DNA and siRNA Transfection Reagent (Polyplus Transfection):

jetPRIME™ Reagent

jetPRIME™ Buffer

siRNA - Silencer® Select Validated siRNA (Applied Biosystems) against Protein Kinase C α

siRNA stock was made of 10 μM concentration (by mixing 5 nM siRNA with 500 μl of H_2O)

5.3 Solutions for cell lysates preparation

RIPA buffer

0.15 M	NaCl
50 mM	Tris-HCl (pH 7.4)
1%	Nonidet P – 40
0.1%	SDS (sodium dodecyl sulfate)
1%	sodium deoxycholate
5 mM	EDTA (ethylenediaminetetraacetic acid)
50 mM	NaF

Protease inhibitors stock solution (100x)

Protease Inhibitor Mix M (Serva)

Phosphatase inhibitors stock solution (100x)

Phosphatase Inhibitor Mix II (Serva)

5.4 SDS-PAGE and Western blotting solutions

Sample buffer - 6x Laemmli buffer

0.39 M	Tris-HCl, pH 6.8
12%	SDS (sodium dodecyl sulfate)
50%	glycerol
0.012%	bromphenol blue

Protein marker

PageRuler® Plus Prestained Protein Ladder SM 1811 (Fermentas)

Solutions for polyacrylamide gel preparation

Protogel

30% acrylamide

0.8% N,N'-methylenbisacrylamide,

filtered through 0,45 mm pores filter

4x Tris/SDS, pH 8.8

1.5 M Tris-HCl (pH 8.8)

0.4% SDS,

filtered through 0,45 mm pores filter

4x Tris/SDS, pH 6.8

0.5 M Tris-HCl (pH 6.8)

0.4% SDS,

filtered through 0,45 mm pores filter

TEMED (Sigma)

APS

SDS-PAGE buffer (1x SDS buffer)

25 mM Tris (pH 8.3)

190 mM glycine

0.1% SDS

Staining solution

20% methanol

10% acetic acid

0.114% Coomassie Brilliant Blue R-250 (Bio-Rad)

Destaining solution

5% methanol

7% acetic acid

Transfer buffer

25 mM Tris

192 mM glycine

20% methanol

0.05% SDS

TBS (Tris–buffered saline)

20 mM Tris-HCl (pH 8.0)

500 mM NaCl

TTBS (Tween tris-buffered saline)

0.05% Tween 20 (Serva) in TBS

Blocking solution

4% BSA (bovine serum albumine) (Milipore) in TBS

Solution for primary and secondary antibodies dilution

1% BSA (bovine serum albumine) (Milipore) in TTBS

Developing solution

SuperSignal® West Pico Chemiluminiscent Substrate (Pierce Biotechnology):

Solution A – SuperSignal® West Pico Stable Peroxide Solution

Solution B - SuperSignal® West Pico Luminol / Enhancer Solution

Solution for horseradish peroxidase – solution A : solution B = 1 : 1

Stripping buffer (100 ml)

4.7 µl	2-merkaptoethanol (14.7 M) (Sigma)
20 ml	10% SDS
3.9 ml	1 M Tris-HCl, pH 6.8

in deionizied water

5.5 List of primary antibodies

PKCα – 1:20000, rabbit, polyclonal (Sigma-Aldrich)

p-PKCα (Ser657) – 1:500, goat, polyclonal (Santa Cruz Biotechnology)

p-PKCα (Thr497) – 1:10000, rabbit, monoclonal (abcam)

Actin – 1:200, goat, polyclonal (Santa Cruz Biotechnology)

5.6 List of secondary antibodies

Donkey anti-goat IgG HRP-conjugated, 1:5000 (Santa Cruz Biotechnology)

Goat anti-rabbit IgG HRP-conjugated, 1:5000 (Santa Cruz Biotechnology)

5.7 Solutions for collagen and matrigel matrices preparation

Collagen R (Collagen type I), 4 mg/ml (Serva)

0.25 M $NaHCO_3$: 2.2g $NaHCO_3$ in 100 ml 1x CMF - HBSS

1x CMF – HBSS: 900 ml distilled water, 8 g NaCl, 0.4 g KCl, 0.06 g KH_2PO_4, 0.35 g $NaHCO_3$, 0.112 g Na_2HPO_4 . 12 H_2O, pH adjusted to 7.4 using 2 M NaOH

Collagen G, 4 mg/ml (BIOCHROM AG)

Fetal bovine serum (FBS) (Sigma)

10x PBS (Invitrogen)

10x H-MEM

BD Matrigel^{TM} Basement Membrane Matrix, Phenol Red Free, 9,5 mg/ml (BD Bioscience)

BD Cell Recovery Solution (BD Bioscience)

5.8 Solutions for matrix degradation and invadopodia assays

FITC-labeled gelatin

0.5% glutaraldehyde in PBS

0.1 M $NaBH_4$

4% paraformaldehyde in 25 mM HEPES

Triton X-100 in PBS

Blocking solution and solution for diluting antibodies – 5% BSA in TBS

Antibodies

Cortactin – 1:100, rabbit, polyclonal (Sanza Cruz Biotechnology)

p – cortactin (Tyr421) – 1.100, rabbit, polyclonal (BioSource)

Alexa Fluor® 546 Goat anti-rabbit IgG – 1:1000 (Invitrogen)

Alexa Fluor® 405 phalloidin – 1:70 (Invitrogen)

Mounting medium

6 g glycerole, 2,4 g mowiol, 6 ml H_2O, 12 ml buffer (60 mM PIPES, 25 mM HEPES, 10 ml EGTA, 1 mM $MgCl_2$, pH 8.3)

DABCO

6. Methods

6.1 Cell cultivation

Cells are cultivated in the incubator under standard conditions of 37°C and 5% CO_2 atmosphere. Cells are cultivated on 100 mm cell culture dishes in 10 ml of complete growth medium. Cells are regularly controlled under the microscope (Nikon Eclipse TS 100) to determine their confluence and check for potential contaminations.

6.2 Cell splitting

According to the cell confluence, cells are splitted every 2 – 4 days.
Prior to working with cells, heat medium and trypsin in 37°C water bath for approximately 15 minutes.

- Aspirate the old medium
- Add 1 ml of trypsin per one dish and rinse gently
- Aspirate trypsin
- Add 1 ml of trypsin again to cover the surface of the dish and incubate in an incubator for 3 - 5 minutes, until cells are detached from the surface of the dish
- Add complete medium (amount of medium depends on needed dilution of cells) into the dish to block the activity of trypsin and resuspend suspension by pipetting up and down
- Transfer the needed amount of cell suspension into new dish
- Add complete medium to the total amount of 10 ml

6.3 Cell stock preparation

Cell stocks are prepared from fully confluent dishes and it is possible to make two cryogenic tubes from one fully confluent dish.

- Aspirate the medium
- Add 1 ml of trypsin per one dish, rinse and aspirate

- Add 1 ml of trypsin again to cover the surface of the dish and incubate in an incubator for 3 – 5 minutes
- After detaching of cells from the surface of the dish, add 4 ml of medium and transfer into 15 ml falcon tube
- Centrifuge the cell suspension at 180 g for 3 minutes at room temperature (Eppendorf Centrifuge 5804R)
- Aspirate the medium gently (pay attention to not disturbing the pellet) and resuspend the pellet in 2 ml of freezing solution (90% FBS, 10% DMSO)
- Fill cryogenic tubes with 1 ml of cell solution per one tube
- Place the cryogenic tubes into isopropanole-filled container and transfer into -70°C freezer for 24 hours
- Next day, transfer the tubes into liquid nitrogen container to store cell stocks

6.4 Cell stock re-culturing

- Put out cryogenic tube from liquid nitrogen container and place on ice
- Thaw cell suspension as fast as possible in 37°C water bath
- Quantitatively transfer the cell suspension into prepared 15 ml falcon tube with 7 ml of complete medium
- Centrifuge the cell suspension at 180 g for 3 minutes at room temperature (Eppendorf Centrifuge 5804R)
- Aspirate the supernatant gently, resuspend the pellet in 7 ml of complete medium by pipetting up and down
- Centrifuge the cell suspension again at 180 g for 3 minutes at room temperature (Eppendorf Centrifuge 5804R)
- Aspirate the supernatant again, resuspend the pellet in 5 ml of complete medium and transfer into new culture dish
- Add 5 ml of complete medium into the dish to reach the total amount of 10 ml of growth medium and cultivate cells in the incubator

6.5 Cell transfection

Cells are transfected with siRNA (10 μM stock) (Applied Biosystems) using jetPRIME^{TM} Transfection Reagent (Polyplus Transfection).

- One day before transfection, seed the cells into 6 well plate, so they are approximately 60 – 80% confluent at the day of transfection
- At the time of transfection, prepare siRNA mixture – pipette 200 μl of jetPRIMETM Buffer into a microtube, add 2.2 μl of siRNA (to the final concentration of 10 nM at the plate) and 4 μl of jetPRIMETM Reagent, vortex for 10 seconds and incubate for 15 minutes at room temperature
- Meanwhile, aspirate the medium from the plate and add 2 ml of fresh complete medium per one 6 well
- After incubation time, gently pipette siRNA mixture to the plate, drop after drop, to cover whole surface of the plate
- Shake gently to spread siRNA mixture over the plate and incubate in the incubator
- After 48 hours, use cells for experiment or prepare cell lysates
- As a negative control, untreated cells are used as well as mock - transfected cells – transfected only with 200 μl of jetPRIMETM Buffer and 4 μl of jetPRIMETM Reagent (with no siRNA added).

6.6 Cell lysates preparation

Cell lysates are prepared under non-sterile conditions and everything is done on ice and as quickly as possible to avoid protein degradation.

- Place fully confluent dish on ice immediately after putting out from the incubator
- Aspirate the medium
- Rinse the dish two times with 5 ml of cold 1x PBS
- Add 1 ml of lysis buffer (RIPA buffer, protease inhibitors (1:100) and phosphatase inhibitors (1:100)) per one 100 mm dish (or 100 – 200 μl of RIPA buffer per one 6 well) and incubate for 12 – 15 minutes in a fridge (4°C) on a rocker (Biosan, MR-1)
- Scrape cells off the dish using plastic cell scraper and transfer cell lysate into prepared microtube

- Push the cell lysate through 21G needle 6 times until the suspension is clear
- Centrifuge the cell lysate at 11 000g for 20 minutes at 0°C (Eppendorf Centrifuge 5417R)
- Transfer the supernatant gently into new microtube and store in a freezer (-20°) or directly prepare samples for SDS-PAGE

6.7 Determination of protein concentration in cell lysates – Folin's method

Protein concentration in cell lysates is assessed by colorimetric assay using Dc Protein Assay kit (Bio-Rad).

- Prepare set of bovine serum albumin (BSA) standards according to the table:

BSA 2 mg/ml (µl)	RIPA buffer (µl)	Final concentration (µg/µl)
0	40	0
5	45	200
10	40	400
20	30	800
37,5	12,5	1500

- Prepare A´ reagent – mix 20 µl of S reagent into 1 ml of A reagent in a microtube
- Thaw cell lysates on ice and mix 25 µl of cell lysate with 25 µl of RIPA buffer in a microtube
- Transfer 25 µl of diluted cell lysate or 25 µl of BSA standard into new microtube and add 125 µl of A´ solution
- Add 1 ml of B solution into each microtube and shortly vortex
- Incubate in dark for at least 15 minutes
- Measure absorbance of the samples and BSA standards at 750 nm wave length (Schimadzu UV 1650 PC)
- Plot the calibration curve based on BSA dilution (plot the absorbance against protein concentration)
- Count protein concentration of the samples according to the calibration curve based on their absorbance

- Adjust protein concentration of the samples to the same value by adding RIPA buffer

6.8 SDS – PAGE samples preparation

- Add ¼ of final volume of 6x Laemmli buffer into each cell lysate sample
- Add 1/20 of final volume of 1 M DTT (dithiothreitol) into each cell lysate sample
- Boil for approximately 10 minutes in heating block at 100°C
- Freeze prepared samples or load them directly on SDS – PAGE gel
- Before loading on the SDS – PAGE gel, boil the samples for 5 – 10 minutes in heating block at 100°C

6.9 Protein Tris-glycine SDS polyacrylaminde gel electrophoresis (SDS-PAGE)

- Assemble an apparatus for polyacrylamide gel preparation
- Prepare polyacrylamide running gel mixture by mixing together its components according to the table (add TEMED and APS at last, because they cause gel polymerization):

Mixture for one 0.75 mm thick running gel (for 1.5 mm thick gel use two-times bigger amounts)			
	7.5%	10%	12%
Deionized water	2.50 ml	2.08 ml	1.75 ml
4x Tri/SDS pH 8,8	1.25 ml	1.25 ml	1.25 ml
Protogel 30%AA/0,8%BisAA	1.25 ml	1.67 ml	2.00 ml
TEMED	3.4 µl	3.4 µl	3.4 µl
APS	16.5 µl	16.5 µl	16.5 µl

- Pour the polyacrylamide running gel mixture into the apparatus between two glass panels and immediately cover with the layer of deionized water to avoid contact with air
- Let the gel polymerize for approximately 20 minutes and afterwards gently remove water with filter paper Whatman

- Prepare polyacrylamide stacking gel mixture according to the table:

Mixture for one 0.75 mm thick stacking gel (for 1.5 mm thick gel use two-times bigger amounts)	
Deionized water	1.550 ml
4x Tri/SDS pH 6,8	0.625 ml
Protogel 30%AA/0,8%BisAA	0.325 ml
TEMED	2.5 µl
APS	12.5 µl

- Pour the polyacrylamide stacking gel mixture over the running gel and put a plastic comb in to make sample wells and let the gel polymerize

Pre-prepared polyacrylamide gel can be stored wrapped in plastic foil in a fridge (4°C) for several days.

- Assemble apparatus for electrophoresis (BIO-RAD Mini Protein III Cell) and put the polyacrylamide gel in, fill the apparatus with 1x SDS buffer
- Remove the plastic comb gently from the gel (pay attention to not disturbing sample wells), wash sample wells with 1x SDS buffer and load prepared and heated samples using Hamilton syringe (for one 0.75 mm well load maximum 20 µl of sample, for one 1.5 mm well load maximum 40 µl of sample)
- Run the stacking gel at 10 mA per one 0.75 mm gel, if there is 1.5 mm gel or two 0.75 mm gels in the apparatus, double the electrical current
- After the dye front reaches running gel, increase electrical current to 20 mA per one 0.75 gel, or 40 mA per one 1,5 mm gel or two 0.75 mm gels
- When the dye front reaches the end of the gel, turn off the electric power supply and take the gel out of the apparatus
- Remove stacking gel and use the gel for Western blot or simple staining

6.10 Western blot

- Assemble blotting sandwich for transfer of proteins from polyacrylamide gel to nitrocellulose membrane as follows: sponge, filter paper Whatman, gel, nitrocellulose membrane (Nitrobind, MSI), filter paper Whatman, sponge (pre-

moisten everything in transfer buffer and assemble sandwich in Petri dish filled with transfer buffer)

- Put the blotting sandwich into the Western blot apparatus (BIO-RAD Trans-blot) and fill the apparatus with transfer buffer
- Transfer the proteins to the membrane at the voltage of 100 V for 1,5 hours, whilst constantly stirring and cooling with ice
- After the blotting, stain the gel in staining solution for 30 minutes and then de-stain it with de-staining solution overnight
- Wash the membrane in TBS and use it for immunodetection of proteins

6.11 Immunodetection of proteins on the membrane

- After washing of the membrane in TBS, block it in blocking solution for 1 hour on a rocker (Biosan, MR-1) in a 37°C incubator
- Then, incubate the membrane in primary antibody solution overnight on a rocker (Biosan, MR-1) in a fridge (4°C)
- Following day, wash the membrane 3 x 10 minutes in TTBS to remove excess primary antibody
- Incubate the membrane in secondary antibody (horseradish peroxidase (HRP)-conjugated) solution for 1 hour on a rocker (Biosan, MR-1) at room temperature
- Wash the membrane 3 x 10 minutes in TTBS to remove excess secondary antibody
- Wash the membrane for 5 minutes in TBS
- Prepare HRP - developing solution, pour it on the membrane to cover the whole surface and incubate it in dark for 2 – 3 minutes
- Detect the signal using developing device LAS-4000

6.12 Stripping of the membrane

- After immunodetection of the proteins on the nitrocellulose membrane using LAS-4000, wash the membrane properly in TBS (wash it at least 3 x 10 minutes)
- Incubate the membrane in stripping buffer for 30 minutes in 50°C in dark on a rocker (Biosan, MR-1)

- Wash the membrane 3 x 10 minutes in TTBS
- Then, block the membrane in blocking solution for 1 hour on a rocker (Biosan, MR-1) in a 37°C incubator
- Next, work according to the normal protocol for immunodetection

6.13 3D collagen preparation for 3D cell morphology assays

- Trypsinize cells (as previously described) to detach from the surface of the plate, add medium and transfer it into 15 ml falcon tube and centrifuge the solution (180 g, 3 min, room temperature, Eppendorf Centrifuge 5804R)
- Gently aspirate the medium and resuspend pellet in 1 – 2 ml of complete medium and count the cell number using counting chamber
- Prepare 2% collagen solution according to the table and keep on ice:

2% collagen solution		
	24 – wells plate (total 500 µl of collagen solution per well)	96 – wells plate (total 80 µl of collagen solution per well)
H-MEM (10x)	52 µl	8.3 µl
1x PBS	156 µl	25 µl
FBS	26 µl	4.2 µl
0,25 M $NaHCO_3$	26 µl	4.2 µl
Collagen type I	261 µl	42 µl

It is essential to keep all the solutions and collagen mixture all the time on ice. When collagen warms up, its consistency changes from liquid to gel.

- Transfer amount of 100000 cells into new microtube per one 24 well and add 500 µl of collagen solution and mix gently by pipetting up and down (for 96 well use 11000 cells with 80 µl of collagen solution) (if needed, add inhibitor or activator into the microtube before collagen addition and incubate for 15 minutes)
- Pipette collagen solution with cells into 24 or 96 well and incubate in a incubator for approximately 45 minutes, so collagen becomes gel-like
- Afterwards, pipette 1 ml of complete medium (if needed, add inhibitor or activator also to the medium) very carefully onto collagen in 24 well (or 150 µl per 96 well) (be careful about not disturbing collagen layer)

- Incubate the plate in an incubator and after 48 hours observe cell morphology at the microscope Nikon Eclipse TE2000-S using Hoffman modulation contrast (MC2) (20x objective)
- Classify the cells according to their morphology using NIS Elements program (Nikon) – count the number of rounded, elongated and "intermediate" cells. Consider the overall shape of the cell and length–width index (cell length divided by cell width). Rounded cells are the cells expressing smooth roundish shape without any protrusions. Elongated cells are polarized cells with one or more protrusions and length-width index value bigger than 2. Intermediate cells are the cells with uncertain morphology, roundish cells with some protrusions or cells with length-width index less than 2. Do not count apoptotic and dividing cells. Count a minimum of 300 cells for each well
- NIS Elements program (Nikon) allows you to mark cells according to their morphology, so one cell is counted only once and the total number of each morphology type at the moment is seen
- Finally, calculate the proportion of rounded, elongated and intermediate cells. Express these values in percents to assess the morphology profile of cells

6.14 Invasivity assay in 3D collagen

For invasivity assays specialized invasion wells are used (µ-Slide Angiogenesis ibiTreat Microscopy Chamber (IBIDI)).

- Prepare 3D collagen solution according to the table and keep on ice:

Collagen solution for invasivity (10 µl) per one IBIDI well	
Collagen R	200 µl (by mixing 100 µl collagen R and 100 µl 1x PBS)
Collagen G	200 µl
$NaHCO_3$	45.8 µl
H-MEM (10x)	45.8 µl

- Pipette 10 µl of collagen solution per one IBIDI well (hold the pipette very near the bottom and pipette vertically to make the collagen layer straight and without bubbles)
- Put the IBIDI plate into the specialized chamber with deionized water (approximately 10 – 20 ml) at the bottom (to avoid drying out)

- Incubate in a incubator for 20 – 30 minutes
- Trypsinize and count cells (as described previously)
- Transfer 100000 cells into microtube and add medium to the total volume 1 ml (if needed, add inhibitor or activator to the microtube as well)
- Pipette 50 µl of cell suspension into each IBIDI well (pipette very carefully, drop after drop, to avoid disturbing collagen layer), put the plate into the chamber and incubate in a incubator
- Following day, aspirate the medium very gently with a pipette (be careful not to destroy collagen) and change the medium for serum-free medium (if needed, add inhibitor or activator into the medium)
- After another 48 hours examine how the cells invaded into 3D collagen using Nikon Eclipse TE2000-S microscope with Hoffman modulation contrast (MC2) (20x objective)
- Using NIS Elements program (Nikon), take a picture of collagen cross-section every 10 µm starting at the surface and heading into the depth
- Count the focused cells in each cross-section
- Calculate relative invasivity index as follows:

$$\text{relative invasivity index} = \frac{\sum \text{number of focused cells in cross-section} \times \text{depth of cross-section in } \mu\text{m}}{\text{total number of cells in all cross-sections}}$$

- To compare between experiments, express the relative invasivity index of untreated cells as 1 and normalize the relative invasivity index to that of untreated cells

6.15 3D matrigel preparation for 3D cell lysates

It is necessary to thaw and keep matrigel all the time on ice. As soon as it warms a little bit up, it starts to become gel-like.

- Trypsinize and count cells (as described previously)
- Transfer amount of 125000 cells into new microtube and add medium to the final volume of 37 µl

- Add FBS, DMEM or Y27632 and incubate for 15 minutes and at last, add matrigel:

Matrigel solution (500 µl) per one 24 well	
BD Matrigel™ Basement Membrane Matrix	420 µl
FBS	19 µl
DMEM / Y27632	25 µl
Cells in DMEM	125000 cells in 37 µl

- Mix the solution gently by pipetting up and down and transfer it into 24 well
- Incubate in a incubator for approximately 45 minutes, so matrigel gains gel consistency
- After that, pipette 1 ml of complete medium (if needed, add inhibitor Y27632 into the medium) over the matrigel layer (be sure not to damage matrigel)
- Incubate matrigel with cells in a incubator for 24 hours
- Next day, prepare 3D cell lysates by dissolving 3D matrigel

6.16 Dissolving of 3D matrigel and preparation of 3D cell lysates

It is essential to perform dissolving of 3D matrigel directly on ice in a cold room at 2 - 4°C. It is also necessary to cool all the solutions and tools in advance.

- Put the 24 well plate with cells in 3D matrigel on ice immediately after putting out from a incubator and take it into the cold room
- Aspirate medium very carefully (be careful not to destroy matrigel) and wash 3 times with 1 ml of cold 1x PBS
- Add 500 µl of BD Cell Recovery solution per each well and using spatula separate matrigel from the bottom of the well
- Transfer matrigel and solution into 15 ml falcon tube using pipette with cut tip
- Add 500 µl of Cell Recovery solution into the well again and transfer matrigel with solution into the same falcon tube using same cut tip (try to minimize the loss of matrigel and cells) and repeat 2 – 3 more times
- Let the matrigel thaw in the solution for approximately 30 minutes and then help its thawing by shaking gently with falcon tube until all the matrigel is thawed

- Centrifuge the solution in pre-cooled centrifuge at 250 g for 5 minutes at 0°C (Eppendorf Centrifuge 5804R)
- Aspirate the supernatant very gently (always be very gentle aspirating the supernatant - try to avoid any loss of cells), resuspend the pellet carefully (cells are very sensitive to die in these steps) in 3 ml of cool 1x PBS and centrifuge again (250 g, 5 minutes, 0°C, Eppendorf Centrifuge 5804R)
- Aspirate the supernatant again and resuspend the pellet in 2 ml of DMEM without FBS and centrifuge again (250 g, 5 minutes, 0°C, Eppendorf Centrifuge 5804R)
- Aspirate DMEM and add 20 µl of lysis buffer (RIPA buffer, protease inhibitors (1:100) and phosphatase inhibitors (1:100)) and incubate for 15 minutes on ice
- Add 7 µl 6x Laemmli buffer and 0.7 µl DTT into each sample, transfer into new microtube and heat for 10 – 15 minutes at 100°C in a heating block

6.17 Preparation of FITC-labeled gelatin-coated coverslips

Perform all the steps of coverslips preparation on ice. Keep the moist chamber or well plate in dark during all the incubations.

- Place clean coverslips on a parafilm inserted into moist chamber
- Pipette big drop of FITC-labeled gelatin on each coverslip and aspirate immediately, so the thin layer of gelatin is created
- Turn coverslip upside down on 100 µl drop of 0,5% glutaraldehyde prepared on parafilm and incubate for 15 minutes in dark
- Afterwards, transfer coverslip into 12 well plate and wash 3 times with 1x PBS (always be careful not to disturb gelatin layer on coverslip – aspirate PBS from the side as well as pipette solutions to the side of the dish)
- Add 1 ml of $NaBH_4$ (5 mg / ml) and incubate for 3 minutes
- Wash 3 times in 1x PBS
- Add 1 ml of 70% ethanol, incubate for 1 minute and transfer coverslip into sterile 12 well plate in a hood (and continue working in sterile environment)
- Add 1 ml of complete media to each well and incubate for 1 hour or more (possibly overnight)
- After the time, wash coverslip 5 times in complete medium

- Trypsinize and count cells (as described previously), transfer 30000 cells into 1 ml of complete medium and pipette gently onto coverslip
- Following day, fix and stain cells according to the immunostaining protocol

6.18 Immunofluorescence staining of cells for gelatin degradation assay

From now on, work in non-sterile conditions again.

- Aspirate the medium from the coverslip and fix cells with 0.5 ml of 4% paraformaldehyde for 15 minutes
- Wash 3 times with 1x PBS
- Permeabilize cells with 1ml of 0.5% Triton X-100 in 1x PBS for 10 minutes
- Wash 3 times with 1x PBS
- Incubate coverslip in 1 ml of blocking solution (5% BSA in TBS) for 30 minutes
- Place the coverslip upside down on a 50 µl drop of primary antibody solution on parafilm in moist chamber and incubate for 2 - 3 hours
- Wash 3 x 10 minutes with 1x PBS
- Place the coverslip upside down on a 100 µl drop of secondary antibody solution on parafilm in moist chamber and incubate for 60 minutes
- Wash 3 x 10 minutes with 1x PBS
- Place the coverslip upside down on a 70 µl drop of phalloidin solution on parafilm in moist chamber and incubate for 15 minutes
- Wash 3 x 10 minutes with 1x PBS
- Rinse the coverslip quickly in deionized water and mount to a 9 µl drop of mounting medium on a mounting slide
- Examine cells using fluorescent microscope Nikon Eclipse TE2000-S (20x/0.40 HMC objective) or confocal microscope Leica DM IRE2
- For degradation assay, use fluorescent microscope Nikon Eclipse TE2000-S (20x/0.40 HMC objective). Take pictures in two different levels – cortactin level (546 nm) - marker of cells and gelatin level (488 nm) - extracellular matrix on which cells were plated. For each experiment, examine seven random fields to quantify gelatin degradation. For analysis, use AnalyzeGelStack program (obtained from Dr.

Buccione). This program allows to measure degradation area (in gelatin level) normalized to the number and area of cells (seen in cortactin level) (degradation area per cell). Express these values as relative degradation – degradation normalized to degradation of control untreated cells

- For better visualization of cells and taking representative pictures, use confocal microscope Leica DM IRE2. Take pictures in three levels – cortactin level (546 nm), actin level (405 nm) and gelatin level (488 nm)

7. Results

7.1 Analysis of protein kinase C α (PKCα) expression and phosphorylation in cells after amoeboid – mesenchymal transition (AMT)

Previous results from our laboratory suggested possible role of PKCα in amoeboid migration. PKCα phosphorylation on Ser657 was significantly lower in A375m2 melanoma cells after AMT, therefore in their mesenchymal state, suggesting that PKCα is more activated in their amoeboid state (Kasalová, 2010).

To find out whether amoeboid or mesenchymal state of cells influences also total PKCα levels or its phosphorylation on Thr497, A375m2 cells were analyzed. Cells were cultivated both in 2D (cultivate dish) and 3D (matrigel) environment, as cells behave differently depending on their cultivation environment. Cultivation of cells in 3D environment more appropriately resembles situation *in vivo*. As 3D matrix, BD Matrigel^{TM} Basement Membrane Matrix (Phenol Red Free, 9,5 mg/ml (BD Bioscience)) was used. AMT was induced by ROCK inhibitor Y27632 that is specific for both ROCK1 and ROCK2 isoforms. Y27632 binds to the active site of the enzyme and blocks kinase activity (Ishizaki et al., 2000). It was shown previously that treatment of amoeboid cells with Y27632 results in AMT because of inhibiting Rho/ROCK signaling pathway (Sahai and Marshall, 2003). The inhibitor concentration of 10μM was used. Cell lysates were made after 24 hours of cell cultivation in the presence of Y27632 in 3D matrigel and after 48 hours of cell cultivation with Y27632 on plastic dish. Samples were separated on 12% polyacrylamide gels and transferred onto nitrocellulose membranes using Western blot method. Total PKCα levels and PKCα phosphorylation on Thr497 were analyzed using immunodetection by specific antibodies (PKCα (Sigma Aldrich) and p-PKCα Thr497 (abcam)).

It was observed, that neither total PKCα level, nor PKCα phosphorylation on Thr497 were changed upon AMT (induced by ROCK inhibitor Y27632). The results were the same for both 2D and 3D environment (Figure 7.1).

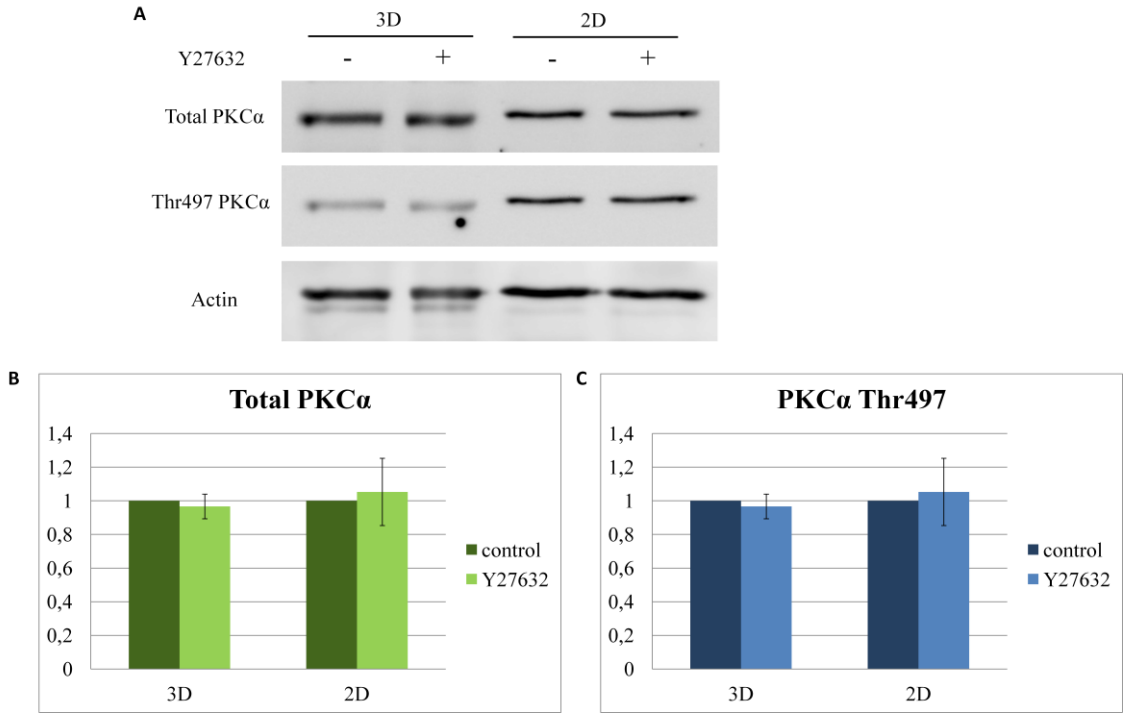

Figure 7.1. Immunoblots of total PKCα and PKCα phosphorylation on Thr497. Cells after AMT (induced by ROCK inhibitor Y27632) express the same amount of PKCα as control cells both in 3D and in 2D environment. Similarly, phosphorylation on Thr497 remains unchanged.
A) Representative immunoblots of total PKCα level (upper line), phosphorylation of PKCα on Thr497 (middle line) and actin as a loading control (lower line). A375m2 cell lysates were made from non-treated (-) and treated (+) cells with ROCK inhibitor (Y27632). Cells were cultured in both 3D and 2D environment.
B) Densitometric quantification of total PKCα levels, evaluation from three independent experiments. Densitometric analysis was made using ImageJ software and values were normalized to that of untreated cells. Error bars represent standard deviations, statistical significance was evaluated according to unpaired two-tailed Student's t-test. Significant difference ($p<0.05$) in comparison to control is indicated by asterisk.
C) Densitometric quantification of PKCα phosphorylation on Thr497, evaluation from three independent experiments. Densitometric analysis was made using ImageJ software and values were normalized to that of untreated cells. Error bars represent standard deviations, statistical significance was evaluated according to unpaired two-tailed Student's t-test. Significant difference ($p<0.05$) in comparison to control is indicated by asterisk.

It is noteworthy that our antibodies detected more bands on the membrane (Figure 7.2). There was 80 kDa band that was according to its size identified as the PKCα enzyme. However, also smaller bands were detected. When using total PKCα antibody smaller bands around 54 and 43 kDa were present. Phosphorylation specific antibody detected only 54 kDa fragment.

It is not clear what these bands represent. In literature, we have not found any note about more bands detected by these antibodies. It is known, however, that PKCα can be cleaved in its hinge region by calpains or other proteases. This way, two fragments are produced – regulatory domain fragment (around 30 kDa) and constitutively active

catalytic fragment (also known as protein kinase M (PKM)). This fragment migrates at 40 – 50 kDa, most frequently observed size is 46 kDa (Touyarot et al., 2002; Touyarot et al., 2000; Leverrier et al., 2002; Kang et al., 2010). It is possible, that fragments detected in our experiment could represent these cleaved fragments of PKCα, however, physiological significance of PKM is still controversial.

For this reason and for clarity, only larger band of 80 kDa was always quantified. Anyway, abundance of these smaller bands always matched the abundance of the upper band both in total PKCα and in PKCα phosphorylation immunoblot analysis.

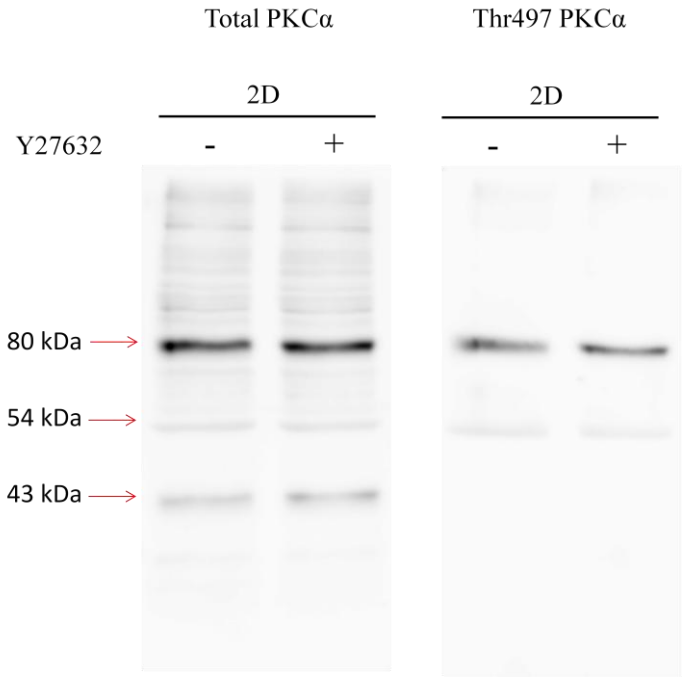

Figure 7.2. Representative immunoblots of A375m2 cell lysates using antibodies against total PKCα and PKCα phosphorylation on Thr497 with molecular weights marked. Using antibody against total PKCα, bands of 80 kDa, 54 kDa and 43 kDa were observed. Using antibody against PKCα phosphorylation, only two upper bands were detected.

Taken together, these results suggest that PKCα is not less active after AMT and therefore propose that PKCα activation is not directly connected to amoeboid invasion.

AMT does not activate PKCα expression or its phosphorylation on Thr497 both in 2D and in 3D environment. In other words, PKCα is not activated downstream of change of invasion mode.

However, there is still possibility that PKCα could reversely regulate amoeboid invasion and play an important role in transitions between these states as will be addressed further.

7.2 PKCα can regulate morphology of cells in 3D collagen – effect of PKCα activator and inhibitor

To investigate the possible role of PKCα in regulating cell morphology that is very important feature of mode of invasion, we performed morphology assays in 3D collagen.

A375m2 human melanoma cell line, K2 rat sarcoma cell line and MDA-MB-231 human breast cancer cell line were used. Cells were seeded into 3D collagen matrix (3 mg/ml Collagen R solution in complete medium (Serva)) and morphology of cells was observed after 48 hours incubation. 48 hours exposure was needed to allow cells to adjust to the 3D environment and adopt accurate shape. Using microscope Nikon Eclipse TE2000-S (20x / 0.40 HMC objective) and NIS Elements program (Nikon), cells were counted and divided into three groups – rounded cells, elongated cells and "intermediate" cells. As rounded cells, cells exhibiting smooth round shape without any protrusion were considered. Elongated cells were the polarized, extended cells with one or more protrusions. Length-width index (cell length divided cell width) of these cells was bigger than 2. Intermediate cells were the cells with uncertain morphology, round-shaped cells with some protrusions or a bit elongated cells that did not match length-width index of 2. Apoptotic and dividing cells were excluded from analysis. Approximately 300 cells were counted for each experiment. At last, proportion of rounded, mesenchymal and intermediate cells was calculated and expressed in percents.

To asses the role of PKCα in cell morphology regulation, activator and inhibitor of PKCα were used. As PKCα activator, phorbol 12-myristate 13-acetate (PMA) was used in final concentration of 162nM. PMA is not PKCα specific activator, it is able to activate all the PKC isoforms. As PKCα inhibitor, Gö6976 was used in 1μM concentration. Gö6976 is PKCα/PKCβ specific inhibitor. However, proteomic analysis did not show any changes in other PKC isoforms than PKCα, so the activator and particularly the inhibitor were considered to be sufficiently specific for our experiments.

Observations of control cells helped us to determine primary morphology of cell lines examined. Analysis confirmed that A375m2 cells are primarily amoeboid and K2 and MDA-MB-231 cells are primarily mesenchymal (Figure 7.3; 7.4).

Upon activator treatment, K2 and MDA-MB-231 cells changed their morphology towards amoeboid. For K2 cells, proportion of amoeboid cells was increased approximately 4 fold and for MDA-MB-231 cells 3 fold increase was observed. In both cases, the number of mesenchymal cells decreased proportionally. This strongly suggests occurrence of MAT. PMA did not have significant effect on A375m2 cells as these cells already were of predominantly rounded morphology.

The other way around, inhibitor treatment resulted in AMT of A375m2 cells, manifested by 2.5 fold increase in proportion of elongated cells. Simultaneously, proportion of rounded cells decreased. Gö6976 did not greatly affect morphology of K2 and MDA-MB-231 cells as these cells were already of mainly elongated morphology (Figure 7.3; 7.4).

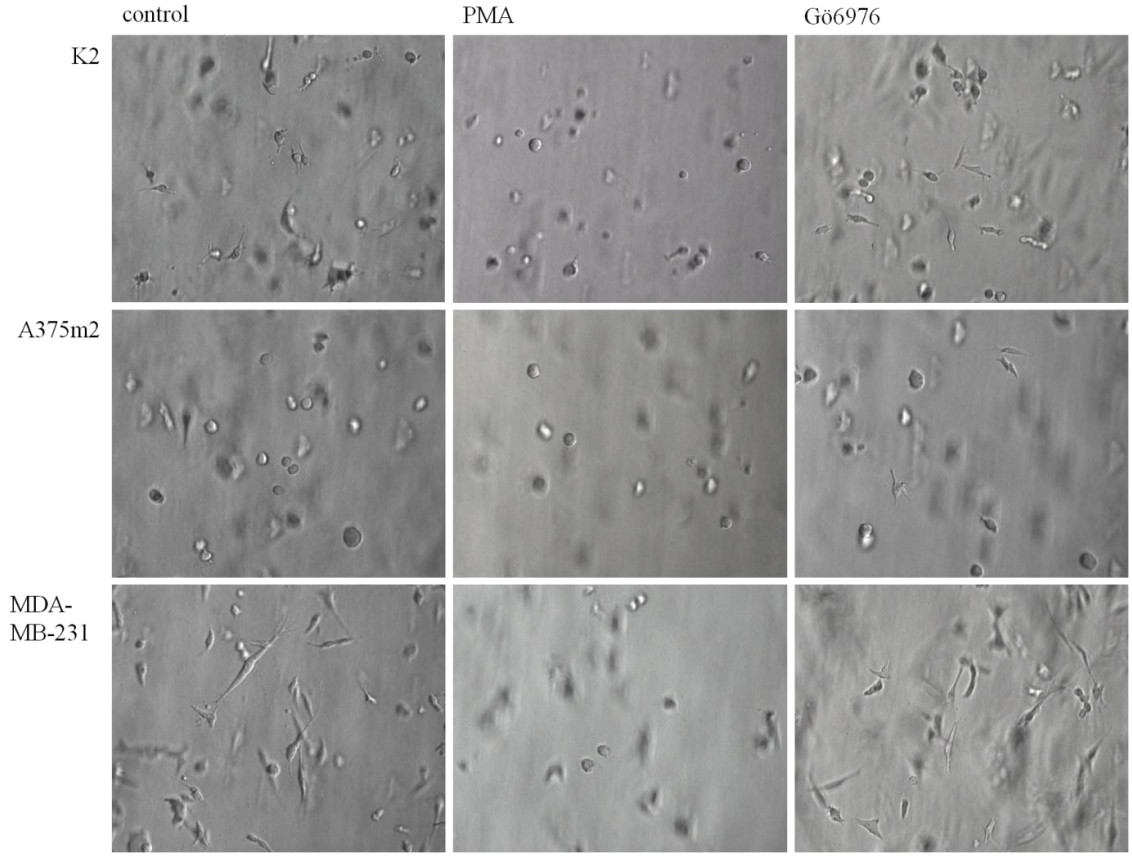

Figure 7.3. Pictures of K2, A375m2 and MDA-MB-231 cells in 3D collagen. K2 and MDA-MD-231 cells show primarily mesenchymal morphology, A375m2 cells are primarily amoeboid (left panel). Morphological changes can be observed upon PKCα activator PMA (middle panel) or PKCα inhibitor Gö6976 treatment (right panel). According to the observations, PKCα activation results in MAT, PKCα inhibition leads to AMT.
Pictures were taken after 48 hours incubation in 3D collagen using microscope Nikon Eclipse TE2000-S with Hoffman modulation contrast (20x / 0.40 HMC objective).

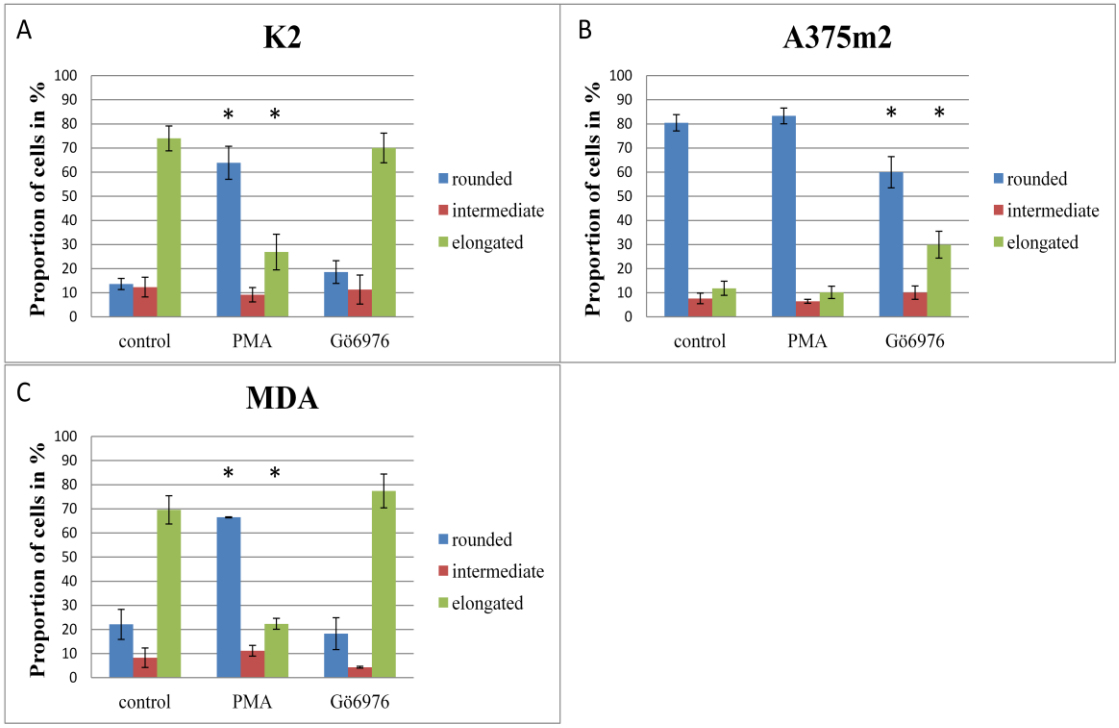

Figure 7.4. Effect of PKCα activator PMA and PKCα inhibitor Gö6976 on morphology of K2, A375m2 and MDA-MB-231 cell lines. Proportion of rounded, elongated and intermediate cells is expressed in percents. K2 and MDA-MB-231 cells exhibited primarily elongated morphology, A375m2 cells were primarily rounded. PKCα activator PMA treatment resulted in more rounded K2 and MDA-MB-231 cells, it did not significantly affect morphology of A375m2 cells. On the other hand, PKCα inhibitor Gö6976 caused change towards elongated shape of A375m2 cells, it did not change morphology of K2 and MDA-MB-231 cells.
A) Morphology of K2 cells.
B) Morphology of A375m2 cells.
C) Morphology of MDA-MB-231 cells.
Approximately 300 cells were observed after 48 hours of incubation in 3D collagen. Cells were analyzed using NIS Elements program (Nikon). Showed results are evaluation from three independent experiments. Error bars represent standard deviations. Statistical significance was evaluated according to unpaired two-tailed Student's t-test. Significant difference ($p<0.05$) in comparison to control is indicated by asterisk.

Morphology of cells is very important marker of invasion mode. Rounded shape of cells is strongly connected to amoeboid invasion and elongated shape to mesenchymal invasion. Although cell morphology is not the only one characteristic of invasion mode, it could be generally said that rounded cells are amoeboid and elongated cells are mesenchymal. Therefore, it could be also suggested that PKC activation caused MAT and PKCα inhibition caused AMT. These observations strongly support the hypothesis that PKCα is important for amoeboid morphology of cancer cells.

7.3 Analysis of expression and phosphorylation of PKCα in cells treated with activator and inhibitor

As PKCα activator and inhibitor are used to specifically activate and inhibit PKCα in these experiments, it was important to know, whether presence of activator or inhibitor influences PKCα status in cell and whether this change can be detected. Therefore, immunoblot analysis of total PKCα expression and its phosphorylation on Thr497 was performed in cells upon activator and inhibitor treatment.

K2, A375m2 and MDA-MB-231 cells were cultured with PKCα activator PMA (final concentration 162nM) or PKCα inhibitor Gö6976 (final concentration 1μM) for 48 hours and then cell lysates were made. Samples were analyzed by Western blot followed by immunodetection using antibodies against total PKCα (Sigma-Aldrich) and its phosphorylation on Thr497 (abcam).

All cell lines showed similar PKCα expression profiles. According to the analysis, control cells and inhibitor treated cells had the same amount of total PKCα, whereas in activator treated cells, amount of PKCα was decreased (Figure 7.5). The level of PKCα phosphorylation on Thr497 in samples had the same overall profile as the total PKCα expression (Figure 7.5).

This could mean that PMA treated cells expressed lower amount of PKCα than control or inhibitor treated cells. However, there is also possibility that prolonged incubation time with PMA can result in enhanced PKCα activation, but also subsequent increased degradation till its depletion (Newton, 1995; Martiny-Baron and Fabbro, 2007). Therefore, also shorter incubation times (10 min, 30 min, 60 min) were analyzed, but no conclusive differences between the lines (control – activator - inhibitor) were seen and no changes in time were observed (data not shown).

Anyway, cell lysates were made after 48 hours because the morphology analysis in 3D collagen was also evaluated after 48 hours. The reason for that is that cells have to adjust themselves to the novel 3D environment and this needs some time.

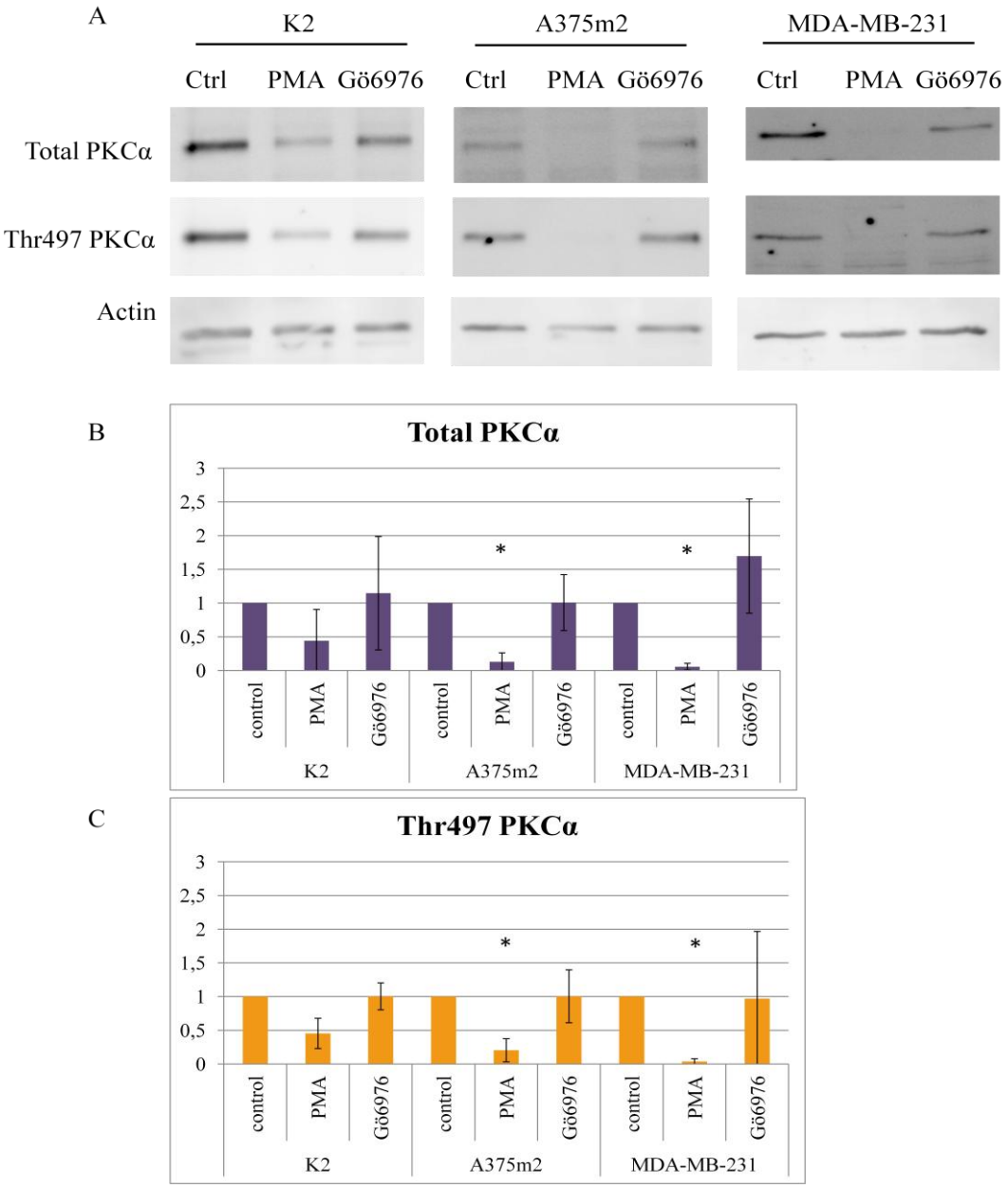

Figure 7.5. Immunoblots of total PKCα and PKCα phosphorylation on Thr497 in K2, A375m2 and MDA-MB-231 cells treated with both PKCα activator PMA and PKCα inhibitor Gö6976. In all cell lines, control and PKCα inhibitor Gö6976 treated cells had similar levels of PKCα expression, whereas in PKCα activator PMA treated cells, PKCα expression was decreased. Phosphorylation of PKCα on Thr497 had the same profile.

A) Representative immunoblots of total PKCα levels (upper line), its phosphorylation on Thr497 and actin verification for the same loadings (lower line) in K2, A375m2 and MDA-MB-231 cells. All cell lines were treated with PKCα activator PMA and PKCα inhibitor Gö6976. Immunoblots are representative from three independent experiments.

B) Densitometric quantification of total PKCα levels, evaluation from three independent experiments. Densitometric analysis was made using ImageJ software, error bars represent standard deviation. Statistical significance was evaluated according to unpaired two-tailed Student's t-test. Significant difference ($p<0.05$) in comparison to control is indicated by asterisk.

C) Densitometric quantification of PKCα phosphorylation on Thr497, evaluation from three independent experiments. Densitometric analysis was made using ImageJ software, error bars represent standard deviation. Statistical significance was evaluated according to unpaired two-tailed Student's t-test. Significant difference ($p<0.05$) in comparison to control is indicated by asterisk.

In addition, to find out whether PKCα phosphorylation on Thr497 changed in respect to total PKCα level, the ratio of phosphorylated PKCα to total PKCα (phosphorylated PKCα divided total PKCα level) was counted (Figure 7.6). However, for all cell lines, no significant or reproducible change of phosphorylation on Thr497 even in respect to total PKCα level was observed.

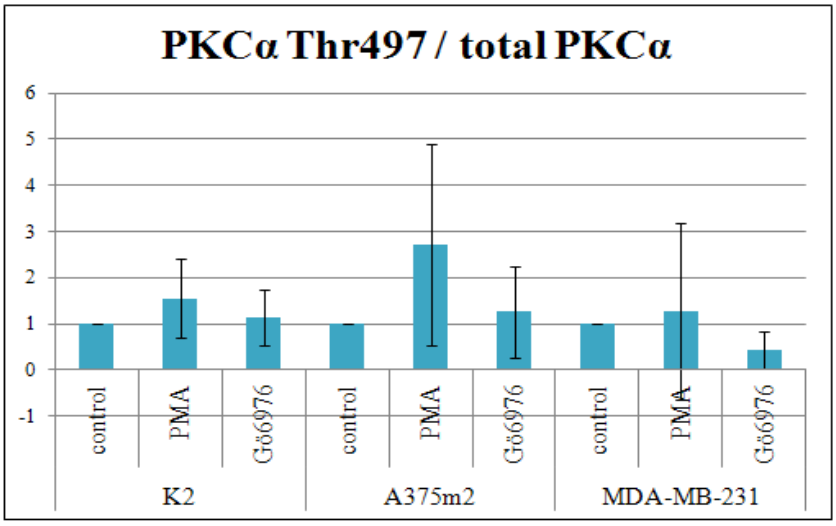

Figure 7.6. Ratio of phosphorylated PKCα on Thr497 to total PKCα.
This value was calculated as phosphorylation level of PKCα divided total PKCα expression level (results from Figure 7.5) to detect if there was any change in phosphorylation on Thr497 respective to total PKCα expression. However, no such reproducible change was according to these results fro three cell lines detected.
Evaluation from three independent experiments is seen, error bars represent standard deviation. Statistical significance was evaluated according to unpaired two-tailed Student's t-test. Significant difference ($p<0.05$) in comparison to control is indicated by asterisk.

These results bring up another question – whether phosphorylation on Thr497 (but also on other two priming phosphorylation sites) really correlates with PKCα activity. As noted previously, this does not have to be always the case (Keranen et al., 1995; Newton, 2000). As the priming phosphorylations correlate more with closed inactive enzyme state (mature enzyme but with bound pseudosubstrate) than with really activated open conformation (activated upon second lipid messengers signals or PMA with pseudosubstrate unbound and ability of phosphorylating its substrates) (Freeley et al., 2011).

7.4 PKCα can regulate morphology of cells in 3D collagen – effect of PKCα siRNA

To further verify specific effect of PKCα isoform on cell morphology, specific downregulation of PKCα expression was performed using siRNA against PKCα and morphology of cells in 3D collagen was examined.

For siRNA-mediated knock-down of PKCα, A375m2 cell line was used. Cells were plated on 6-well plates one day before, so they were 60 – 80% confluent at the day of transfection. Cells were transfected using transfection system jetPRIME™ (Polyplus transfection). Cells were transfected either with siRNA (Silencer® Select Validated siRNA (Applied Biosystems)) or only with transfection reagens (without siRNA) to exclude possible role of transfection reagens in influencing cell morphology (these cells are called MOCK cells). Moreover, as a control, also untreated cells were examined. The final concentration of siRNA used was 10 μM. After 48 hours since transfection, cell lysates were made or cells were seeded into 3D collagen matrix (3 mg/ml Collagen R in growth medium (Collagen type I) (Serva)). Morphology of cells in 3D collagen was examined after 48 hours since collagen preparation. 48 hours incubation time was needed to allow cells to adapt to the novel 3D environment. Cells were observed using microscope Nikon Eclipse TE2000-S (20x / 0.40 HMC objective) and cell morphology was evaluated using NIS Elements program (Nikon) as described previously. Approximately 300 cells were counted for each experiment. Lastly, proportion of rounded, mesenchymal and intermediate cells was calculated and expressed in percents.

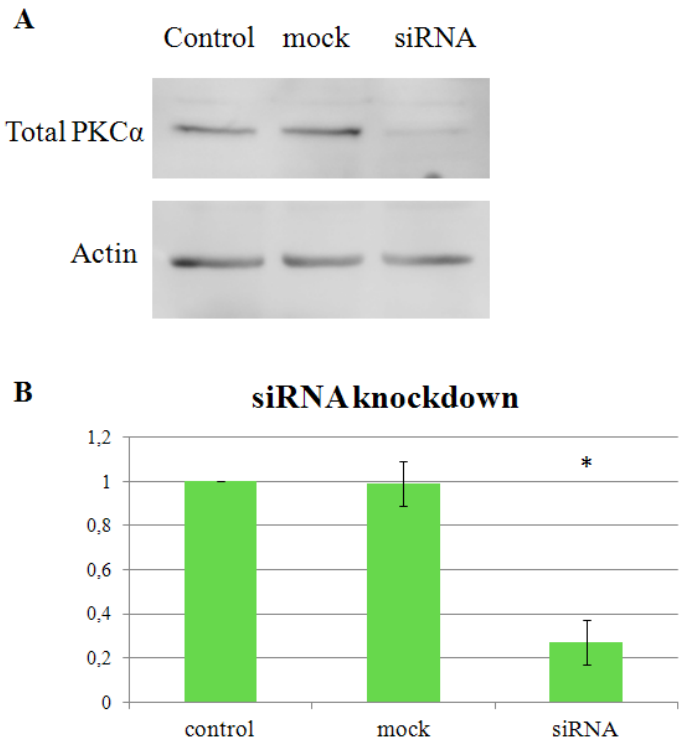

Figure 7.7. Knockdown of PKCα using siRNA in A375m2 cells. By siRNA transfection into A375m2 cells, the level of total PKCα expression was decreased to approximately 30% of initial PKCα expression. A) Representative immunoblots of total PKCα level (upper panel) in control cells (first line), mock cells (transfected only with transfection reagens, without siRNA) (second line) and siRNA transfected cells (third line). Also, actin blot as a verification of the same loadings was performed (lower panel).
B) Densitometric quantification of total PKCα levels, evaluation from three independent experiments. Densitometric analysis was made using ImageJ software, error bars represent standard deviation. Statistical significance was evaluated according to unpaired two-tailed Student's t-test. Significant difference ($p<0.05$) in comparison to control is indicated by asterisk.

To verify the efficiency of siRNA mediated silencing, the control Western blot analysis was made (Figure 7.7). Whole cell lysates from 48 hours transfected cells were made and analyzed by immunoblot using total PKCα antibody (Sigma-Aldrich).

Our results showed that control cells (totally untreated) had the same level of total PKCα as mock cells (transfected only with transfection reagens without siRNA). This confirms that transfection reagens itself did not influence total PKCα expression. Importantly, in siRNA treated cells, total PKCα expression level was significantly lower in comparison to control and mock cells. These cells expressed total PKCα at level only of 30% of initial PKCα expression of control and mock cells.

Analysis of cell morphology confirmed that A375m2 cells are primarily amoeboid. In addition, control and mock cells had very similar morphology profiles which confirms that transfection reagens did not have indirect unspecific effect on cell morphology.

Furthermore, siRNA treated cells exhibited more mesenchymal morphology profile than control and mock cells, suggesting induction of AMT. Proportion of elongated cells increased 2 fold and there was a little increase in proportion of intermediate cells too. Consistently, proportion of rounded cells decreased (Figures 7.8; 7.9).

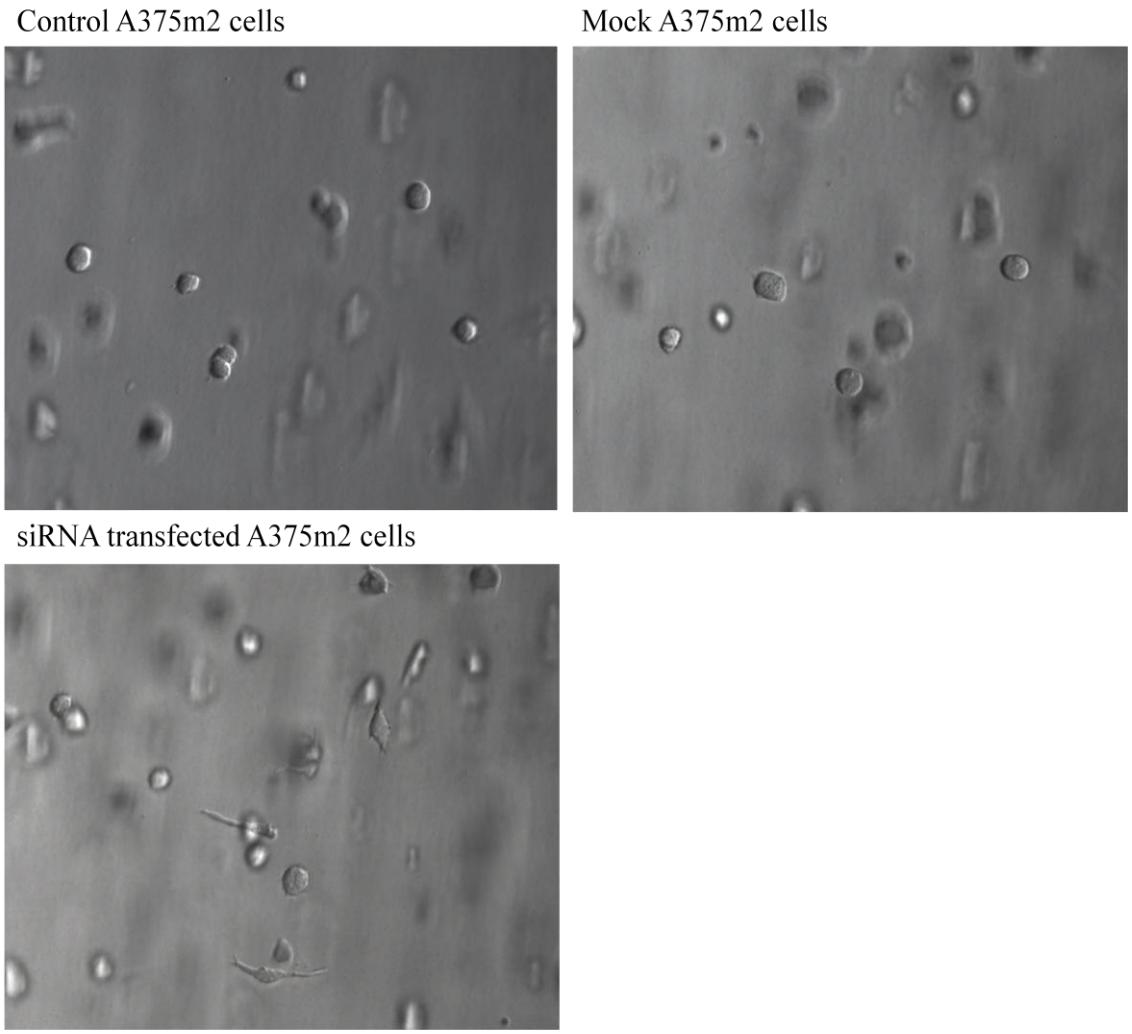

Figure 7.8. Pictures of A375m2 in 3D collagen – effect of PKCα downregulation. Control A375m2 cells (upper left panel) as well as mock cells (transfected only with transfection reagens without siRNA) (upper right panel) showed rounded morphology. Upon siRNA treatment, proportion of elongated cells significantly increased (lower panel).
Pictures were taken after 48 hours incubation in 3D collagen using microscope Nikon Eclipse TE2000-S with Hoffman modulation contrast (20x / 0.40 HMC objective).

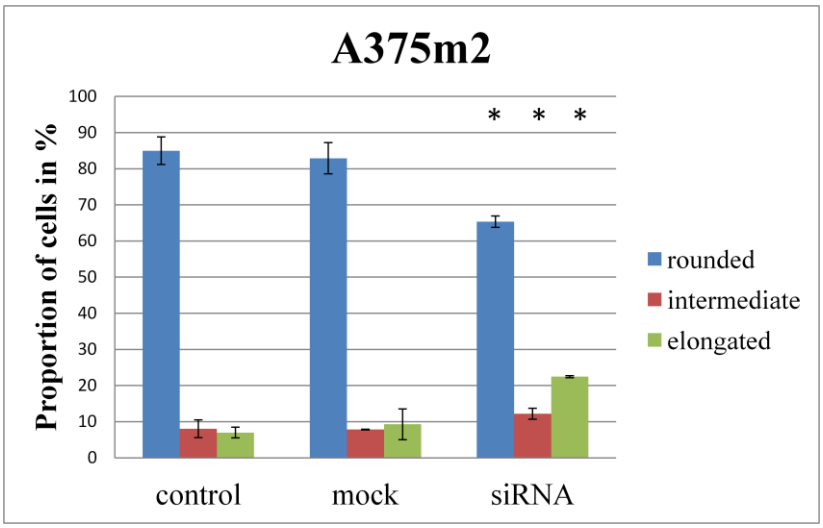

Figure 7.9. Effect of PKCα knockdown on morphology of A375m2 cells. As noted previously, A375m2 cells are primarily amoeboid. For control, mock cells (transfected only with transfection reagens, not with siRNA) showed similar morphology. Most importantly, siRNA transfected cells exhibited decrease in number of rounded cells and increase in number of intermediate and elongated cells, suggesting AMT.
Approximately 300 cells were observed after 48 hours of incubation in 3D collagen. Cells were analyzed using NIS Elements program (Nikon). Showed results are evaluation from three independent experiments. Error bars represent standard deviations. Statistical significance was evaluated according to unpaired two-tailed Student's t-test. Significant difference ($p<0.05$) in comparison to control is indicated by asterisk.

To sum up, these results suggest that PKCα could have role in amoeboid morphology and presumably also invasion.

7.5 PKCα can regulate invasion of cells *in vitro* – effect of PKCα activator and inhibitor

Next, invasivity of cells *in vitro* was analyzed to determine the effect of PKCα on capacity of cells to invade 3D collagen.

Again, K2, A375m2 and MDA-MB-231 cell lines were used. For invasion assay, specialized invasion wells were used (µ-Slide Angiogenesis ibiTreat Microscopy Chamber (IBIDI)). Invasion wells were filled with collagen solution (containing 2 mg/ml Collagen R (Serva) and 4 mg/ml Collagen G (Biochrom)) and when collagen gained gel-like consistency, cell suspension (in full growth medium) was added on top of collagen. Next day, medium was aspirated and changed for serum-free medium with PKCα activator PMA or PKCα inhibitor Gö6976. PMA was added to reach final concentration of 162 nM and Gö6976 was added to final concentration of 1 µM. Cells

were allowed to invade into 3D collagen for 48 hours and then relative invasivity of cells was examined using microscope Nikon Eclipse TE2000-S (20x / 0.40 HMC objective). Using NIS Elements program (Nikon), the most flat field in well was found (usually in the middle of the well) and it was focused on cells on the surface. Next, images of collagen cross-sections were taken every 10 µm heading towards the bottom. Then, focused cells in every cross-section were counted and relative invasivity index was calculated as follows:

$$\text{relative invasivity index} = \frac{\sum \text{number of focused cells in cross-section} \times \text{depth of cross-section in } \mu\text{m}}{\text{total number of cells in all cross-sections}}$$

To compare between experiments, relative invasivity index was normalized to that of untreated cells.

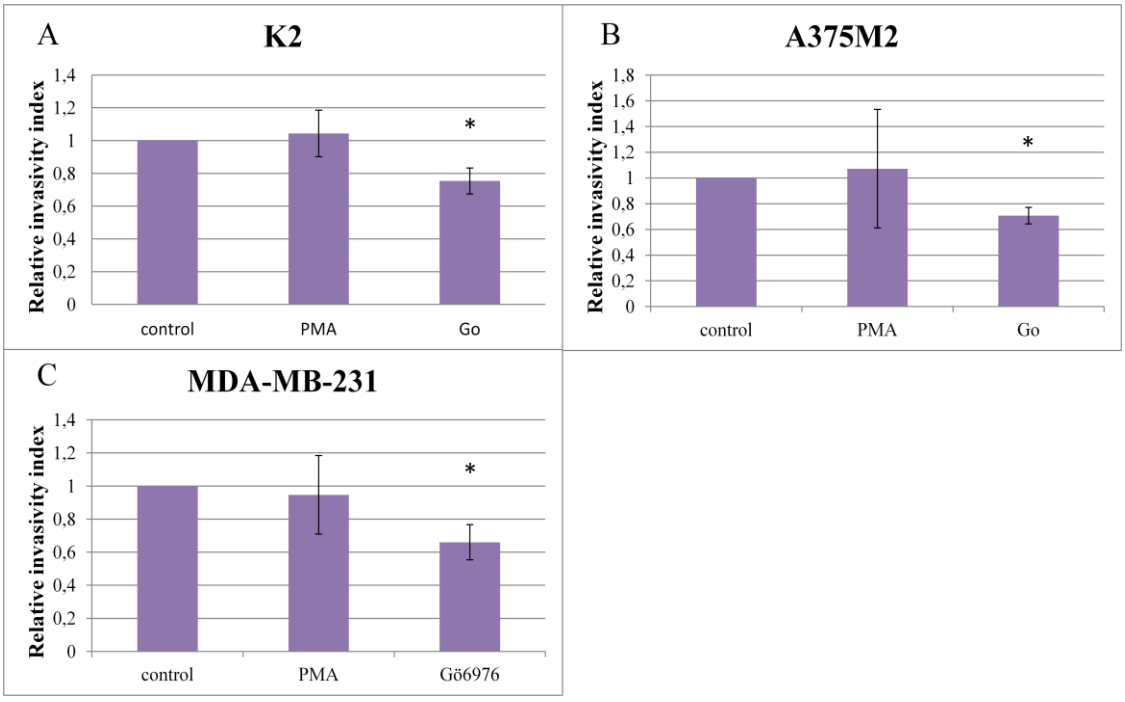

Figure 7.10. Invasivity analysis of K2, A375m2 and MDA-MB-231 cells and effect of PKCα activator PMA and PKCα inhibitor Gö6976 on cell invasivity *in vitro*. Observations revealed that PKCα activator PMA treatment did not change invasivity of cells in vitro in any of three cell lines. However, upon PKCα inhibition by Gö6976, invasivity of all three cell lines was significantly decreased.
A) Invasivity analysis of K2 cells.
B) Invasivity analysis of A375m2 cells.
C) Invasivity analysis of MDA-MB-231 cells.
Showed results are calculated from four independent experiments. Cross-sections were taken and analyzed by NIS Elements program (Nikon). Error bars represent standard deviations. Statistical significance was evaluated according to unpaired two-tailed Student's t-test. Significant difference ($p<0.08$) in comparison to control is indicated by asterisk.

In *in vitro* invasion analysis, all investigated cell lines showed similar responses to PKCα activation and inhibition. Incubation of cells with PKCα activator PMA did not significantly change cell invasion potential of any of three cell lines examined. On the other hand, PKCα inhibitor Gö6976 treatment resulted in significant decrease in cell invasion abilities of all three cell lines. This decrease was 1.3 fold in the case of K2 cells, 1.5 fold in the case of MDA-MB-231 cells and 1.4 fold in the case of A375m2 cells. Together, PKCα inhibition caused reduction of cell invasion to approximately 70% of initial cell invasion of control cells in all three cell lines (this represents approximately 1.4 fold decrease).

It is interesting, that although PKCα activation did not have any specific effect on cell invasion, PKCα inhibition significantly reduced cell invasion potential of all three cell lines investigated. Nevertheless, this *in vitro* invasion analysis gave us important evidence that PKCα could be involved in regulating of cell invasivity.

7.6 PKCα can regulate invasion of cells *in vitro* – effect of PKCα siRNA

To further evaluate specific effect of PKCα on cell invasion, specific knockdown of PKCα was performed by siRNA and cells were used for *in vitro* invasion analysis.
A375m2 were plated on 6 well plate so to be 60 – 80% confluent at the day of transfection. Cells were transfected with siRNA against PKCα (Silencer® Select Validated siRNA (Applied Biosystems)) using jetPRIME^{TM} transfection system (Polyplus transfection). Final concentration of PKCα was 10 μM. As a control, control cells (totally untreated), but also mock cells (transfected only with transfection reagens, not with siRNA) were used to prove that transfection reagens did not have any unspecific effect on cell invasion. After 48 hours, transfected cells were transferred into growth medium and cell suspension was plated onto pre-prepared collagen gel in specialized invasion wells (μ-Slide Angiogenesis ibiTreat Microscopy Chamber (IBIDI)). Next day, growth medium was replaced for serum-free medium and cells were allowed to invade into 3D collagen. After 48 hour incubation, images of collagen cross-sections were taken every 10 μm starting at the surface and heading to the bottom.

Focused cells in every cross-section were counted and relative invasivity index was calculated:

$$\text{relative invasivity index} = \frac{\sum \text{number of focused cells in cross-section} \times \text{depth of cross-section in } \mu m}{\text{total number of cells in all cross-sections}}$$

To compare between experiments, relative invasivity index was normalized to that of untreated cells.

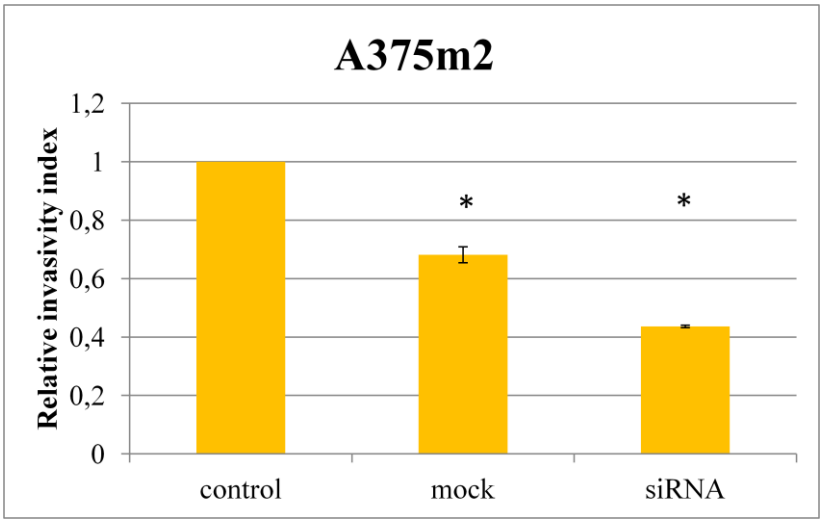

Figure 7.11. Invasivity analysis of A375m2 cells and effect of PKCα knockdown on cell invasivity *in vitro*. According to our observations, mock cells (transfected only with transfection reagens, not with siRNA) exhibited lower invasivity than control cells. However, more important fact is that siRNA treated cells exhibited significantly decreased invasivity comparing to control cells, but this decrease in invasivity was also significant comparing to mock cells.
Showed results are calculated from two independent experiments. Cross-sections were taken and analyzed by NIS Elements program (Nikon). Error bars represent standard deviations. Statistical significance ($p<0.05$) was evaluated according to unpaired two-tailed Student's t-test. Significant difference ($p<0.05$) in comparison to control is indicated by asterisk.

For siRNA mediated silencing, untreated cells as well as mock cells (transfected only with transfection reagent without siRNA) were used as a control that transfection reagens itself did not have any unspecific effect on cell invasion. It is noteworthy, therefore, that mock cells invaded into 3D collagen significantly less than control cells (Figure 7.11). This could suggest a possible effect of transfection reagens on cell behavior, specifically on cell invasion (as none unspecific effect of transfection reagens was observed on cell morphology).

More importantly, siRNA mediated knockdown of PKCα resulted in a considerable 2.5 fold decrease in cell invasion comparing to control cells. Moreover, the ability of siRNA treated cells to invade into 3D collagen was reduced 1.5 fold comparing to mock cells too (Figure 7.11).

In vitro invasion analysis of siRNA transfected cells showed that PKCα downregulation reduced cell invasivity in 3D collagen. This is in consistence with previous experiments where PKCα inhibition also resulted in significant decrease in cell invasion potential. Together, these results propose important role of PKCα in cell invasivity.

7.7 Effect of PKCα activator and inhibitor on invadopodia formation and ECM degradation

To further elucidate how PKCα could regulate cell invasion, its effect on invadopodia formation and ECM degradation was investigated.

ECM degradation is very important feature of mesenchymal cells. Mesenchymal cells produce enzymes (matrix metalloproteinases, cathepsins, serine proteases and other) that are able to cleave and degrade ECM components and this way they make a path for their migration. On the other hand, amoeboid cells are not dependent on ECM degradation, rather, they produce acto-myosin force to squeeze through ECM fibers (reviewed in Paňková et al., 2010). Importantly, upon inhibition of proteolysis in mesenchymal cells, transition from mesenchymal to amoeboid invasion mode was observed (Wolf et al., 2003). Therefore, ECM degradation by cells is very important marker of mesenchymal mode of invasion.

Mesenchymal cells form specific structures into which their ECM degradation ability is situated. These structures are called invadopodia (reviewed in Weaver, 2006; Buccione et al., 2004). Invadopodia are actin-rich membrane protrusions containing also actin-regulatory proteins (Arp2/3, N-WASP, cortactin), adhesion molecules (integrins), signaling molecules (Src) and matrix degrading enzymes (MT1-MMP, MMP-2, MMP-9).

When cells are seeded on thin layer of fluorescently-labeled gelatin, invadopodia formation and gelatin degradation by cells can be visualized. In microscope, invadopodia are visible as punctuate structures, in which actin and cortactin (or phospho-cortactin) co-localize. Gelatin degradation is visible as areas that lack FITC-labeled gelatin (they are seen as dark areas in otherwise green gelatin). Typically, degradation areas occur beneath invadopodia and this way, functional (invadopodia

under which gelatin degradation can be seen) and non-functional (invadopodia without any gelatin degradation beneath) invadopodia can be distinguished.
To analyze the effect of PKCα activation and inhibition on invadopodia formation and ECM degradation, and to find out whether PKCα-mediated effect on the ratio of mesenchymal / amoeboid state of our cells correlated with its effect on matrix-degrading activity, above described assay was used.

A375m2 cell line was used. First, FITC-labeled gelatin-coated coverslips were prepared and then, cells were plated on them. PKCα activator PMA and PKCα inhibitor Gö6976 were added (PMA in concentration of 162nM and Gö6976 in concentration of 1 μM) and cells were allowed to adhere to gelatin and to degrade it for 24 hours. Next day, cells were fixed, permeabilized and stained to visualize actin and cortactin or phospho-cortactin. For actin staining, fluorescently labeled phalloidin (Alexa Fluor® 405 phalloidin (Invitrogen)) was used. For cortactin staining, first primary rabbit antibodies against cortactin (Santa Cruz Biotechnology) or phospho-cortactin (BioSource) were used and then secondary fluorescently-labeled antibody (Alexa Fluor® 546 Goat anti-rabbit IgG (Invitrogen)) was used. After staining, coverslips were mounted on a mounting slide and cells were prepared for microscopy.
For gelatin degradation assay, fluorescent microscope Nikon Eclipse TE2000-S was used (20x / 0.40 HMC objective). Images were taken in two different levels – cortactin level (546 nm) and gelatin level (488 nm). For each experiment, seven random fields were examined. Evaluation was done using AnalyzeGelStack software (obtained from Dr. Buccione). This software allows to measure degradation area normalized to the number and area of cells (degradation area per cell). Degradation area of treated cells was always normalized to degradation area of control untreated cells.
For better visualization of cells and of invadopodia, confocal microscope Leica DM IRE2 was used. Images were taken in three levels – cortactin level (546 nm), actin level (405 nm) and gelatin level (488 nm).

Invadopodia analysis can be done manually from microscopic images of cells. As noted previously, invadopodia can be seen as dots where actin and cortactin (or phospho-cortactin) co-localize. By counting these punctuate structures in each cell, number of invadopodia per cell can be determined. Moreover, functionality of each invadopodia can be investigated by presence or absence of gelatin degradation under each dot.

Interestingly, in spite of the fact that A375m2 are primarily amoeboid, they are able to form invadopodia (Baldassarre et al., 2003). However, in our conditions used, invadopodia analysis was not successful. This was for a few technical obstacles which we did not have time to resolve.

First, cortactin staining (marker of invadopodia) was mostly disperse, sometimes punctuate, but mostly with no larger distinct dots (that could represent invadopodia) observed. Moreover, actin staining did not detect any bigger dots too and therefore actin and cortactin co-localization could not be observed. Consequently, it was very hard to distinguish between background signal and signal that could mark invadopodia sites.

Despite of this fact, invadopodia were considered as larger cortactin puncta in cells. However, only part of cells in sample produced invadopodia. It was necessary to look for the cells with invadopodia in the sample and this could have lead to the non-representative selection of cells. Furthermore, there was still problem with punctuate background of cells and many cells seemed to produce tens of invadopodia. Moreover, only observation of samples in confocal microscope provided sufficiently focused and resoluted images to visualize these small cell structures adequately. However, this required bigger zooming and visualization of only one or few cells per field and so, it would have required visualization of many more fields to be statistically significant. Therefore, analysis of invadopodia formation could have been misleading.

For all these complications, invadopodia analysis was excluded from analysis of the effect of PKCα on cancer cell invasion.

Nevertheless, A375m2 cells degraded gelatin efficiently and so gelatin degradation and the effect of PKCα activation and inhibition on gelatin degradation was investigated.

Our analysis revealed interesting information (Figure 7.12, 7.13). As noted previously, A375m2 cells are primarily amoeboid and their invasion is proteolysis-independent. It is interesting, therefore, that also control A375m2 cells were capable of matrix degradation (Figure 7.13).

As seen from the graph and images (Figure 7.12, 7.13), gelatin degrading ability of PKCα inhibitor Gö6976 treated cells remained unchanged in comparison to control cells. On the other hand, PKCα activation by PMA resulted in greatly reduced gelatin degrading ability of A375m2 cells. This suggests even more amoeboid phenotype of A375m2 cells and it in consistence with previous morphology results which showed that PKCα plays role in amoeboid invasion.

It is also interesting, that treatment with PKCα inhibitor did not show any effect on gelatin degradation, if PKCα activator did. This could be caused by inefficient dose of inhibitor for changes in matrix degrading abilities.

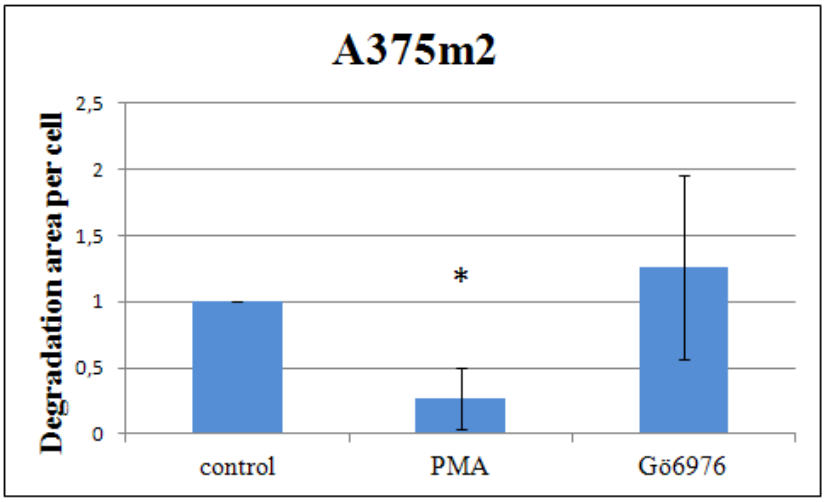

Figure 7.12. Gelatin degradation by A375m2 cells and effect of PKCα activator PMA and PKCα inhibitor Gö6976 on matrix degrading activity of these cells.
Incubation with PKCα inhibitor Gö6976 did not show any change in gelatin degradation area per cell comparing to control. On the other hand, PKCα activator PMA treatment resulted in significant decrease in degradation area.
Showed results are calculated from three independent experiments. Images were analyzed by AnalyzeGelStack software. Error bars represent standard deviations. Statistical significance was evaluated according to unpaired two-tailed Student's t-test. Significant difference ($p<0.05$) in comparison to control is indicated by asterisk.

Notably, some inconsistencies in gelatin degradation were observed. It seemed like two different reasons of gelatin absence can be distinguished. There was detected "genuine" gelatin degradation (by matrix degrading enzymes that were secreted by cells) (for typical gelatin degradation see Figure 7.13 – control A375m2 cells). However, there were also areas where no gelatin was present, but a higher signal was observed on the edges of these areas, as if gelatin was not proteolytically cleaved, but torn (see Figure 7.13 – Gö6976 treated A375m2 cells). These areas were localized mostly at the edges of cells, whereas gelatin degradation by enzymes localized predominantly underneath cell body. This supports the possibility, that gelatin was torn by traction forces generated by cells while contracting their membrane protrusions.

It is therefore a question, whether also these sites can be considered as gelatin degradation. It is important to note, however, that although these sites are probably not degraded by matrix degrading enzymes, they are not present in all cells in the sample

and sometimes also differences between different conditions were seen. So, it was not a stable value that remained unchanged. Therefore, these torn sites could represent another feature of migrating cells – strength of their protrusions contraction that can be changed upon different conditions (here - treatment with activator or inhibitor).

Unfortunately, it was not possible to distinguish between these two types of lack of gelatin during gelatin degradation evaluation using AnalyzeGelStack software and so, these results were very hard to interpret.

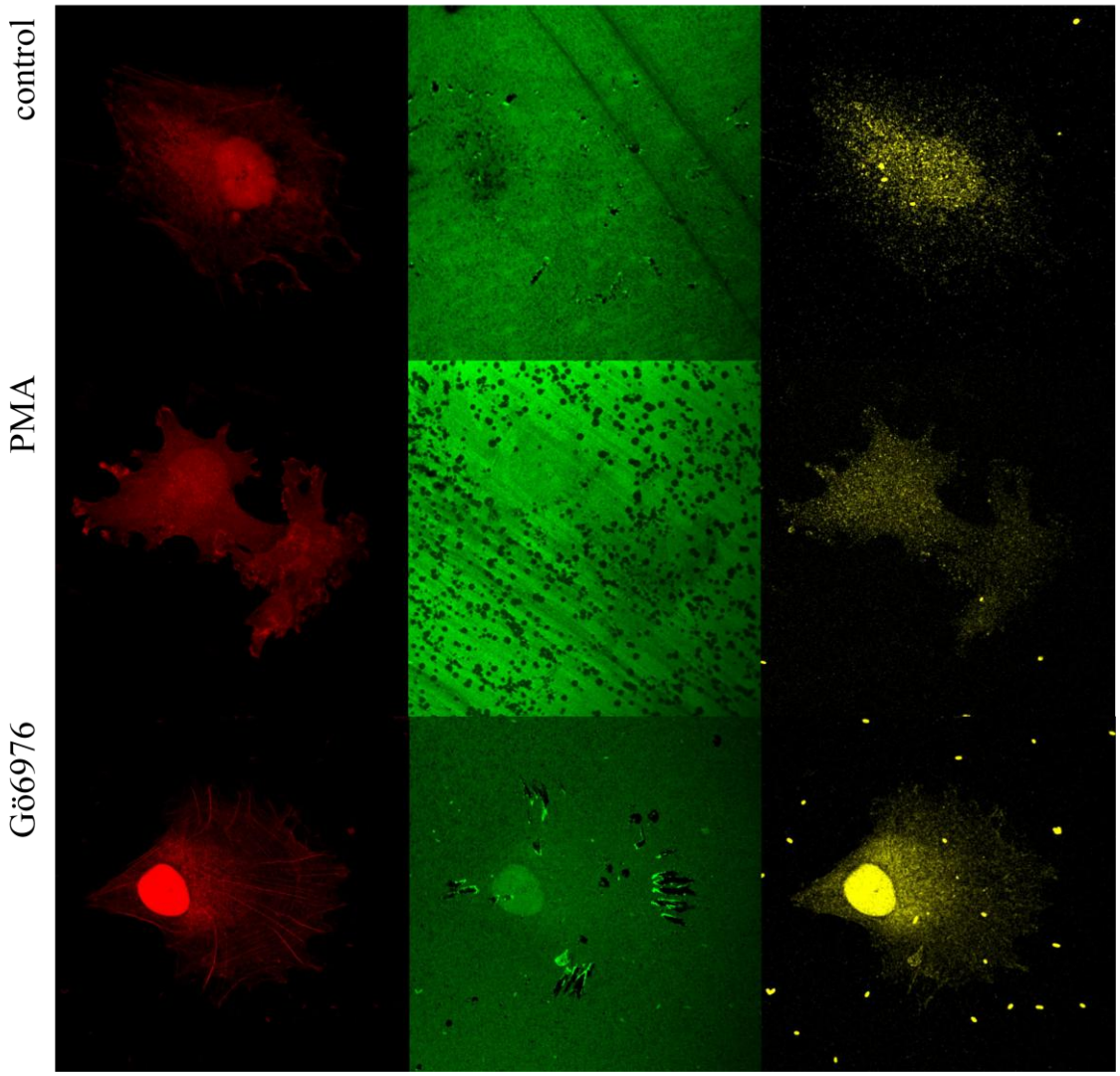

Figure 7.13. Representative images of A375m2 cells plated on fluorescently-labeled gelatin and effect of PKCα activator PMA (middle panel) and inhibitor Gö6976 (lower panel) on gelatin degradation comparing to control cells (upper panel).
Note, that gelatin layer of PMA treated cells is a little bit disrupted on its own, no gelatin degradation by cells can be observed.
Images were taken using confocal microscope Leica DM IRE2.

To sum up, our investigations showed that A375m2 cells are able to produce invadopodia and degrade extracellular matrix although being amoeboid. PKCα inhibitor Gö6976 did not have great effect on gelatin degradation. However, it was obvious, that PKCα activator PMA decreased gelatin degrading ability of A375m2 cells, supporting even more amoeboid phenotype of these cells and suggesting that PKCα is important pro-amoeboid protein.

7.8 Effect of PKCα siRNA on ECM degradation

To investigate specific effect of PKCα on ECM degradation, PKCα was specifically downregulated by siRNA and matrix degradation assay was performed.

Again, 60 – 80% confluent A375m2 cells were transfected with PKCα siRNA (Silencer® Select Validated siRNA (Applied Biosystems)). Cells were transfected by jetPRIME^{TM} transfection system (Polyplus transfection) with final concentration of siRNA 10 μM. As a control, totally untreated cells, but also mock cells (transfected only with transfection reagens, not with siRNA) were used to exclude unspecific effect of transfection reagens on matrix degradation. After 48 hours since transfection, cells were plated onto prepared FITC-labeled gelatin-coated coverslips. Overnight, cells were allowed to adhere and degrade gelatin and next day, cells were fixed and stained for actin and cortactin (or phospho-cortactin). For actin staining, fluorescently labeled phalloidin (Alexa Fluor® 405 phalloidin (Invitrogen)) was used. For cortactin staining, first primary rabbit antibodies against cortactin (Santa Cruz Biotechnology) or phospho-cortactin (BioSource) were used and then secondary fluorescently-labeled antibody (Alexa Fluor® 546 Goat anti-rabbit IgG (Invitrogen)) was used. Finally, coverslips were mounted on a mounting slide.

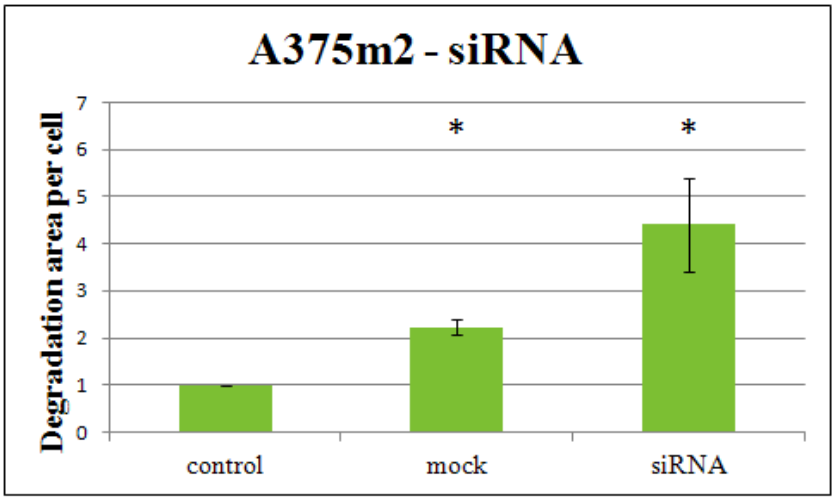

Figure 7.14. Gelatin degradation by A375m2 cells and effect of PKCα downregulation on matrix degrading activity. PKCα silencing in A375m2 cells resulted in more than four-times enhanced gelatin degradation area comparing to control cells and two-times bigger gelatin degradation area in comparison to mock cells.
Showed results are calculated from two independent experiments. Images were analyzed by AnalyzeGelStack software. Error bars represent standard deviations. Statistical significance was evaluated according to unpaired two-tailed Student's t-test. Significant difference ($p<0.05$) in comparison to control is indicated by asterisk.

Images for gelatin degradation assay were taken by fluorescent microscope Nikon Eclipse TE2000-S was used (20x / 0.40 HMC objective). Images were taken in cortactin level (546 nm) and gelatin level (488 nm). Seven random fields were analyzed in each experiment using AnalyzeGelStack software (obtained from Dr. Buccione). Using this software, degradation area normalized to the number and area of cells (degradation area per cell) was measured. Values were normalized to value of control untreated cells.
Confocal microscope Leica DM IRE2 was used for better cell visualization and taking representative pictures. Three levels (cortactin level (546 nm), actin level (405 nm) and gelatin level (488 nm)) were always imagined.

As noted previously (Chapter 7.7), under conditions used, invadopodia analysis could not be performed and the effect of PKCα siRNA on invadopodia formation and functionality could not be investigated.

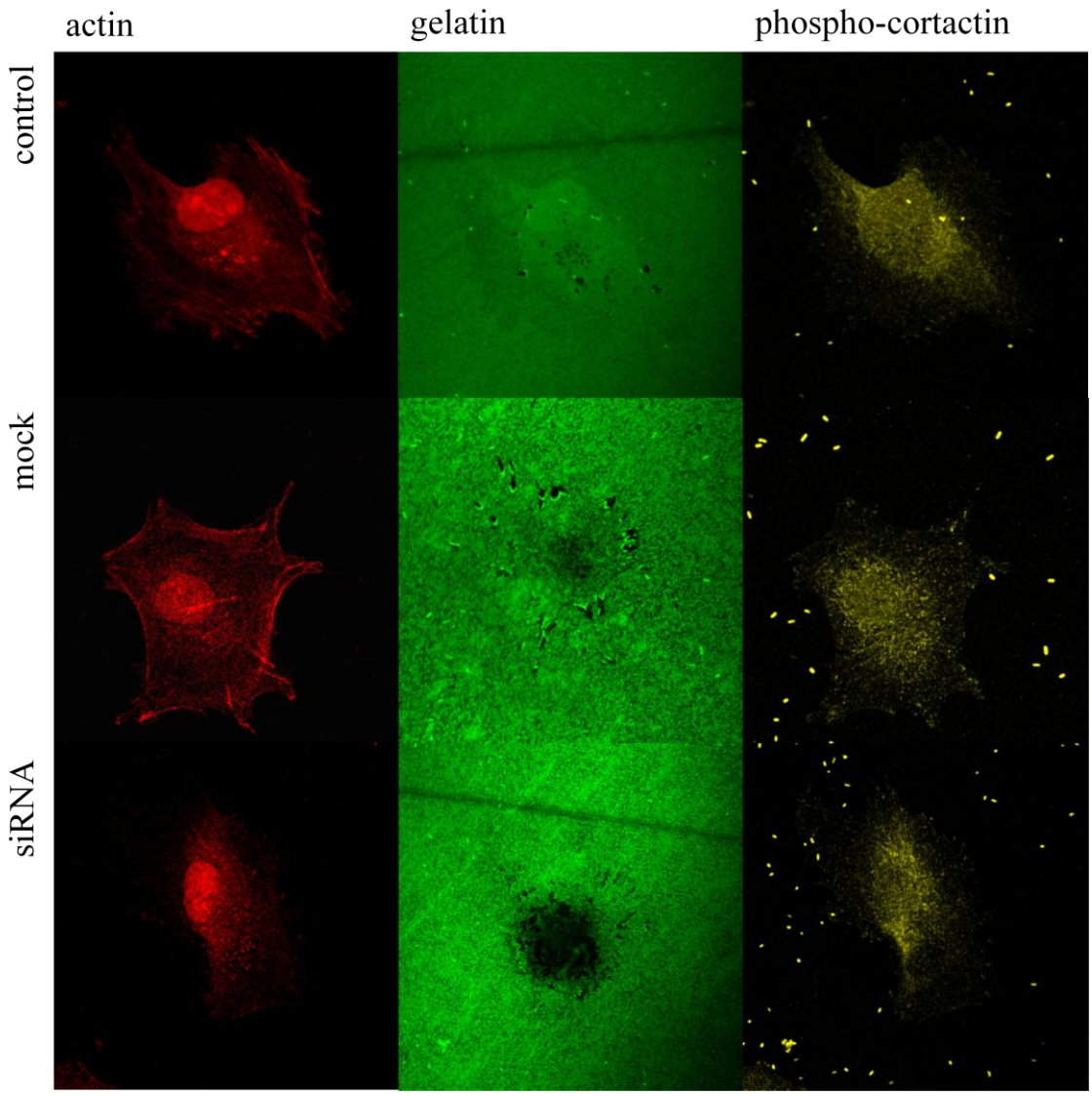

Figure 7.15. Images of A375m2 cells plated on fluorescently-labeled gelatin and effect of PKCα downregulation on gelatin degradation. Control A375m2 cells (upper panel) are able to degrade gelatin. This ability is a bit higher in mock cells (middle panel). Importantly, siRNA treatment (lower panel) greatly enhanced gelatin degradation ability of A375m2 cells.
Images were taken using confocal microscope Leica DM IRE2.

Nonetheless, area of degraded gelatin by cells was evaluated.

As a control, untreated cells, but also mock (transfected with only transfection reagens without siRNA) cells were used to verify, that transfection reagens does not have any indirect effect on gelatin degradation. As seen from the graph (Figure 7.14), mock cells exhibited two times enhanced matrix degrading ability and this difference was statistically significant, so a little effect of transfection reagens could not be excluded during analysis.

Anyway, siRNA transfected cells showed two-fold increase of gelatin degradation comparing to mock cells. This increase was even more significant comparing to control untreated cells, where siRNA transfected cells showed more than four times greater gelatin degradation area (Figure 7.15).

siRNA mediated downregulation of PKCα resulted in considerable increase in gelatin degradation. This suggests that PKCα is important pro-amoeboid protein and upon its silencing, cells can switch from amoeboid to mesenchymal mode of invasion.

8. Discussion

The aim of this thesis was to investigate the possible role of protein kinase C α (PKCα) in amoeboid mode of cancer cell invasion.

PKCα is very important protein regulating many signaling pathways in cell such as proliferation, differentiation, polarity, secretion, apoptosis and tumorigenesis. PKCα was also shown to regulate cell migration and invasion.
Previous results from our laboratory suggested that PKCα could be particularly involved in amoeboid invasiveness of cancer cells (Kasalová, 2010). Proteomic analysis of amoeboid A375m2 cells revealed, that phosphorylation of PKCα at Ser657 is reduced upon induction of amoeboid-mesenchymal transition (AMT) (induced by inhibitor of ROCK kinase), although total PKCα expression level remained unchanged. This was observed both in 2D and in 3D environment. Decrease in the phosphorylation at Ser657 was also confirmed by immunoblot analysis, however, only in 3D environment (Kasalová, 2010). This suggests that mesenchymal state of A375m2 cells is connected to decreased activity of PKCα.

To further elucidate PKCα status in A375m2 cells in their amoeboid (primary) or mesenchymal state (induced by inhibitor of ROCK kinase), PKCα expression and PKCα phosphorylation at Thr497 were investigated. Phosphorylation at Thr497 is one of three priming phosphorylations (together with above noted Ser657 and also Thr638) that are required for PKCα maturation, because of enabling subsequent activation by second lipid messengers upon specific extracellular signals (Newton, 2010).
It was observed, that total PKCα expression level remained unchanged upon AMT (induced by inhibitor of ROCK kinase) both in 2D and in 3D environment. This result was in consistence with proteomic analysis performed previously (Kasalová, 2010) and was not surprising since 24 hours incubation time may not be long enough for change of PKCα gene expression. Moreover, activity of protein is regulated not just through its amount in cell (expression level), but more often through influencing its activation status (e.g. by phosphorylation or dephosphorylation).
However, PKCα phosphorylation levels at Th497 were not changed upon AMT in A375m2 cells cultured in 2D and 3D environments. These results suggest that PKCα

activation status did not probably changed upon AMT and therefore PKCα activation is not exclusively associated with amoeboid invasion as was suggested previously.
Nevertheless, it is important to note, that amoeboid invasion is very complex process with many signaling pathways involved. In our case, AMT was induced by inhibition of just one essential pathway, and almost at its downstream end, very close to the effector proteins. This was enough to induce AMT, as the cells changed their morphology and maybe also some other signaling pathways were adapted, but it is very probable that not all pathways were influenced. So, AMT does not have to necessarily influence PKCα expression or activation.
Furthermore, if we propose that PKCα somehow regulates Rho/ROCK pathway, upon inhibition of ROCK kinase, this pathway is still off, not depending on upstream regulators such as PKCα. Therefore, these cells would be still mesenchymal, no matter how the PKCα activation status would be.
As a result, PKCα expression and activation could remain unchanged even after transition of amoeboid cells to mesenchymal state. But still, this does not exclude the possibility, that PKCα could be upstream of signaling pathways regulating cell invasion and this way, PKCα could regulate amoeboid invasivity of cancer cells and transitions between modes of cell invasion.

So, to further elucidate the possible role of PKCα in amoeboid invasion, morphology analysis, invasivity analysis and gelatin-degradation analysis were performed. PKCα activator PMA, PKCα inhibitor Gö6976 and siRNA against PKCα were used to manipulate the PKCα activation status.

Morphology analysis revealed that PKCα is very important protein for cell morphology. PKCα activation resulted in mesenchymal-amoeboid transition (MAT) of mesenchymal K2 and MDA-MB-231 cell lines. It did not change morphology of amoeboid A375m2 cells, but it is not surprising, as these cells already exhibited amoeboid morphology. The other way around, PKCα inhibition lead to amoeboid-mesenchymal transition (AMT) of amoeboid A375m2 cells. Consistently with these results, siRNA mediated downregulation of PKCα caused AMT of amoeboid A375m2 cells. PKCα inhibition did not cause any change in morphology of K2 and MDA-MB-231 cells as these cells were already mesenchymal.

As PKCα activation resulted in MAT and PKCα inhibition or downregulation resulted in AMT, it is obvious, that PKCα is important pro-amoeboid protein presumably regulating also amoeboid morphology.

It is noteworthy, that morphology assay in 3D collagen evaluates only morphology of cells (rounded or elongated), not directly invasion mode (amoeboid or mesenchymal), because invasion mode is complex process characterized by many more features. Nevertheless, it is generally accepted that rounded cells are considered to migrate in an amoeboid way and elongated cells are strongly connected to mesenchymal invasion mode. In this context and also often in literature, rounded morphology implies amoeboid invasion mode and elongated cells are considered to be mesenchymal (Paňková et al., 2012; Berton et al., 2009; Carragher et al., 2006; Fujita et al., 2011; Gadea et al., 2008; Wolf et al., 2003).

As PKCα activator and PKCα inhibitor were used in our experiments, it was necessary to investigate the effect of activator and inhibitor used on PKCα status in cells.

Immunoblot analysis revealed that upon PKCα inhibitor Gö6976 PKCα treatment expression and phosphorylation remained unchanged. Gö6976 is PKCα and PKCβI specific inhibitor that interacts with ATP binding site (Martiny-Baron et al., 1993). Therefore, it is not surprising, that Gö6976 did not have any effect on PKCα expression. Furthermore, this is also in consistence with previously performed proteomic analysis of A375m2 cells after AMT (Kasalová, 2010). Its effect on PKCα phosphorylation is also understandable as there is no reason to think that blocking of nucleotide binding site should influence enzyme phosphorylation.

This analysis also revealed that total PKCα level as well as phosphorylation at Thr497 was significantly decreased upon PKCα activator PMA treatment in A375m2 and MDA-MB-231 cells. The reduction in PKCα expression level and also in PKCα phosphorylation at Thr497 was observed also in K2 cells, albeit the decrease was not statistically significant.

These results suggest that PMA treated cells express lower amount of PKCα than control cells. However, there could be also another explanation. PMA belongs to the group of phorbol esters that are very potent activators of PKCs. This ability is due to their similarity to diacylglycerol (natural PKC activator) – they can bind and activate PKC (Kikkawa et al., 1983). Phorbol esters are not easily metabolized and therefore incubation with phorbol esters causes enhanced PKC activity (Newton, 1995). In a

longer incubation time, however, this can result also in enhanced PKC degradation (Martiny-Baron and Fabbro, 2007).

So, to verify that we could detect PMA and Gö6976 mediated changes in the activity of PKCα, also shorter incubation times (10 min, 30min, 60 min) were analyzed for PKCα expression and phosphorylation. However, no conclusive differences between the control, PMA and Gö6976 treated cells were observed, as well as there were no differences between distinct incubation times.

Nonetheless, cells were still incubated with PMA and Gö6976 for 48 hours in 3D collagen for morphology assays, because this time was necessary for cells to adjust to the 3D environment. Similarly, 48 and 24 hours incubation times were used during invasivity assays or gelatin degradation assays, respectively, because these experiments required this time for cells to invade into 3D collagen or to degrade gelatin.

It is therefore a question, whether this prolonged incubation time with PMA really caused enhanced PKCα activation also after 48 (or 24) hours, or whether it conversely decreased PKCα activity. Although total level of PKCα in cells was decreased, PKCα could still have faster turnover or it could be more activated even if the amount was lower.

Another possibility for detection of PKCα activity marked by Thr497 phosphorylation was to investigate whether PKCα phosphorylation changed in respect to the PKCα expression. However, the ratio of phosphorylated PKCα to total PKCα showed no change in phosphorylation at Thr497 in respect to total PKCα.

This proposes that in control, PMA and Gö6976 treated cells the proportion of phosphorylated PKCα respective to total PKCα is still the same and phosphorylation did not change upon PMA or Gö6976 treatment.

This brought up another question – whether phosphorylation at Thr497 really marks PKCα activity. As stated previously, phosphorylation at Thr497 is one of three priming phosphorylations of PKCα (together with phosphorylation at Ser657 and Thr638) (Newton, 2010). These three phosphorylations are required for PKCα activity, however, their phosphorylation does not mean PKCα is active. They are phosphorylated after enzyme synthesis and they cause that enzyme adopts stable, closed conformation with pseudosubstrate bound to the substrate-binding site. The enzyme is matured, but inactive. Its activation can occur just upon interaction with second lipid messengers, recruitment to the membrane and subsequent release of pseudosubstrate from substrate-

binding cavity – and gain of open, catalytically active conformation (Newton, 2010; Newton, 1995).

Thus, phosphorylations on these priming sites correlate more with mature, closed, but catalytically inactive conformation of the enzyme than with open, catalytically active enzyme state (Freeley, 2011).

Therefore, priming phosphorylations are not probably the best markers for PKCα activation, different markers would be better – PKCα translocation to the membrane, specific phosphorylations that occur only under specific conditions or specialized PKC assay kit that measures PKC activity. Notably, also in literature, priming phosphorylations are rarely used to determine PKCα activation (PKCα phosphorylation was used for verifying PKCα activity for example in Hu et al., 2010). Most often, only remark that cells were treated with activator or inhibitor (and so PKCα is active or inactive, respectively) is stated, without additional confirmation by analyzing of PKCα phosphorylation status (and this is done also in papers that investigate the role of PKCα in regulating RhoA (Holinstat et al., 2003; Madigan et al., 2009; Dovas et al., 2010)).

Next, *in vitro* invasivity assays into 3D collagen were performed to elucidate the effect of PKCα directly on cell invasiveness. Although PKCα activator did not significantly influence invasivity of cells, PKCα inhibition resulted in considerable decrease in invading abilities of all three cell lines used (K2, A375m2 and MDA-MB-231). In consistence, siRNA mediated silencing of PKCα caused dramatic decrease in invasiveness of A375m2 cells.

These results suggest that PKCα is probably involved in regulating of signaling pathways that can mediate and enhance such a complex process as cell invasivity.

This is in consistence with previous results which shown that PKCα regulates cell invasion and migration in several cancer cell lines. Inhibition of PKCα decreased invasion of urinary bladder carcinoma (Koivunen et al., 2006), colon carcinoma (Masur et al., 2001), renal cell carcinoma (Engers et al., 2000), breast carcinoma (Parsons et al., 2002), multiple myeloma (Podar et al., 2002), glioma (Hu et al., 2010), breast cancer (Lønne et al., 2010) and endometrial cancer cells (Haughian nad Bradford, 2009). PKCα activation and overexpression were shown to increase cancer cell migration (Masur et al., 2001; Parsons et al., 2002; Podar et al., 2002; Haughian nad Bradford, 2009). Consistently, PKCα knockdown lead to decrease in cancer cell invasion (Masur et al., 2001; Lønne et al., 2010; Haughian nad Bradford, 2009). To investigate cancer cell

invasion and migration, methods as Dunn chemotaxis chamber assay, transwell chamber migration assay and wound healing migration assay were employed. However, this study was first to show invasion into 3D collagen matrix (not just through matrix membrane) that resembles more the environment of invasion *in vivo*.

These results are also important for more practical reason. As PKCα inhibition resulted in decreased invasivity, a potential role for PKCα inhibitors in anti-metastatic therapy should be considered.

So far, PKCα specific inhibitor aprinocarsen was tested already in clinical trials of breast and ovarian cancer and also of hematologic malignancies (NHL – non-Hodkin lymphoma) or prostate cancer patients (Lahn et al., 2004a; Lahn et al., 2004b; Lahn et al., 2006). Results of these studies did not convincingly show improvement during PKCα inhibitor treatment and suggested that also other characteristics of tumor cells should be considered while using this treatment.

Remarkably, PKCα was shown to be a marker of breast cancer aggressiveness as patients with PKCα-positive tumors exhibited poorer prognosis than patients with PKCα-negative tumors (Lønne et al., 2010).

Moreover, also effect of PKCα on extracellular matrix degrading abilities of A375m2 cells was investigated to further elucidate the possible mechanisms through which PKCα could regulate cell invasiveness.

Although being amoeboid, A375m2 cells were previously shown to form invadopodia and degrade ECM (Baldassarre et al., 2003). Consistently, also in our experiments, A375m2 cells were able to degrade gelatin. Importantly, although PKCα inhibition did not have any effect on gelatin degradation, PKCα activation resulted in greatly decreased gelatin degrading abilities of A375m2 cells. This suggests that PKC activation further increased amoeboid phenotype of A375m2 cells presumably by negatively regulating of matrix degrading enzymes expression or secretion. Results obtained from experiments with siRNA transfected cells were consistent with this hypothesis, gelatin degradation was greatly increased upon siRNA mediated PKCα silencing.

Taken together, these results support the proposed role of PKCα in amoeboid phenotype and invasiveness of cancer cells and suggest that PKCα could be involved in regulating ECM degrading abilities of cells, possibly through the regulation of matrix degrading enzymes expression or secretion.

In contrast with our results, in literature it was documented that PKCα could regulate MMPs expression through MAP kinase cascade and therefore enhance extracellular matrix degradation typical for mesenchymal invasion.

First, it was observed that PKCα can activate MAP kinase cascade through activation of Raf1 and subsequent activation of MEK1 and p42-MAPK in connection to cell proliferation (Schönwasser et al., 1998). Then, evidence that PKCα regulates Raf, ERK and JNK and subsequently also NF-κB and AP1 transcription factors to mediate MMP-9 expression were provided directly in association with HT-1080 fibrosarcoma cell invasion induced by PMA (Hwang et al., 2010; Hwang et al., 2011). This was confirmed also for invasion of glioblastoma cells (Lin et al., 2010). PKCα also influences TNFα-induced MMP-9 expression through JNK1/2 and c-Jun in A549 cells (alveolar epithelial cell carcinoma) (Lee et al., 2010). Moreover, in these cells, PKCα was shown to regulate expression of urokinase plasminogen-activator (uPA) upon IL-1β treatment and this was connected to increased migration (Cheng et al., 2009). PKCα was also shown to influence MMP-1, uPA and uPAR of hepatocellular carcinoma cells (Wu et al., 2008) and expression of MMP-1 and MMP-9 in breast cancer cells (Kim et al., 2011). Furthermore, activated PKCα was shown to translocate specifically from cytosol to podosomes and mediate gelatin degradation (Xiao et al., 2010). In addition, PKCα activation was shown to induce invasion of breast cancer cells in cooperation with Src that is important pro-mesenchymal protein (Tan et al., 2006).

Together, these results suggest that PKCα can regulate MAP kinase signaling pathway and induce expression of extracellular matrix degrading enzymes. However, in these studies, only gelatin zymography that evaluates amount of gelatin degrading enzymes was used. It would be interesting to investigate also potential role of PKCα-induced MAP kinase cascade on gelatin degradation assay with cells plated on extracellular matrix substrates.

These results suggest that PKCα plays an important role also in mesenchymal invasion. Importantly, this is not in conflict with the role of PKCα in amoeboid invasion. Effect of PKCα activation can differ in different conditions. It could be dependent on the specific cancer cell type and signaling environment, where PKCα could presumably regulate distinct specific signaling pathways or could regulate these pathways in a different way. Further analysis will be needed to elucidate this possibility.

Notably, interesting observation was done during gelatin degradation analysis.

It seemed like sites without gelatin had two mechanisms of origin. It was possible to distinguish between "genuine" gelatin degradation and somehow "torn" gelatin sites. "Genuine" gelatin degradation was simply degraded gelatin (by matrix degrading enzymes) at some areas, localized underneath cell body, often organized into little punctuate structures. But also other type of sites without gelatin was observed, these sites looked like gelatin was torn, because there was higher signal at the edges of the area as if gelatin from the site was just transferred to the sides. These areas occurred mostly at the cell edges and protrusions and this suggests that gelatin was torn by contractile forces of cell protrusions.

It is noteworthy that these torn sites were not present in all cells within the sample and also some differences were observed upon PKCα activator or inhibitor, which means, that occurrence of these torn sites could be affected by changed conditions. Therefore, these torn sites could potentially represent another characteristic of invading cells – strength of their protrusions contraction.

To verify that these sites are really torn and not degraded, MMPs inhibitor could be used. Comparing gelatin degradation (and tearing) between untreated cells and cells treated with MMPs inhibitor, it could be seen whether these sites are really MMPs-independent and occurred as a result of contraction forces of cell protrusions. This approach could be also used in further gelatin degradation analysis to exclude these indirect effects and estimate only specific effect of activator and inhibitor on gelatin degradation by matrix degrading enzymes as while analyzing the gelatin degradation using AnalyzeGelStack software, it was not possible to distinguish between these two types of gelatin degradation.

Another option is to modify gelatin-coated coverslips preparation and make gelatin somehow stiffer to be rigid enough to resist contractile forces of cell protrusions.

In future research, to further elucidate the effect of PKCα on matrix degrading abilities of cells, in gel gelatin zymography could be also performed. This analysis would help to elucidate whether and how PKCα affects matrix degrading proteins expression or secretion and also would help to identify which enzymes are influenced.

Regarding analyses performed, there was one interesting fact observed – sometimes, PKCα activator PMA did not have any effect on cells even when PKCα inhibitor Gö6976 had effect on cells and vice versa. In invasivity assay, although Gö6976

changed invasiveness of cells significantly, upon PMA treatment no change was observed. Similarly, PMA treatment significantly influenced gelatin degradation abilities of cells, however, Gö6976 did not have any specific effect.

This might be explained by different mechanisms of action between activator and inhibitor. While PKCα activator PMA acts through the recruitment of the enzyme to the membrane and therefore forces the closed enzyme state to adopt open conformation and become active, PKCα inhibitor Gö6976 inhibits probably both closed and open conformation of the enzyme by occupying nucleotide-binding site. Therefore, also pool of the enzyme on which activator or inhibitor can act differs. Moreover, different concentrations of activator or inhibitor could be needed for different actions – whereas one concentration of Gö6976 is enough for changing cell invasiveness, it does not have to have also effect on gelatin degradation (and conversely in the case of PMA). Also, 48 hours incubation time in the case of invasivity assay and 24 hours incubation time in the case of gelatin degradation assay could have slightly different effects on specific PKCα activation or inhibition.

These complications with using activator and inhibitor could be overcome in further experiments by using an additional experimental system – constructs with dominantly negative PKCα and constitutively active PKCα. These could be transiently transfected into cells or stable lines expressing these enzymes could be prepared. Experiments performed in this study, but with these new cell lines, would confirm results gained in this study and additionally specify the role of PKC in amoeboid invasion of cancer cells. In this study, siRNA mediated silencing of PKCα was performed to verify specificity of PKCα in our experiments. In future research, these experiments could be supplemented by re-expression of PKCα after siRNA mediated downregulation to the initial level of PKCα expression. In addition, also PKCα overexpression in cells could be applied.

Together, all our results suggest a possible role of PKCα in amoeboid invasion of cancer cells. We hypothesize that PKCα could activate small GTPase RhoA or ROCK kinase that are important for amoeboid type of invasion. Rho/ROCK signaling pathway controls phosphorylation of myosin light chain and mediates enhanced acto-myosin contractility that is critical feature of amoeboid cells (Sahai and Marshall, 2003; Wyckoff et al., 2006; Mierke et al., 2008). However, it is likely that PKCα does not phosphorylate RhoA or ROCK directly, rather, PKCα could phosphorylate some regulators of RhoA and ROCK. In literature, evidences were documented that PKCα

could regulate Rho/ROCK signaling pathway through their upstream regulators and these changes in signaling can be connected to cell adhesion and cytoskeletal reorganization.

Earlier results showed that PKCα can be activated upon thrombin treatment and can enhance RhoA activity in endothelial cells and mediate cell contraction (Mehta et al., 2001; Singh et al., 2007). PKCα can phosphorylate p115RhoGEF that is specific Rho guanine nucleotide exchange factor and this way increases its activity (Holinstat et al., 2003). Therefore, also RhoA activity is increased and this is connected to regulation of stress fibers formation and cell contraction (Holinstat et al., 2003).

One of the PKCα substrates is also RhoGDIα (Dovas et al., 2010). RhoGDIα is a cytosolic protein that binds GDP-bound small RhoGTPases RhoA, Rac1 and Cdc42 and prevents them from exchange of GDP to GTP (DerMardirossian and Bokoch, 2005). PKCα can phosphorylate RhoGDIα at Ser34 and this way it reduces its affinity for RhoA (but not for Rac1 or Cdc42) (Dovas et al., 2010). So, RhoA can be activated by GTP binding and downstream signaling is enhanced as was observed by loss of focal adhesions (Dovas et al., 2010). Also PIP_2 is needed for RhoGDIα phosphorylation, probably for correct PKCα localization and orientation in the membrane (Dovas et al., 2010). Moreover, αvβ3 integrin and syndecan4-mediated PKCα activation enhances RhoA activity to form focal adhesions and maintain stress fibers (Dovas et al., 2006; Avalos et al., 2009).

Recently, also results that connect PKCα directly to regulation of Rho/ROCK signaling pathway were published. PKCα could regulate localization of small GTPase Rnd3 (also called RhoE) (Madigan et al., 2009). Rnd3 can bind ROCK kinase and prevents its downstream signaling - upon Rnd3 binding, phosphorylation of MLCP was inhibited and formation of ROCK-induced stress fibers was disturbed (Riento et al., 2003). Moreover, Rnd3 competes with PDK1 for binding to ROCK kinase and thus prevents its correct localization to the plasma membrane (Pinner and Sahai, 2008). PKCα was shown to phosphorylate Rnd3 and Rnd3 was upon this phosphorylation translocated to the internal membranes (Madigan et al., 2009). Consequently, Rnd3 is far away from ROCK kinase and cannot inhibit its pathway, therefore Rho/ROCK signaling is enhanced (Madigan et al., 2009). Moreover, Raf kinase pathway activation, that could be regulated by PKCα (Hwang et al., 2010), was shown to be associated with Rnd3 expression (Hansen et al., 2000).

To verify that PKCα has a direct effect on RhoA activity in our cells used, RhoGTPase assay could be performed. This assay determines the amount of GTP-bound Rho in respect to total Rho in cells (treated with PKCα activator or inhibitor, siRNA treated cells or cells expressing dominantly negative form or constitutively active PKCα as described above). Moreover, using phospho-specific antibodies, also activation of other parts of this signaling cascade can be determined – phospho-ROCK kinase or phospho-MLC (myosin light chain). Novel PKCα targets that could downstream activate Rho/ROCK pathway could be potentially identified by interaction screen and possibly *in vitro* phosphorylation analysis and further verify for their role in cytoskeletal dynamics and activating Rho/ROCK pathway.

To sum up, our results suggest that PKCα regulates amoeboid invasion of cancer cells and plays important role in transitions between amoeboid and mesenchymal modes of cancer cell invasiveness.

Metastases are the worst complication of cancer patients treatment. Therefore, the better understanding of mechanisms of cancer cell invasion is necessary for efficient anti-metastatic therapy.

9. Conclusions

- PKCα expression remained unchanged after amoeboid-mesenchymal transition (induced by inhibitor of ROCK kinase) of A375m2 cells cultivated both in 2D and in 3D environment
- Similarly, phosphorylation of PKCα at Thr497 was not affected by amoeboid-mesenchymal transition (induced by inhibitor of ROCK kinase) in A375m2 cells cultivated both in 2D and in 3D environment
- Treatment with PKCα activator PMA lead to mesenchymal-amoeboid transition of mesenchymal K2 and MDA-MB-231 cells, it did not have any effect on morphology of amoeboid A375m2 cells as these were already amoeboid
- The other way around, PKCα inhibition by PKCα inhibitor Gö6976 caused amoeboid-mesenchymal transition of A375m2 amoeboid cell line, morphology of mesenchymal K2 and MDA-MB-231 cells remained unchanged as these cells were already mesenchymal
- Likewise, siRNA-mediated downregulation of PKCα lead to amoeboid-mesenchymal transition of A375m2 amoeboid cells
- Ability of invading into 3D collagen was significantly decreased upon PKCα inhibitor Gö6976 in all three cells lines used (K2, A375m2 and MDA-MB-231), PKCα activator did not have significant effect on cell invasion
- Correspondingly, siRNA mediated silencing of PKCα resulted in reduced invading ability of A375m2 cells
- Although incubation with PKCα inhibitor Gö6976 did not influence gelatin degradation area of A375m2, PKCα activator PMA treatment greatly decreased gelatin degradation abilities of A375m2 cells
- In consistence, siRNA mediated knockdown of PKCα increased matrix degrading ability of A375m2 cells

10. References

Aimes, R. T. and J. P. Quigley (1995). "Matrix metalloproteinase-2 is an interstitial collagenase. Inhibitor-free enzyme catalyzes the cleavage of collagen fibrils and soluble native type I collagen generating the specific 3/4- and 1/4-length fragments." J Biol Chem 270(11): 5872-6.

Alberts, B., A. Johnson, et al. (2002). "Molecular Biology of the Cell." Garland Science, 4th edition, p. 1325.

Amano, M., K. Chihara, et al. (1997). "Formation of actin stress fibers and focal adhesions enhanced by Rho-kinase." Science 275(5304): 1308-11.

Amano, M., M. Ito, et al. (1996). "Phosphorylation and activation of myosin by Rho-associated kinase (Rho-kinase)." J Biol Chem 271(34): 20246-9.

Anilkumar, N., M. Parsons, et al. (2003). "Interaction of fascin and protein kinase Calpha: a novel intersection in cell adhesion and motility." Embo J 22(20): 5390-402.

Avalos, A. M., A. D. Valdivia, et al. (2009). "Neuronal Thy-1 induces astrocyte adhesion by engaging syndecan-4 in a cooperative interaction with alphavbeta3 integrin that activates PKCalpha and RhoA." J Cell Sci 122(Pt 19): 3462-71.

Babwah, A. V., L. B. Dale, et al. (2003). "Protein kinase C isoform-specific differences in the spatial-temporal regulation and decoding of metabotropic glutamate receptor1a-stimulated second messenger responses." J Biol Chem 278(7): 5419-26.

Baldassarre, G., B. Belletti, et al. (2005). "p27(Kip1)-stathmin interaction influences sarcoma cell migration and invasion." Cancer Cell 7(1): 51-63.

Baldassarre, M., A. Pompeo, et al. (2003). "Dynamin participates in focal extracellular matrix degradation by invasive cells." Mol Biol Cell 14(3): 1074-84.

Balendran, A., G. R. Hare, et al. (2000). "Further evidence that 3-phosphoinositide-dependent protein kinase-1 (PDK1) is required for the stability and phosphorylation of protein kinase C (PKC) isoforms." FEBS Lett 484(3): 217-23.

Ballestrem, C., B. Hinz, et al. (2001). "Marching at the front and dragging behind: differential alphaVbeta3-integrin turnover regulates focal adhesion behavior." J Cell Biol 155(7): 1319-32.

Bass, M. D., M. R. Morgan, et al. (2008). "p190RhoGAP is the convergence point of adhesion signals from alpha 5 beta 1 integrin and syndecan-4." J Cell Biol 181(6): 1013-26.

Bazzi, M. D. and G. L. Nelsestuen (1990). "Protein kinase C interaction with calcium: a phospholipid-dependent process." Biochemistry 29(33): 7624-30.

Behn-Krappa, A. and A. C. Newton (1999). "The hydrophobic phosphorylation motif of conventional protein kinase C is regulated by autophosphorylation." Curr Biol 9(14): 728-37.

Belletti, B., M. S. Nicoloso, et al. (2008). "Stathmin activity influences sarcoma cell shape, motility, and metastatic potential." Mol Biol Cell 19(5): 2003-13.

Berton, S., B. Belletti, et al. (2009). "The tumor suppressor functions of p27(kip1) include control of the mesenchymal/amoeboid transition." Mol Cell Biol 29(18): 5031-45.

Besson, A., M. Gurian-West, et al. (2004). "p27Kip1 modulates cell migration through the regulation of RhoA activation." Genes Dev 18(8): 862-76.

Birkedal-Hansen, H. (1995). "Proteolytic remodeling of extracellular matrix." Curr Opin Cell Biol 7(5):

728-35.

Bornancin, F. and P. J. Parker (1996). "Phosphorylation of threonine 638 critically controls the dephosphorylation and inactivation of protein kinase Calpha." Curr Biol 6(9): 1114-23.

Bornancin, F. and P. J. Parker (1997). "Phosphorylation of protein kinase C-alpha on serine 657 controls the accumulation of active enzyme and contributes to its phosphatase-resistant state." J Biol Chem 272(6): 3544-9.

Bosco, E. E., J. C. Mulloy, et al. (2009). "Rac1 GTPase: a "Rac" of all trades." Cell Mol Life Sci 66(3): 370-4.

Brabek, J., C. T. Mierke, et al. (2010). "The role of the tissue microenvironment in the regulation of cancer cell motility and invasion." Cell Commun Signal 8: 22.

Breitkreutz, D., L. Braiman-Wiksman, et al. (2007). "Protein kinase C family: on the crossroads of cell signaling in skin and tumor epithelium." J Cancer Res Clin Oncol 133(11): 793-808.

Bretscher, A., K. Edwards, et al. (2002). "ERM proteins and merlin: integrators at the cell cortex." Nat Rev Mol Cell Biol 3(8): 586-99.

Bretscher, A., K. Edwards, et al. (2002). "ERM proteins and merlin: integrators at the cell cortex." Nat Rev Mol Cell Biol 3(8): 586-99.

Brooks, P. C., S. Stromblad, et al. (1996). "Localization of matrix metalloproteinase MMP-2 to the surface of invasive cells by interaction with integrin alpha v beta 3." Cell 85(5): 683-93.

Buccione, R., J. D. Orth, et al. (2004). "Foot and mouth: podosomes, invadopodia and circular dorsal ruffles." Nat Rev Mol Cell Biol 5(8): 647-57.

Calderwood, D. A., R. Zent, et al. (1999). "The Talin head domain binds to integrin beta subunit cytoplasmic tails and regulates integrin activation." J Biol Chem 274(40): 28071-4.

Carlier, M. F., A. Ducruix, et al. (1999). "Signalling to actin: the Cdc42-N-WASP-Arp2/3 connection." Chem Biol 6(9): R235-40.

Carragher, N. O., S. M. Walker, et al. (2006). "Calpain 2 and Src dependence distinguishes mesenchymal and amoeboid modes of tumour cell invasion: a link to integrin function." Oncogene 25(42): 5726-40.

Castagna, M., Y. Takai, et al. (1982). "Direct activation of calcium-activated, phospholipid-dependent protein kinase by tumor-promoting phorbol esters." J Biol Chem 257(13): 7847-51.

Cau, J. and A. Hall (2005). "Cdc42 controls the polarity of the actin and microtubule cytoskeletons through two distinct signal transduction pathways." J Cell Sci 118(Pt 12): 2579-87.

Cazaubon, S., F. Bornancin, et al. (1994). "Threonine-497 is a critical site for permissive activation of protein kinase C alpha." Biochem J 301 (Pt 2): 443-8.

Clark, E. A., W. G. King, et al. (1998). "Integrin-mediated signals regulated by members of the rho family of GTPases." J Cell Biol 142(2): 573-86.

Coleman, M. L., E. A. Sahai, et al. (2001). "Membrane blebbing during apoptosis results from caspase-mediated activation of ROCK I." Nat Cell Biol 3(4): 339-45.

Conesa-Zamora, P., M. J. Lopez-Andreo, et al. (2001). "Identification of the phosphatidylserine binding site in the C2 domain that is important for PKC alpha activation and in vivo cell localization." Biochemistry 40(46): 13898-905.

Corbalan-Garcia, S., M. Guerrero-Valero, et al. (2007). "The C2 domains of classical/conventional PKCs are specific PtdIns(4,5)P(2)-sensing domains." Biochem Soc Trans 35(Pt 5): 1046-8.

Coussens, L., P. J. Parker, et al. (1986). "Multiple, distinct forms of bovine and human protein kinase C suggest diversity in cellular signaling pathways." Science 233(4766): 859-66.

Cunningham, C. C. (1995). "Actin polymerization and intracellular solvent flow in cell surface blebbing." J Cell Biol 129(6): 1589-99.

Curmi, P. A., O. Gavet, et al. (1999). "Stathmin and its phosphoprotein family: general properties, biochemical and functional interaction with tubulin." Cell Struct Funct 24(5): 345-57.

Dahl, K. N., A. J. Ribeiro, et al. (2008). "Nuclear shape, mechanics, and mechanotransduction." Circ Res 102(11): 1307-18.

Datta, R., H. Kojima, et al. (1997). "Caspase-3-mediated cleavage of protein kinase C theta in induction of apoptosis." J Biol Chem 272(33): 20317-20.

Daub, H., J. V. Olsen, et al. (2008). "Kinase-selective enrichment enables quantitative phosphoproteomics of the kinome across the cell cycle." Mol Cell 31(3): 438-48.

DerMardirossian, C. and G. M. Bokoch (2005). "GDIs: central regulatory molecules in Rho GTPase activation." Trends Cell Biol 15(7): 356-63.

Deryugina, E. I., B. Ratnikov, et al. (2001). "MT1-MMP initiates activation of pro-MMP-2 and integrin alphavbeta3 promotes maturation of MMP-2 in breast carcinoma cells." Exp Cell Res 263(2): 209-23.

Devreotes, P. N. and S. H. Zigmond (1988). "Chemotaxis in eukaryotic cells: a focus on leukocytes and Dictyostelium." Annu Rev Cell Biol 4: 649-86.

Dharmawardhane, S., D. Brownson, et al. (1999). "Localization of p21-activated kinase 1 (PAK1) to pseudopodia, membrane ruffles, and phagocytic cups in activated human neutrophils." J Leukoc Biol 66(3): 521-7.

d'Ortho, M. P., H. Stanton, et al. (1998). "MT1-MMP on the cell surface causes focal degradation of gelatin films." FEBS Lett 421(2): 159-64.

Dovas, A. and J. R. Couchman (2005). "RhoGDI: multiple functions in the regulation of Rho family GTPase activities." Biochem J 390(Pt 1): 1-9.

Dovas, A., Y. Choi, et al. (2010). "Serine 34 phosphorylation of rho guanine dissociation inhibitor (RhoGDIalpha) links signaling from conventional protein kinase C to RhoGTPase in cell adhesion." J Biol Chem 285(30): 23296-308.

Dovas, A., A. Yoneda, et al. (2006). "PKCbeta-dependent activation of RhoA by syndecan-4 during focal adhesion formation." J Cell Sci 119(Pt 13): 2837-46.

Doyle, A. D., F. W. Wang, et al. (2009). "One-dimensional topography underlies three-dimensional fibrillar cell migration." J Cell Biol 184(4): 481-90.

Dutil, E. M., L. M. Keranen, et al. (1994). "In vivo regulation of protein kinase C by trans-phosphorylation followed by autophosphorylation." J Biol Chem 269(47): 29359-62.

Dutil, E. M. and A. C. Newton (2000). "Dual role of pseudosubstrate in the coordinated regulation of protein kinase C by phosphorylation and diacylglycerol." J Biol Chem 275(14): 10697-701.

Dutil, E. M., A. Toker, et al. (1998). "Regulation of conventional protein kinase C isozymes by phosphoinositide-dependent kinase 1 (PDK-1)." Curr Biol 8(25): 1366-75.

Egeblad, M. and Z. Werb (2002). "New functions for the matrix metalloproteinases in cancer progression." Nat Rev Cancer 2(3): 161-74.

Elfenbein, A., J. M. Rhodes, et al. (2009). "Suppression of RhoG activity is mediated by a syndecan 4-synectin-RhoGDI1 complex and is reversed by PKCalpha in a Rac1 activation pathway." J Cell Biol 186(1): 75-83.

Emoto, Y., Y. Manome, et al. (1995). "Proteolytic activation of protein kinase C delta by an ICE-like protease in apoptotic cells." Embo J 14(24): 6148-56.

Engers, R., S. Mrzyk, et al. (2000). "Protein kinase C in human renal cell carcinomas: role in invasion and differential isoenzyme expression." Br J Cancer 82(5): 1063-9.

Evans, J. H., D. Murray, et al. (2006). "Specific translocation of protein kinase Calpha to the plasma membrane requires both Ca2+ and PIP2 recognition by its C2 domain." Mol Biol Cell 17(1): 56-66.

Facchinetti, V., W. Ouyang, et al. (2008). "The mammalian target of rapamycin complex 2 controls folding and stability of Akt and protein kinase C." Embo J 27(14): 1932-43.

Farooqui, R. and G. Fenteany (2005). "Multiple rows of cells behind an epithelial wound edge extend cryptic lamellipodia to collectively drive cell-sheet movement." J Cell Sci 118(Pt 1): 51-63.

Foster, R., K. Q. Hu, et al. (1996). "Identification of a novel human Rho protein with unusual properties: GTPase deficiency and in vivo farnesylation." Mol Cell Biol 16(6): 2689-99.

Frankel, P., C. Pellet-Many, et al. (2008). "Chondroitin sulphate-modified neuropilin 1 is expressed in human tumour cells and modulates 3D invasion in the U87MG human glioblastoma cell line through a p130Cas-mediated pathway." EMBO Rep 9(10): 983-9.

Freeley, M., D. Kelleher, et al. (2011). "Regulation of Protein Kinase C function by phosphorylation on conserved and non-conserved sites." Cell Signal 23(5): 753-62.

Friedl, P. (2004). "Prespecification and plasticity: shifting mechanisms of cell migration." Curr Opin Cell Biol 16(1): 14-23.

Friedl, P., S. Borgmann, et al. (2001). "Amoeboid leukocyte crawling through extracellular matrix: lessons from the Dictyostelium paradigm of cell movement." J Leukoc Biol 70(4): 491-509.

Friedl, P. and E. B. Brocker (2000). "The biology of cell locomotion within three-dimensional extracellular matrix." Cell Mol Life Sci 57(1): 41-64.

Friedl, P. and D. Gilmour (2009). "Collective cell migration in morphogenesis, regeneration and cancer." Nat Rev Mol Cell Biol 10(7): 445-57.

Friedl, P., P. B. Noble, et al. (1994). "Locomotor phenotypes of unstimulated CD45RAhigh and CD45ROhigh CD4+ and CD8+ lymphocytes in three-dimensional collagen lattices." Immunology 82(4): 617-24.

Friedl, P., P. B. Noble, et al. (1995). "Migration of coordinated cell clusters in mesenchymal and epithelial cancer explants in vitro." Cancer Res 55(20): 4557-60.

Friedl, P. and K. Wolf (2010). "Plasticity of cell migration: a multiscale tuning model." J Cell Biol 188(1): 11-9.

Friedl, P., K. S. Zanker, et al. (1998). "Cell migration strategies in 3-D extracellular matrix: differences in morphology, cell matrix interactions, and integrin function." Microsc Res Tech 43(5): 369-78.

Fujita, M., Y. Otsuka, et al. (2011). "X-ray irradiation and Rho-kinase inhibitor additively induce invasiveness of the cells of the pancreatic cancer line, MIAPaCa-2, which exhibits mesenchymal and amoeboid motility." Cancer Sci 102(4): 792-8.

Gadea, G., M. de Toledo, et al. (2007). "Loss of p53 promotes RhoA-ROCK-dependent cell migration and invasion in 3D matrices." J Cell Biol 178(1): 23-30.

Gadea, G., L. Lapasset, et al. (2002). "Regulation of Cdc42-mediated morphological effects: a novel function for p53." Embo J 21(10): 2373-82.

Gadea, G., V. Sanz-Moreno, et al. (2008). "DOCK10-mediated Cdc42 activation is necessary for amoeboid invasion of melanoma cells." Curr Biol 18(19): 1456-65.

Gao, T., J. Brognard, et al. (2008). "The phosphatase PHLPP controls the cellular levels of protein kinase C." J Biol Chem 283(10): 6300-11.

Gao, T. and A. C. Newton (2002). "The turn motif is a phosphorylation switch that regulates the binding of Hsp70 to protein kinase C." J Biol Chem 277(35): 31585-92.

Gatti, A. and P. J. Robinson (1997). "Okadaic acid interferes with phorbol-ester-mediated down-regulation of protein kinase C-alpha, C-delta and C-epsilon." Eur J Biochem 249(1): 92-7.

Giannelli, G., J. Falk-Marzillier, et al. (1997). "Induction of cell migration by matrix metalloprotease-2 cleavage of laminin-5." Science 277(5323): 225-8.

Gould, C. M., N. Kannan, et al. (2009). "The chaperones Hsp90 and Cdc37 mediate the maturation and stabilization of protein kinase C through a conserved PXXP motif in the C-terminal tail." J Biol Chem 284(8): 4921-35.

Guasch, R. M., P. Scambler, et al. (1998). "RhoE regulates actin cytoskeleton organization and cell migration." Mol Cell Biol 18(8): 4761-71.

Guo, F., M. Debidda, et al. (2006). "Genetic deletion of Rac1 GTPase reveals its critical role in actin stress fiber formation and focal adhesion complex assembly." J Biol Chem 281(27): 18652-9.

Gysin, S. and R. Imber (1996). "Replacement of Ser657 of protein kinase C-alpha by alanine leads to premature down regulation after phorbol-ester-induced translocation to the membrane." Eur J Biochem 240(3): 747-50.

Hagerty, L., D. H. Weitzel, et al. (2007). "ROCK1 phosphorylates and activates zipper-interacting protein kinase." J Biol Chem 282(7): 4884-93.

Hansen, S. H., M. M. Zegers, et al. (2000). "Induced expression of Rnd3 is associated with transformation of polarized epithelial cells by the Raf-MEK-extracellular signal-regulated kinase pathway." Mol Cell Biol 20(24): 9364-75.

Hansra, G., F. Bornancin, et al. (1996). "12-O-Tetradecanoylphorbol-13-acetate-induced dephosphorylation of protein kinase Calpha correlates with the presence of a membrane-associated protein phosphatase 2A heterotrimer." J Biol Chem 271(51): 32785-8.

Hansra, G., P. Garcia-Paramio, et al. (1999). "Multisite dephosphorylation and desensitization of conventional protein kinase C isotypes." Biochem J 342 (Pt 2): 337-44.

Harley, B. A., H. D. Kim, et al. (2008). "Microarchitecture of three-dimensional scaffolds influences cell migration behavior via junction interactions." Biophys J 95(8): 4013-24.

Hauge, C., T. L. Antal, et al. (2007). "Mechanism for activation of the growth factor-activated AGC kinases by turn motif phosphorylation." Embo J 26(9): 2251-61.

Haughian, J. M. and A. P. Bradford (2009). "Protein kinase C alpha (PKCalpha) regulates growth and invasion of endometrial cancer cells." J Cell Physiol 220(1): 112-8.

He, Z. and M. Tessier-Lavigne (1997). "Neuropilin is a receptor for the axonal chemorepellent Semaphorin III." Cell 90(4): 739-51.

Hegerfeldt, Y., M. Tusch, et al. (2002). "Collective cell movement in primary melanoma explants:

plasticity of cell-cell interaction, beta1-integrin function, and migration strategies." Cancer Res 62(7): 2125-30.

Hilger, R. A., M. E. Scheulen, et al. (2002). "The Ras-Raf-MEK-ERK pathway in the treatment of cancer." Onkologie 25(6): 511-8.

Holinstat, M., D. Mehta, et al. (2003). "Protein kinase Calpha-induced p115RhoGEF phosphorylation signals endothelial cytoskeletal rearrangement." J Biol Chem 278(31): 28793-8.

House, C. and B. E. Kemp (1987). "Protein kinase C contains a pseudosubstrate prototope in its regulatory domain." Science 238(4834): 1726-8.

Hu, J. G., X. F. Wang, et al. (2010). "Activation of PKC-alpha is required for migration of C6 glioma cells." Acta Neurobiol Exp (Wars) 70(3): 239-45.

Hurley, J. H. (2006). "Membrane binding domains." Biochim Biophys Acta 1761(8): 805-11.

Hwang, Y. P. and H. G. Jeong (2010). "Metformin blocks migration and invasion of tumour cells by inhibition of matrix metalloproteinase-9 activation through a calcium and protein kinase Calpha-dependent pathway: phorbol-12-myristate-13-acetate-induced/extracellular signal-regulated kinase/activator protein-1." Br J Pharmacol 160(5): 1195-211.

Hwang, Y. P., H. J. Yun, et al. (2010). "Suppression of PMA-induced tumor cell invasion by dihydroartemisinin via inhibition of PKCalpha/Raf/MAPKs and NF-kappaB/AP-1-dependent mechanisms." Biochem Pharmacol 79(12): 1714-26.

Hwang, Y. P., H. J. Yun, et al. (2011). "Suppression of phorbol-12-myristate-13-acetate-induced tumor cell invasion by piperine via the inhibition of PKCalpha/ERK1/2-dependent matrix metalloproteinase-9 expression." Toxicol Lett 203(1): 9-19.

Hyatt, S. L., L. Liao, et al. (1994). "Identification and characterization of alpha-protein kinase C binding proteins in normal and transformed REF52 cells." Biochemistry 33(5): 1223-8.

Charras, G. T., C. K. Hu, et al. (2006). "Reassembly of contractile actin cortex in cell blebs." J Cell Biol 175(3): 477-90.

Cheng, C. Y., H. L. Hsieh, et al. (2009). "IL-1 beta induces urokinase-plasminogen activator expression and cell migration through PKC alpha, JNK1/2, and NF-kappaB in A549 cells." J Cell Physiol 219(1): 183-93.

Cho, W. and R. V. Stahelin (2006). "Membrane binding and subcellular targeting of C2 domains." Biochim Biophys Acta 1761(8): 838-49.

Chou, M. M., W. Hou, et al. (1998). "Regulation of protein kinase C zeta by PI 3-kinase and PDK-1." Curr Biol 8(19): 1069-77.

Ikenoue, T., K. Inoki, et al. (2008). "Essential function of TORC2 in PKC and Akt turn motif phosphorylation, maturation and signalling." Embo J 27(14): 1919-31.

Inoue, M., A. Kishimoto, et al. (1977). "Studies on a cyclic nucleotide-independent protein kinase and its proenzyme in mammalian tissues. II. Proenzyme and its activation by calcium-dependent protease from rat brain." J Biol Chem 252(21): 7610-6.

Ishizaki, T., M. Maekawa, et al. (1996). "The small GTP-binding protein Rho binds to and activates a 160 kDa Ser/Thr protein kinase homologous to myotonic dystrophy kinase." Embo J 15(8): 1885-93.

Ivetic, A. and A. J. Ridley (2004). "Ezrin/radixin/moesin proteins and Rho GTPase signalling in leucocytes." Immunology 112(2): 165-76.

Johnson, J. E., J. Giorgione, et al. (2000). "The C1 and C2 domains of protein kinase C are independent

membrane targeting modules, with specificity for phosphatidylserine conferred by the C1 domain." Biochemistry 39(37): 11360-9.

Kar, S., S. Subbaram, et al. (2010). "Redox-control of matrix metalloproteinase-1: a critical link between free radicals, matrix remodeling and degenerative disease." Respir Physiol Neurobiol 174(3): 299-306.

Kasalová L. (2010). "In vitro analysis of amoeboi-mesenchymal transition of A375m2 melanoma cells." Charles University in Prague, Faculty of Science, Master's thesis.

Kawakami, Y., J. Kitaura, et al. (2003). "A Ras activation pathway dependent on Syk phosphorylation of protein kinase C." Proc Natl Acad Sci U S A 100(16): 9470-5.

Kazanietz, M. G., S. Wang, et al. (1995). "Residues in the second cysteine-rich region of protein kinase C delta relevant to phorbol ester binding as revealed by site-directed mutagenesis." J Biol Chem 270(37): 21852-9.

Keely, P. J., J. K. Westwick, et al. (1997). "Cdc42 and Rac1 induce integrin-mediated cell motility and invasiveness through PI(3)K." Nature 390(6660): 632-6.

Keller, H. and P. Eggli (1998). "Protrusive activity, cytoplasmic compartmentalization, and restriction rings in locomoting blebbing Walker carcinosarcoma cells are related to detachment of cortical actin from the plasma membrane." Cell Motil Cytoskeleton 41(2): 181-93.

Kelly, T., Y. Yan, et al. (1998). "Proteolysis of extracellular matrix by invadopodia facilitates human breast cancer cell invasion and is mediated by matrix metalloproteinases." Clin Exp Metastasis 16(6): 501-12.

Keranen, L. M., E. M. Dutil, et al. (1995). "Protein kinase C is regulated in vivo by three functionally distinct phosphorylations." Curr Biol 5(12): 1394-1403.

Keum, E., Y. Kim, et al. (2004). "Syndecan-4 regulates localization, activity and stability of protein kinase C-alpha." Biochem J 378(Pt 3): 1007-14.

Kikkawa, U., Y. Takai, et al. (1983). "Protein kinase C as a possible receptor protein of tumor-promoting phorbol esters." J Biol Chem 258(19): 11442-5.

Kim, S., J. Han, et al. (2012). "Berberine suppresses the TPA-induced MMP-1 and MMP-9 expressions through the inhibition of PKC-alpha in breast cancer cells." J Surg Res 176(1): e21-9.

Kimura, K., M. Ito, et al. (1996). "Regulation of myosin phosphatase by Rho and Rho-associated kinase (Rho-kinase)." Science 273(5272): 245-8.

Kinch, M. S. and K. Carles-Kinch (2003). "Overexpression and functional alterations of the EphA2 tyrosine kinase in cancer." Clin Exp Metastasis 20(1): 59-68.

Kishimoto, A., N. Kajikawa, et al. (1983). "Proteolytic activation of calcium-activated, phospholipid-dependent protein kinase by calcium-dependent neutral protease." J Biol Chem 258(2): 1156-64.

Kishimoto, A., K. Mikawa, et al. (1989). "Limited proteolysis of protein kinase C subspecies by calcium-dependent neutral protease (calpain)." J Biol Chem 264(7): 4088-92.

Kiyokawa, E., Y. Hashimoto, et al. (1998). "Evidence that DOCK180 up-regulates signals from the CrkII-p130(Cas) complex." J Biol Chem 273(38): 24479-84.

Koivunen, J., V. Aaltonen, et al. (2004). "Protein kinase C alpha/beta inhibitor Go6976 promotes formation of cell junctions and inhibits invasion of urinary bladder carcinoma cells." Cancer Res 64(16): 5693-701.

Kopfstein, L. and G. Christofori (2006). "Metastasis: cell-autonomous mechanisms versus contributions by the tumor microenvironment." Cell Mol Life Sci 63(4): 449-68.

Lahn, M., G. Kohler, et al. (2004a). "Protein kinase C alpha expression in breast and ovarian cancer." Oncology 67(1): 1-10.

Lahn, M., K. Sundell, et al. (2004b). "Protein kinase C-alpha in prostate cancer." BJU Int 93(7): 1076-81.

Lahn, M., K. Sundell, et al. (2006). "The role of protein kinase C-alpha in hematologic malignancies." Acta Haematol 115(1-2): 1-8.

Lammermann, T. and M. Sixt (2009). "Mechanical modes of 'amoeboid' cell migration." Curr Opin Cell Biol 21(5): 636-44.

Lauffenburger, D. A. and A. F. Horwitz (1996). "Cell migration: a physically integrated molecular process." Cell 84(3): 359-69.

Lecuit, T. and P. F. Lenne (2007). "Cell surface mechanics and the control of cell shape, tissue patterns and morphogenesis." Nat Rev Mol Cell Biol 8(8): 633-44.

Lee, J. Y., Y. A. Hannun, et al. (2000). "Functional dichotomy of protein kinase C (PKC) in tumor necrosis factor-alpha (TNF-alpha) signal transduction in L929 cells. Translocation and inactivation of PKC by TNF-alpha." J Biol Chem 275(38): 29290-8.

Lee, I. T., C. C. Lin, et al. (2010). "TNF-alpha induces matrix metalloproteinase-9 expression in A549 cells: role of TNFR1/TRAF2/PKCalpha-dependent signaling pathways." J Cell Physiol 224(2): 454-64.

Lemmon, M. A. (2008). "Membrane recognition by phospholipid-binding domains." Nat Rev Mol Cell Biol 9(2): 99-111.

Leontieva, O. V. and J. D. Black (2004). "Identification of two distinct pathways of protein kinase Calpha down-regulation in intestinal epithelial cells." J Biol Chem 279(7): 5788-801.

Leung, T., X. Q. Chen, et al. (1998). "Myotonic dystrophy kinase-related Cdc42-binding kinase acts as a Cdc42 effector in promoting cytoskeletal reorganization." Mol Cell Biol 18(1): 130-40.

Liacini, A., J. Sylvester, et al. (2003). "Induction of matrix metalloproteinase-13 gene expression by TNF-alpha is mediated by MAP kinases, AP-1, and NF-kappaB transcription factors in articular chondrocytes." Exp Cell Res 288(1): 208-17.

Lin, C. W., S. C. Shen, et al. (2010). "12-O-tetradecanoylphorbol-13-acetate-induced invasion/migration of glioblastoma cells through activating PKCalpha/ERK/NF-kappaB-dependent MMP-9 expression." J Cell Physiol 225(2): 472-81.

Liu, J. F., Y. C. Fong, et al. (2010). "Cyclooxygenase-2 enhances alpha2beta1 integrin expression and cell migration via EP1 dependent signaling pathway in human chondrosarcoma cells." Mol Cancer 9: 43.

Lo, C. M., H. B. Wang, et al. (2000). "Cell movement is guided by the rigidity of the substrate." Biophys J 79(1): 144-52.

Lonne, G. K., L. Cornmark, et al. (2010). "PKCalpha expression is a marker for breast cancer aggressiveness." Mol Cancer 9: 76.

Maaser, K., K. Wolf, et al. (1999). "Functional hierarchy of simultaneously expressed adhesion receptors: integrin alpha2beta1 but not CD44 mediates MV3 melanoma cell migration and matrix reorganization within three-dimensional hyaluronan-containing collagen matrices." Mol Biol Cell 10(10): 3067-79.

Madigan, J. P., B. O. Bodemann, et al. (2009). "Regulation of Rnd3 localization and function by protein kinase C alpha-mediated phosphorylation." Biochem J 424(1): 153-61.

Maekawa, M., T. Ishizaki, et al. (1999). "Signaling from Rho to the actin cytoskeleton through protein kinases ROCK and LIM-kinase." Science 285(5429): 895-8.

Makagiansar, I. T., S. Williams, et al. (2007). "Differential phosphorylation of NG2 proteoglycan by ERK and PKCalpha helps balance cell proliferation and migration." J Cell Biol 178(1): 155-65.

Mandeville, J. T., M. A. Lawson, et al. (1997). "Dynamic imaging of neutrophil migration in three dimensions: mechanical interactions between cells and matrix." J Leukoc Biol 61(2): 188-200.

Manser, E., C. Chong, et al. (1995). "Molecular cloning of a new member of the p21-Cdc42/Rac-activated kinase (PAK) family." J Biol Chem 270(42): 25070-8.

Martiny-Baron, G., M. G. Kazanietz, et al. (1993). "Selective inhibition of protein kinase C isozymes by the indolocarbazole Gö 6976." J Biol Chem 268(13): 9194-9197.

Martiny-Baron, G. and D. Fabbro (2007). "Classical PKC isoforms in cancer." Pharmacol Res 55(6): 477-86.

Mashukova, A., A. S. Oriolo, et al. (2009). "Rescue of atypical protein kinase C in epithelia by the cytoskeleton and Hsp70 family chaperones." J Cell Sci 122(Pt 14): 2491-503.

Masur, K., K. Lang, et al. (2001). "High PKC alpha and low E-cadherin expression contribute to high migratory activity of colon carcinoma cells." Mol Biol Cell 12(7): 1973-82.

McGrew, B. R., D. W. Nichols, et al. (1992). "Phosphorylation occurs in the amino terminus of the Raf-1 protein." Oncogene 7(1): 33-42.

Mehta, D., A. Rahman, et al. (2001). "Protein kinase C-alpha signals rho-guanine nucleotide dissociation inhibitor phosphorylation and rho activation and regulates the endothelial cell barrier function." J Biol Chem 276(25): 22614-20.

Miao, H., E. Burnett, et al. (2000). "Activation of EphA2 kinase suppresses integrin function and causes focal-adhesion-kinase dephosphorylation." Nat Cell Biol 2(2): 62-9.

Mierke, C. T., D. Rosel, et al. (2008). "Contractile forces in tumor cell migration." Eur J Cell Biol 87(8-9): 669-76.

Miki, H., S. Suetsugu, et al. (1998). "WAVE, a novel WASP-family protein involved in actin reorganization induced by Rac." Embo J 17(23): 6932-41.

Mishima, T., M. Naotsuka, et al. (2010). "LIM-kinase is critical for the mesenchymal-to-amoeboid cell morphological transition in 3D matrices." Biochem Biophys Res Commun 392(4): 577-81.

Mochly-Rosen, D. and A. S. Gordon (1998). "Anchoring proteins for protein kinase C: a means for isozyme selectivity." Faseb J 12(1): 35-42.

Montcourrier, P., P. H. Mangeat, et al. (1990). "Cathepsin D in breast cancer cells can digest extracellular matrix in large acidic vesicles." Cancer Res 50(18): 6045-54.

Mosior, M. and R. M. Epand (1993). "Mechanism of activation of protein kinase C: roles of diolein and phosphatidylserine." Biochemistry 32(1): 66-75.

Mosior, M. and A. C. Newton (1995). "Mechanism of interaction of protein kinase C with phorbol esters. Reversibility and nature of membrane association." J Biol Chem 270(43): 25526-33.

Mouneimne, G., V. DesMarais, et al. (2006). "Spatial and temporal control of cofilin activity is required for directional sensing during chemotaxis." Curr Biol 16(22): 2193-205.

Mueller, M. M. and N. E. Fusenig (2004). "Friends or foes - bipolar effects of the tumour stroma in cancer." Nat Rev Cancer 4(11): 839-49.

Murphy, G. and J. Gavrilovic (1999). "Proteolysis and cell migration: creating a path?" Curr Opin Cell

Biol 11(5): 614-21.

Nakahara, H., L. Howard, et al. (1997). "Transmembrane/cytoplasmic domain-mediated membrane type 1-matrix metalloprotease docking to invadopodia is required for cell invasion." Proc Natl Acad Sci U S A 94(15): 7959-64.

Nakashima, S. (2002). "Protein kinase C alpha (PKC alpha): regulation and biological function." J Biochem 132(5): 669-75.

Nalefski, E. A., M. A. Wisner, et al. (2001). "C2 domains from different Ca2+ signaling pathways display functional and mechanistic diversity." Biochemistry 40(10): 3089-100.

Newton, A. C. (1993). "Interaction of proteins with lipid headgroups: lessons from protein kinase C." Annu Rev Biophys Biomol Struct 22: 1-25.

Newton, A. C. (1995). "Protein kinase C: structure, function, and regulation." J Biol Chem 270(48): 28495-8.

Newton, A. C. (2001). "Protein kinase C: structural and spatial regulation by phosphorylation, cofactors, and macromolecular interactions." Chem Rev 101(8): 2353-64.

Newton, A. C. (2010). "Protein kinase C: poised to signal." Am J Physiol Endocrinol Metab 298(3): E395-402.

Newton, A. C. and L. M. Keranen (1994). "Phosphatidyl-L-serine is necessary for protein kinase C's high-affinity interaction with diacylglycerol-containing membranes." Biochemistry 33(21): 6651-8.

Ng, T., M. Parsons, et al. (2001). "Ezrin is a downstream effector of trafficking PKC-integrin complexes involved in the control of cell motility." Embo J 20(11): 2723-41.

Ng, T., D. Shima, et al. (1999). "PKCalpha regulates beta1 integrin-dependent cell motility through association and control of integrin traffic." Embo J 18(14): 3909-23.

Ng, T., A. Squire, et al. (1999). "Imaging protein kinase Calpha activation in cells." Science 283(5410): 2085-9.

Niggli, V. (2003). "Microtubule-disruption-induced and chemotactic-peptide-induced migration of human neutrophils: implications for differential sets of signalling pathways." J Cell Sci 116(Pt 5): 813-22.

Niggli, V. and J. Rossy (2008). "Ezrin/radixin/moesin: versatile controllers of signaling molecules and of the cortical cytoskeleton." Int J Biochem Cell Biol 40(3): 344-9.

Niggli, V., M. Schmid, et al. (2006). "Differential roles of Rho-kinase and myosin light chain kinase in regulating shape, adhesion, and migration of HT1080 fibrosarcoma cells." Biochem Biophys Res Commun 343(2): 602-8.

Nishita, M., C. Tomizawa, et al. (2005). "Spatial and temporal regulation of cofilin activity by LIM kinase and Slingshot is critical for directional cell migration." J Cell Biol 171(2): 349-59.

Nishizuka, Y. (1984). "The role of protein kinase C in cell surface signal transduction and tumour promotion." Nature 308(5961): 693-8.

Nobes, C. D. and A. Hall (1995). "Rho, rac, and cdc42 GTPases regulate the assembly of multimolecular focal complexes associated with actin stress fibers, lamellipodia, and filopodia." Cell 81(1): 53-62.

Nobes, C. D. and A. Hall (1999). "Rho GTPases control polarity, protrusion, and adhesion during cell movement." J Cell Biol 144(6): 1235-44.

Nobes, C. D., I. Lauritzen, et al. (1998). "A new member of the Rho family, Rnd1, promotes disassembly of actin filament structures and loss of cell adhesion." J Cell Biol 141(1): 187-97.

Oka, N., M. Yamamoto, et al. (1997). "Caveolin interaction with protein kinase C. Isoenzyme-dependent regulation of kinase activity by the caveolin scaffolding domain peptide." J Biol Chem 272(52): 33416-21.

Orr, J. W., L. M. Keranen, et al. (1992). "Reversible exposure of the pseudosubstrate domain of protein kinase C by phosphatidylserine and diacylglycerol." J Biol Chem 267(22): 15263-6.

Orr, J. W. and A. C. Newton (1992). "Interaction of protein kinase C with phosphatidylserine. 2. Specificity and regulation." Biochemistry 31(19): 4667-73.

Orr, J. W. and A. C. Newton (1994). "Intrapeptide regulation of protein kinase C." J Biol Chem 269(11): 8383-7.

Pajerowski, J. D., K. N. Dahl, et al. (2007). "Physical plasticity of the nucleus in stem cell differentiation." Proc Natl Acad Sci U S A 104(40): 15619-24.

Palazzo, A. F., C. H. Eng, et al. (2004). "Localized stabilization of microtubules by integrin- and FAK-facilitated Rho signaling." Science 303(5659): 836-9.

Palecek, S. P., J. C. Loftus, et al. (1997). "Integrin-ligand binding properties govern cell migration speed through cell-substratum adhesiveness." Nature 385(6616): 537-40.

Paluch, E., M. Piel, et al. (2005). "Cortical actomyosin breakage triggers shape oscillations in cells and cell fragments." Biophys J 89(1): 724-33.

Pankova, D., N. Jobe, et al. (2012). "NG2-mediated Rho activation promotes amoeboid invasiveness of cancer cells." Eur J Cell Biol.

Pankova, K., D. Rosel, et al. (2010). "The molecular mechanisms of transition between mesenchymal and amoeboid invasiveness in tumor cells." Cell Mol Life Sci 67(1): 63-71.

Parker, P. J., L. Coussens, et al. (1986). "The complete primary structure of protein kinase C--the major phorbol ester receptor." Science 233(4766): 853-9.

Parri, M., F. Buricchi, et al. (2007). "EphrinA1 activates a Src/focal adhesion kinase-mediated motility response leading to rho-dependent actino/myosin contractility." J Biol Chem 282(27): 19619-28.

Parri, M., M. L. Taddei, et al. (2009). "EphA2 reexpression prompts invasion of melanoma cells shifting from mesenchymal to amoeboid-like motility style." Cancer Res 69(5): 2072-81.

Parsons, M., M. D. Keppler, et al. (2002). "Site-directed perturbation of protein kinase C- integrin interaction blocks carcinoma cell chemotaxis." Mol Cell Biol 22(16): 5897-911.

Pears, C., S. Stabel, et al. (1992). "Studies on the phosphorylation of protein kinase C-alpha." Biochem J 283 (Pt 2): 515-8.

Peyton, S. R., P. D. Kim, et al. (2008). "The effects of matrix stiffness and RhoA on the phenotypic plasticity of smooth muscle cells in a 3-D biosynthetic hydrogel system." Biomaterials 29(17): 2597-607.

Pinner, S. and E. Sahai (2008). "PDK1 regulates cancer cell motility by antagonising inhibition of ROCK1 by RhoE." Nat Cell Biol 10(2): 127-37.

Podar, K., Y. T. Tai, et al. (2002). "Vascular endothelial growth factor-induced migration of multiple myeloma cells is associated with beta 1 integrin- and phosphatidylinositol 3-kinase-dependent PKC alpha activation." J Biol Chem 277(10): 7875-81.

Provenzano, P. P., K. W. Eliceiri, et al. (2006). "Collagen reorganization at the tumor-stromal interface facilitates local invasion." BMC Med 4(1): 38.

Provenzano, P. P., D. R. Inman, et al. (2008). "Contact guidance mediated three-dimensional cell migration is regulated by Rho/ROCK-dependent matrix reorganization." Biophys J 95(11): 5374-84.

Provenzano, P. P., D. R. Inman, et al. (2008). "Contact guidance mediated three-dimensional cell migration is regulated by Rho/ROCK-dependent matrix reorganization." Biophys J 95(11): 5374-84.

Rabinovitz, I., A. Toker, et al. (1999). "Protein kinase C-dependent mobilization of the alpha6beta4 integrin from hemidesmosomes and its association with actin-rich cell protrusions drive the chemotactic migration of carcinoma cells." J Cell Biol 146(5): 1147-60.

Rabinovitz, I., L. Tsomo, et al. (2004). "Protein kinase C-alpha phosphorylation of specific serines in the connecting segment of the beta 4 integrin regulates the dynamics of type II hemidesmosomes." Mol Cell Biol 24(10): 4351-60.

Ramnath, N. and P. J. Creaven (2004). "Matrix metalloproteinase inhibitors." Curr Oncol Rep 6(2): 96-102.

Ridley, A. J., H. F. Paterson, et al. (1992). "The small GTP-binding protein rac regulates growth factor-induced membrane ruffling." Cell 70(3): 401-10.

Riento, K., R. M. Guasch, et al. (2003). "RhoE binds to ROCK I and inhibits downstream signaling." Mol Cell Biol 23(12): 4219-29.

Rohatgi, R., L. Ma, et al. (1999). "The interaction between N-WASP and the Arp2/3 complex links Cdc42-dependent signals to actin assembly." Cell 97(2): 221-31.

Ron, D., C. H. Chen, et al. (1994). "Cloning of an intracellular receptor for protein kinase C: a homolog of the beta subunit of G proteins." Proc Natl Acad Sci U S A 91(3): 839-43.

Ron, D. and D. Mochly-Rosen (1995). "An autoregulatory region in protein kinase C: the pseudoanchoring site." Proc Natl Acad Sci U S A 92(2): 492-6.

Rosel, D., J. Brabek, et al. (2008). "Up-regulation of Rho/ROCK signaling in sarcoma cells drives invasion and increased generation of protrusive forces." Mol Cancer Res 6(9): 1410-20.

Sabeh, F., R. Shimizu-Hirota, et al. (2009). "Protease-dependent versus -independent cancer cell invasion programs: three-dimensional amoeboid movement revisited." J Cell Biol 185(1): 11-9.

Sahai, E., R. Garcia-Medina, et al. (2007). "Smurf1 regulates tumor cell plasticity and motility through degradation of RhoA leading to localized inhibition of contractility." J Cell Biol 176(1): 35-42.

Sahai, E. and C. J. Marshall (2002). "ROCK and Dia have opposing effects on adherens junctions downstream of Rho." Nat Cell Biol 4(6): 408-15.

Sahai, E. and C. J. Marshall (2003). "Differing modes of tumour cell invasion have distinct requirements for Rho/ROCK signalling and extracellular proteolysis." Nat Cell Biol 5(8): 711-9.

Sanders, L. C., F. Matsumura, et al. (1999). "Inhibition of myosin light chain kinase by p21-activated kinase." Science 283(5410): 2083-5.

Sanz-Moreno, V., G. Gadea, et al. (2008). "Rac activation and inactivation control plasticity of tumor cell movement." Cell 135(3): 510-23.

Sanz-Moreno, V. and C. J. Marshall (2010). "The plasticity of cytoskeletal dynamics underlying neoplastic cell migration." Curr Opin Cell Biol 22(5): 690-6.

Sharkey, N. A., K. L. Leach, et al. (1984). "Competitive inhibition by diacylglycerol of specific phorbol ester binding." Proc Natl Acad Sci U S A 81(2): 607-10.

Sharma, K., C. Kumar, et al. (2010). "Quantitative analysis of kinase-proximal signaling in

lipopolysaccharide-induced innate immune response." J Proteome Res 9(5): 2539-49.

Shea, K. F., C. M. Wells, et al. (2008). "ROCK1 and LIMK2 interact in spread but not blebbing cancer cells." PLoS One 3(10): e3398.

Sheetz, M. P., D. P. Felsenfeld, et al. (1998). "Cell migration: regulation of force on extracellular-matrix-integrin complexes." Trends Cell Biol 8(2): 51-4.

Schechtman, D. and D. Mochly-Rosen (2001). "Adaptor proteins in protein kinase C-mediated signal transduction." Oncogene 20(44): 6339-47.

Schmidt, S. and P. Friedl (2010). "Interstitial cell migration: integrin-dependent and alternative adhesion mechanisms." Cell Tissue Res 339(1): 83-92.

Schonwasser, D. C., R. M. Marais, et al. (1998). "Activation of the mitogen-activated protein kinase/extracellular signal-regulated kinase pathway by conventional, novel, and atypical protein kinase C isotypes." Mol Cell Biol 18(2): 790-8.

Sidani, M., D. Wessels, et al. (2007). "Cofilin determines the migration behavior and turning frequency of metastatic cancer cells." J Cell Biol 179(4): 777-91.

Singh, I., N. Knezevic, et al. (2007). "Galphaq-TRPC6-mediated Ca2+ entry induces RhoA activation and resultant endothelial cell shape change in response to thrombin." J Biol Chem 282(11): 7833-43.

Soker, S., S. Takashima, et al. (1998). "Neuropilin-1 is expressed by endothelial and tumor cells as an isoform-specific receptor for vascular endothelial growth factor." Cell 92(6): 735-45.

Stetler-Stevenson, W. G., S. Aznavoorian, et al. (1993). "Tumor cell interactions with the extracellular matrix during invasion and metastasis." Annu Rev Cell Biol 9: 541-73.

Stylli, S. S., A. H. Kaye, et al. (2008). "Invadopodia: at the cutting edge of tumour invasion." J Clin Neurosci 15(7): 725-37.

Suetsugu, S., H. Miki, et al. (2001). "Enhancement of branching efficiency by the actin filament-binding activity of N-WASP/WAVE2." J Cell Sci 114(Pt 24): 4533-42.

Sun, X. G. and S. A. Rotenberg (1999). "Overexpression of protein kinase Calpha in MCF-10A human breast cells engenders dramatic alterations in morphology, proliferation, and motility." Cell Growth Differ 10(5): 343-52.

Sward, K., K. Dreja, et al. (2000). "Inhibition of Rho-associated kinase blocks agonist-induced Ca2+ sensitization of myosin phosphorylation and force in guinea-pig ileum." J Physiol 522 Pt 1: 33-49.

Takai, Y., A. Kishimoto, et al. (1979). "Calcium-dependent activation of a multifunctional protein kinase by membrane phospholipids." J Biol Chem 254(10): 3692-5.

Tamariz, E. and F. Grinnell (2002). "Modulation of fibroblast morphology and adhesion during collagen matrix remodeling." Mol Biol Cell 13(11): 3915-29.

Tan, I., C. H. Ng, et al. (2001). "Phosphorylation of a novel myosin binding subunit of protein phosphatase 1 reveals a conserved mechanism in the regulation of actin cytoskeleton." J Biol Chem 276(24): 21209-16.

Tan, M., P. Li, et al. (2006). "Upregulation and activation of PKC alpha by ErbB2 through Src promotes breast cancer cell invasion that can be blocked by combined treatment with PKC alpha and Src inhibitors." Oncogene 25(23): 3286-95.

Tolde, O., D. Rosel, et al. (2010). "The structure of invadopodia in a complex 3D environment." Eur J Cell Biol 89(9): 674-80.

Totsukawa, G., Y. Wu, et al. (2004). "Distinct roles of MLCK and ROCK in the regulation of membrane protrusions and focal adhesion dynamics during cell migration of fibroblasts." J Cell Biol 164(3): 427-39.

Totsukawa, G., Y. Yamakita, et al. (2000). "Distinct roles of ROCK (Rho-kinase) and MLCK in spatial regulation of MLC phosphorylation for assembly of stress fibers and focal adhesions in 3T3 fibroblasts." J Cell Biol 150(4): 797-806.

Ulrich, T. A., E. M. de Juan Pardo, et al. (2009). "The mechanical rigidity of the extracellular matrix regulates the structure, motility, and proliferation of glioma cells." Cancer Res 69(10): 4167-74.

Van Goethem, E., R. Poincloux, et al. (2010). "Matrix architecture dictates three-dimensional migration modes of human macrophages: differential involvement of proteases and podosome-like structures." J Immunol 184(2): 1049-61.

Velasco, G., C. Armstrong, et al. (2002). "Phosphorylation of the regulatory subunit of smooth muscle protein phosphatase 1M at Thr850 induces its dissociation from myosin." FEBS Lett 527(1-3): 101-4.

Wang, H. R., A. A. Ogunjimi, et al. (2006). "Degradation of RhoA by Smurf1 ubiquitin ligase." Methods Enzymol 406: 437-47.

Watanabe, M., C. Y. Chen, et al. (1994). "Saccharomyces cerevisiae PKC1 encodes a protein kinase C (PKC) homolog with a substrate specificity similar to that of mammalian PKC." J Biol Chem 269(24): 16829-36.

Weaver, A. M. (2006). "Invadopodia: specialized cell structures for cancer invasion." Clin Exp Metastasis 23(2): 97-105.

Wei, Y., M. Lukashev, et al. (1996). "Regulation of integrin function by the urokinase receptor." Science 273(5281): 1551-5.

Wilkinson, S., H. F. Paterson, et al. (2005). "Cdc42-MRCK and Rho-ROCK signalling cooperate in myosin phosphorylation and cell invasion." Nat Cell Biol 7(3): 255-61.

Wolf, K. and P. Friedl (2005). "Functional imaging of pericellular proteolysis in cancer cell invasion." Biochimie 87(3-4): 315-20.

Wolf, K. and P. Friedl (2006). "Molecular mechanisms of cancer cell invasion and plasticity." Br J Dermatol 154 Suppl 1: 11-5.

Wolf, K. and P. Friedl (2009). "Mapping proteolytic cancer cell-extracellular matrix interfaces." Clin Exp Metastasis 26(4): 289-98.

Wolf, K., I. Mazo, et al. (2003). "Compensation mechanism in tumor cell migration: mesenchymal-amoeboid transition after blocking of pericellular proteolysis." J Cell Biol 160(2): 267-77.

Wolf, K., Y. I. Wu, et al. (2007). "Multi-step pericellular proteolysis controls the transition from individual to collective cancer cell invasion." Nat Cell Biol 9(8): 893-904.

Wu, T. T., Y. H. Hsieh, et al. (2008). "Reduction of PKC alpha decreases cell proliferation, migration, and invasion of human malignant hepatocellular carcinoma." J Cell Biochem 103(1): 9-20.

Wyckoff, J. B., S. E. Pinner, et al. (2006). "ROCK- and myosin-dependent matrix deformation enables protease-independent tumor-cell invasion in vivo." Curr Biol 16(15): 1515-23.

Xiao, H., X. H. Bai, et al. "The protein kinase C cascade regulates recruitment of matrix metalloprotease 9 to podosomes and its release and activation." Mol Cell Biol 30(23): 5545-61.

Yamaguchi, H., M. Lorenz, et al. (2005). "Molecular mechanisms of invadopodium formation: the role of the N-WASP-Arp2/3 complex pathway and cofilin." J Cell Biol 168(3): 441-52.

Yamazaki, D., S. Kurisu, et al. (2009). "Involvement of Rac and Rho signaling in cancer cell motility in 3D substrates." Oncogene 28(13): 1570-83.

Yamazaki, D., S. Suetsugu, et al. (2003). "WAVE2 is required for directed cell migration and cardiovascular development." Nature 424(6947): 452-6.

Yanai, M., C. M. Kenyon, et al. (1996). "Intracellular pressure is a motive force for cell motion in Amoeba proteus." Cell Motil Cytoskeleton 33(1): 22-9.

Yang, L., L. Wang, et al. (2006). "Gene targeting of Cdc42 and Cdc42GAP affirms the critical involvement of Cdc42 in filopodia induction, directed migration, and proliferation in primary mouse embryonic fibroblasts." Mol Biol Cell 17(11): 4675-85.

Yang, N., O. Higuchi, et al. (1998). "Cofilin phosphorylation by LIM-kinase 1 and its role in Rac-mediated actin reorganization." Nature 393(6687): 809-12.

Yonemura, S., T. Matsui, et al. (2002). "Rho-dependent and -independent activation mechanisms of ezrin/radixin/moesin proteins: an essential role for polyphosphoinositides in vivo." J Cell Sci 115(Pt 12): 2569-80.

Yumura, S., H. Mori, et al. (1984). "Localization of actin and myosin for the study of ameboid movement in Dictyostelium using improved immunofluorescence." J Cell Biol 99(3): 894-9.

Zaidel-Bar, R., M. Cohen, et al. (2004). "Hierarchical assembly of cell-matrix adhesion complexes." Biochem Soc Trans 32(Pt3): 416-20.

Zhang, G., M. G. Kazanietz, et al. (1995). "Crystal structure of the cys2 activator-binding domain of protein kinase C delta in complex with phorbol ester." Cell 81(6): 917-24.

Zhao, Z. S. and E. Manser (2005). "PAK and other Rho-associated kinases--effectors with surprisingly diverse mechanisms of regulation." Biochem J 386(Pt 2): 201-14.